Norwegian University of Life Sciences

Master's Thesis 2024 60 ECTS

Faculty of Environmental Sciences and Natural Resource Management

Innate immune responses of *Alternaria* toxins *in vitro*: Receptor activation and modulation of signal transduction

Booshra Ahmed

Master of Science in Ecology

Abstract

Introduction: Mycotoxins are toxic secondary metabolites produced by fungi (*Aspergillus*, *Penicillium*, *Fusarium*, and *Alternaria*) and pose a significant concern in the realm of food safety, occupational and public health. Exposure (i.e. inhalation, dermal, ingestion) to mycotoxins in agriculture and industrial settings such as compound feed mills, farming, and animal husbandry is prevalent and an occupational health concern. Certain mycotoxins have been described to be immunosuppressive by inhibiting the triggering effect of lipopolysaccharide (LPS) on the NF-κB-signaling pathway, that is necessary to engage the immune system.

Objective: This study investigates the immunotoxic effects and inflammasome activation of *Alternaria* toxins—specifically Alternariol (AOH) and Alternariol monomethyl ether (AME)—in an *in vitro* model using engineered HEK-293 Toll-Like Receptor (TLR2 & TLR4) and IL-1β reporter cells, as well as THP-1 cells.

Methods: Experimental parameters involve exposing THP-1 cells and HEK-293 reporter cells encompassing HEK null, TLR2, and TLR4, and HEK IL-1β, HEK Null 1v cells to varying concentrations of mycotoxins (i.e., AOH- 30, 6, 1.2, 0.24 µM; AME- 10, 2.5, 0.625, 0.156 µM), with dimethyl sulfoxide (DMSO 0.1%) as vehicle control. A TLR2 ligand LTA and LPS for TLR4, and THP-1, were used to activate the response/signaling pathway. Assessment methods include alamar-Blue for cell viability and QuantiBlue assays for detecting and quantifying SEAP activity, that serves as a reporter for NF-κB activation. Levels of proinflammatory cytokine IL-1β secretion are measured by ELISA. Bioactive IL-1β is measured by the HEK IL-1β inflammasome assay, and qPCR is used to quantify the gene expression of IL-1β.

Result: LPS and LTA activation of TLR receptors led to an increase in the NF-κB signal. However, combination exposure of LPS and LTA with mycotoxins reduced the increased NF-κB signal in both receptors (TLR2 and TLR4) for both mycotoxins (AOH and AME). AOH and AME also reduced the secretion and gene expression of the key pro-inflammatory cytokine IL- 1β in the inflammasome THP-1/IL-1β assay, when co-exposed to LPS. Some effect of exposure to LPS/LTA and mycotoxins on the cell viability was also seen though no dose-dependent significant reduction was apparent.

Conclusion: The results indicate an immunomodulating effect of AOH and AME mycotoxins on LPS- or LTA-induced activation of TLR via the downstream NF-κB signaling pathway. This study

highlighted the need for improved monitoring and control of these mycotoxins to ensure the safety of food supply and protect the health of people related to agriculture and the food industry.

Graphical abstract

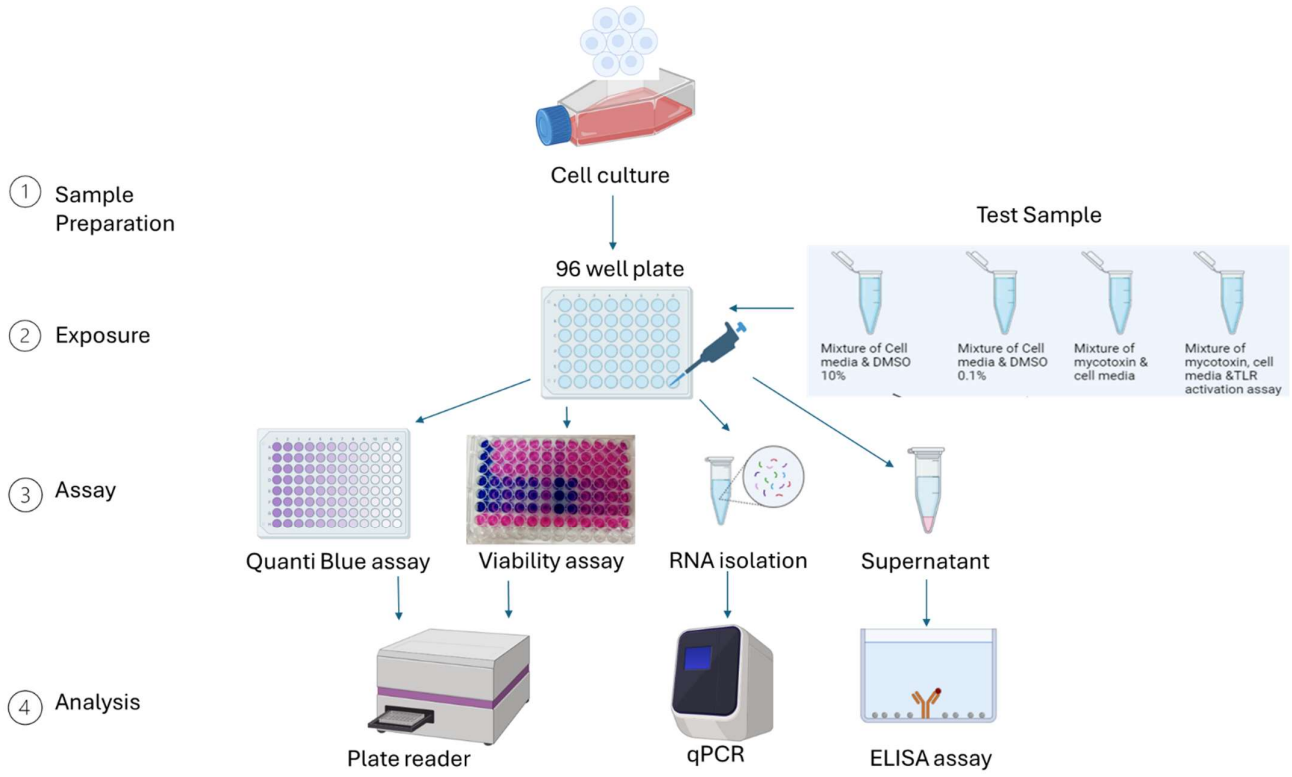

Acknowledgment

This thesis was performed at the Department of Toxicology, the National Occupational Health in Norway (STAMI) as part of master's program in Ecology at the Norwegian University of Life Sciences (NMBU). The author would like to express her deepest gratitude to everyone who assisted her along the way. Special thanks to the university for providing me with this opportunity.

The author is especially grateful to her supervisors, Pål Graff and Solveig Krapf, as well as Steen Møllerup and Anne Straumfors, for their invaluable support, guidance, and encouragement. A special thank you to Solveig for supporting, motivating, and believing in me throughout this journey.

Thanks to PARC for funding and the opportunity to conduct the study.

To everyone at STAMI, especially people from TOKS, thank you for your kindness and support. Thank you Shan Narui, Rita Bæra, Rubiyat Islam, Mrinal Kumar Das, Øyvind Pernell Haugen for your support and Knowledge. Thanks to Andreas Solberg Segan, for his kind gesture whenever I faced confusion. Thanks to those who have assisted me in this project in various ways. Isra Qudrat, special thanks to you for countless hours of discussion in the lab.

I would like to give my deep appreciation to my sister Onee and friend Ayesha and Tabassum for their support throughout my master's journey. And finally, I am indebted also to my family for their unconditional love, continuous support and encouragement throughout my studies. Marine, thank you so much for always assuring me that I could do this.

Booshra Ahmed
14th June 2024
Ås, Norway.

Table of Contents

Abbreviations

AOH - Alternariol

AME - Alternariol Monomethyl Ether

DMSO - Dimethylsulfoxide

DON-Deoxynivalenol

ELISA - Enzyme-Linked Immunosorbent Assay

FBS - Fetal Bovine Serum

HEK cells - Human Embryonic Kidney cells

IL-1β - Interleukin 1 beta

LPS - Lipopolysaccharide

LTA - Lipoteichoic acid

MQ-H2O - Milli-Q water

mRNA - Messenger RNA

NF-κB Nuclear Factor kappa-light-chain-enhancer of activated B cells

PAMPs - Pathogen-Associated Molecular Patterns

PARC - Partnership for Chemicals Risk Assessment

PBS - Phosphate Buffered Saline

PMA - Phorbol 12-Myristate 13-Acetate

qPCR - Quantitative Polymerase Chain Reaction

rcf – Relative centrifugation force

RNA - Ribonucleic acid

rpm – Round per minute

SEAP – Secreted Embryonic Alkaline Phosphatase

STAMI - The National Institute of Occupational Health in Norway (Norwegian: Statens arbeidsmiljøinstitutt)

THP-1 cell - Human Leukemia Monocytic cell

TLR – Toll Like Receptor

TLR2 – TOLL-like receptor 2

TLR4 – TOLL-like receptor 4

°C– Degrees Celsius

µM: – Micromolar

µg – Microgram

µL – Microliter

mL – Milliliter

ng – Nanogram

mg – Milligram

1. Introduction

1.1. Mycotoxins

1.1.1. Secondary metabolites

Many organisms produce secondary metabolites including plants, fungi, and bacteria. These are not directly involved in the core processes of growth, development, or reproduction (Isah et al., 2019) rather, substances that make them competitive in their own environment (Teoh, 2016). Secondary metabolites are not essential for the growth or survival of the producing organism but play crucial roles in ecological interactions and adaptation (Bills, 2016). Mycotoxins are toxic secondary metabolites produced by certain fungi (i.e. *Aspergillus, Penicillium, Fusarium*, and *Alternaria*) (Aichinger et al., 2021, Bernhoft et al., 2022, Bennett and Klich, 2003, Solhaug et al., 2016 a). Approximately 1000 secondary metabolites produced by fungal compounds, the most widely known are aflatoxins, trichothecenes, fumonisins, ochratoxin, cytochalasins, and various indole-terpene tremor genic compounds (Bräse, 2013). Mycotoxins tend to be more problematic than fungi because mycotoxins occur in food, livestock, and indoor environments contaminated by mold leading to high daily exposure for their widespread occurrence (Bills, 2016). Also, all fungal metabolites are not considered as mycotoxin, nature of their targets and concentration plays significant role in this classification. In general, fungal metabolites are toxic to bacteria, such as penicillin. Also, mushroom poisons, a fungal metabolite excluded from mycotoxin classification due to the distinction between molds and larger fungi, as well as intentional consumption and accidental exposure (Bennett et al., 2003).

1.1.2. Mycotoxin and toxicology

Mycotoxin toxicology is a critical area of study that focuses on the adverse effects of mycotoxins on human and animal health. Mycotoxins can exert various toxic effects, including acute and chronic toxicity, immunosuppression, carcinogenicity, and dermal irritation (Archinger et al., 2021, Bennett and Klich, 2003). While all mycotoxins are of fungal origin, not all fungus-produced toxic compounds are considered mycotoxins. The concentration of both the mycotoxin and the metabolite is important. Antibiotics are typically fungal products that are primarily toxic to bacteria (for example, penicillin). Mycotoxins are made by fungi and are toxic to vertebrates and other animal groups in low concentrations. Mycotoxins are hard to define in toxicology but are also classified as hepatotoxins, nephrotoxins, neurotoxins, immunotoxins, and so forth (Bennett, 1987).

1.1.3. Mycotoxins impact on human health

The impact of mycotoxins on human health is of significant concern. Mycotoxins are known for their diverse chemical structures and subsequent biological effects includes cytotoxicity, genotoxicity and mutagenicity, endocrine disruption and immunomodulation (Archinger et al., 2021). The health effects of mycotoxin exposure can vary depending on the specific toxin, the level and duration of exposure, and individual susceptibility (Archinger et al., 2021). Some mycotoxins, such as aflatoxins, ochratoxin A, fumonisins, and trichothecenes, have been extensively studied and are known to pose significant health risks to humans (Bennett and Klich, 2003). These mycotoxins can affect multiple organ systems and have been linked to liver cancer, kidney disease, neural tube defects, immune system suppression, and gastrointestinal disorders (Archinger et al., 2021). The potential impact of *Alternaria* toxins on the gastrointestinal barrier function, which is critical for preventing the entry of harmful substances into the bloodstream. *Alternaria* toxins can directly impair the functional status of intestinal cells by altering membrane fluidity, their migratory potential and membrane-cytoskeletal communication axes (Bernhoft et al., 2022). Consequently, ingestion of mycotoxins is considered a crucial risk factor for health (Solhaug et al., 2016 a).

In Asia gastrointestinal problems and diarrhea have been attributed to the consumption of *Fusarium*-contaminated grain. The presence of Deoxynivalenol (DON) at reported concentrations of 3–93 mg/kg in grain for human consumption was reported (Pinton et al., 2014). Exposure to *fusarium* toxin DON has been associated with a wide range of adverse health effects in humans and animals, including acute and chronic toxicity, immunosuppression, and gastrointestinal disorders (Bernhoft et al., 2022, Sural and Mezes, 2005). Regulations or guidelines for DON in food and feed have been implemented in more than 40 countries (Pinton et al., 2010). A recommended level of 1 ppm of DON has been set by the Food and Drug Administration (FDA) in the USA for bran, flour, and germ intended for human consumption (FDA, 2024). The European Commission resolved to restrict the amount of DON in feed from 0.9 to 5 mg/kg for complementary and complete feedstuffs, depending on the species, and in food from 0.2 to 1.75 mg/kg for cereals and derived products, depending on the exposed population (European Union Commission 2006).

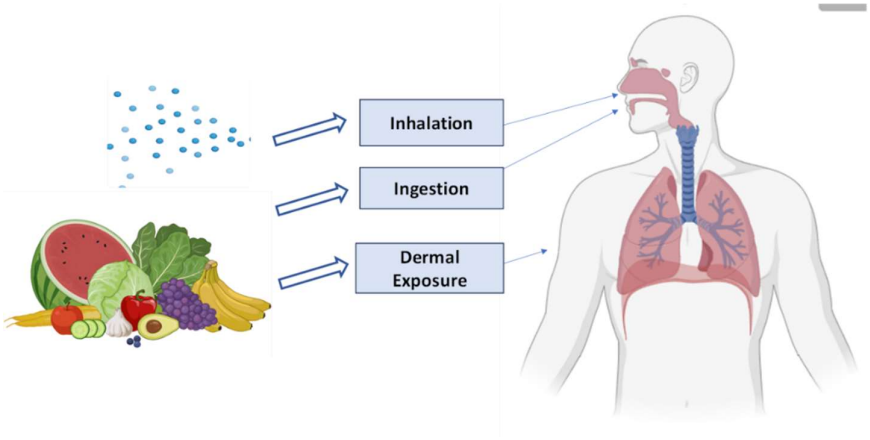

Figure 1.1: Mycotoxin exposure routes (BioRender.com).

The potential impact of DON on human health may occur after ingestion of contaminated foods such as oats, barley, wheat, corn, or other grains (Sobrova et al., 2010). After ingestion of contaminated food or feed, intestinal epithelial cells may be exposed to high concentrations of toxicants, potentially affecting intestinal functions (Pinton et al., 2014). In humans, exposure to DON can cause nausea, vomiting, diarrhea, abdominal pain (Stoev, 2024), and headache. Long-term exposure to DON has been linked to immune system suppression, which can increase the risk of infections and other health problems. The toxicity of DON is due to its ability to inhibit protein synthesis by binding to the ribosome, which can lead to the production of abnormal proteins and cell death. DON can also induce oxidative stress and inflammation, which can contribute to its toxic effects (Archinger et al., 2021).

The majority of investigated human health effects of mycotoxin exposure are through ingestion of contaminated food products. However, occupational exposure is also important where exposure typically occurs through inhalation and dermal contact. While most mycotoxins are non-volatile, they can be present in airborne dust and fungal spores and fragments, which serve as carriers of mycotoxins to the respiratory system, farmers who are involved in storage, threshing and milling tasks are most susceptible ((Halstensen et al., 2008, Straumfors et al., 2015, Mayer et al., 2016, Viegas et al., 2016, Viegas et al., 2018, Stoev, 2024). Inhalation of Aflatoxin poses significant occupational health concern globally (Malik et al., 2014). Aflatoxin B1 (AFB1) is the most recognized hazardous mycotoxin, found in agricultural products, due to its hepatocarcinogen properties (Stoev, 2024). Malik et al., 2014 observed that aflatoxin was significantly detected in Bronchoalveolar lavage and serum samples of food grain workers (32.6%) than non-food grain workers (9.1%), in India. Another study carried out in Egypt observed higher concentration of serum aflatoxin among the workers who were exposed to wheat (mill or bakery) rather than controlled groups (Saad-Hussein et al., 2014).

Dermal contact is a frequent exposure route, in environments where workers come into direct contact with contaminated materials such as food, feed and waste. This risk is heightened in settings where workers wear short-sleeved clothing or handle solutions containing mycotoxins. Dust particles containing mycotoxins may deposit on the skin, facilitating dermal absorption, while contaminated work surfaces may also contribute to dermal exposure through direct contact (Viegas et al., 2016, Viegas et al., 2018). Penetration of beauvericin (BEA) and enniatins (ENNs) into intact and damaged human skin has been demonstrated in an *in vitro* Franz diffusion cell study, where they found that all tested mycotoxins can penetrate the skin with ENN B exhibiting the highest permeation and BEA the lowest (Taevernier et al., 2016).

1.1.4. Mycotoxins in Agriculture

In recent times food and feed have been contaminated by mycotoxin in larger extensions. Both pre- and post-harvest seasons make agricultural products susceptible to mycotoxin contamination (Luo et al., 2021). These naturally occurring compounds can contaminate various agricultural products, including cereals, fruits, and vegetables at various stages of the food chain, leading to potential health risks for humans and animals (Aichinger et al. 2021, Bernhoft et al., 2022, Solhaug et al, 2016 a). From agricultural production to processing, storage, and ultimately consumption, humans and animals may be daily exposed. The presence of mycotoxins in the food chain has global occurrence due to their ubiquity and resilience in various environmental conditions (Aichinger et al.2021, Bernhoft et al., 2022).

Cereal species (such as wheat, oats, barley, maize) are mostly contaminated by plant pathogenic *Fusarium* species in the growing season, causing *Fusarium* Head Blight (FHB) leading to yield losses and reduced grain quality. On the other hand, *Fusarium* mycotoxins are commonly found in cereals which include deoxynivalenol (DON), zearalenone (ZEA), T-2 toxin, and HT-2 toxin (Bernhoft et al., 2012). According to Bernhoft et al., 2022; DON (main marker of *Fusarium* mycotoxin load) concentrations were significantly lower in the organic production system instead of no significant difference between production systems. The estimated mycotoxin concentration in the cereals grown in conventional systems is higher (62%) than the organically produced cereals (Data from systemic review and meta-analysis from field experiments, farm survey and retail survey-based studies). According to the studies, wheat has lower resistance against *fusarium* infection compared to other small-grain cereals, whereas oats are more susceptible to T-2, and HT-2 (Bernhoft et al., 2022).

On the other hand, replicated field experiments which are designed to control the environmental parameters and agronomic conditions to investigate the conditions of mycotoxin and *Fusarium*

infection is not possible due to confounding effects of climate/weather and other environmental parameters (Bernhoft et al., 2022). But still some field experiments suggest no relation between *fusarium* infection and mycotoxin concentration. However, taller cultivars had lower levels of FHB but the same concentration of mycotoxin (Góral et al., 2019). According to some field experiments suggest that growing wheat in organic condition reduces stress resulting from intensive mineral fertilization and chemical crop protection in the fungus (Champeil et al., 2004). Also, it was referring to the fact that high weed density had a protective effect against *fusarium* infection (Munger et al., 2014). But the difference in the concentration is created in conventional than the organic due to elevated level of fertilizer input, which increases the concentrations of DON (Bernhoft et al., 2022). From the farm surveys (pedoclimatic condition and agronomic protocols should be considered), it was reported that both DON and *Fusarium* infection levels increased with nitrogen (N) fertilization (Lemmens et al., 2004), use of fungicides (Bernhoft et al., 2022), reduced tillage (Bernhoft et al., 2022), and maize as a preceding crop (Beyer et al., 2006). Weather conditions have prevalent impact on contamination level (Bernhoft et al., 2022).

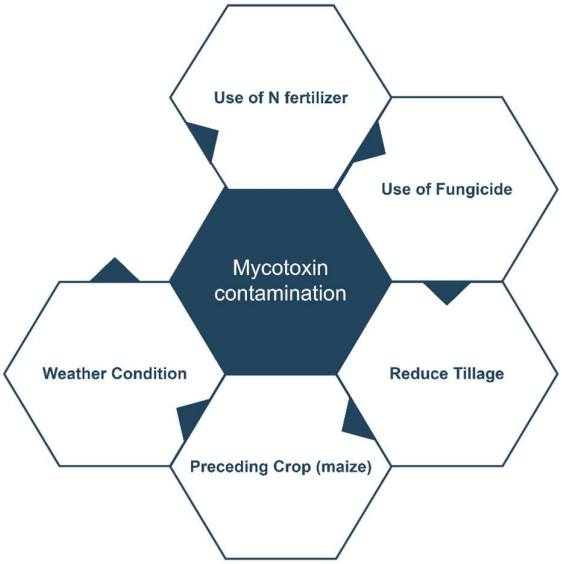

Figure 1.2: Factors that influence mycotoxin contamination.

According to the studies, crop rotation is a good approach to reducing *Fusarium* and mycotoxin contamination in the crops (Bernhoft et al., 2022). Harvesting non-*fusarium* host plants (oilseed rape, potatoes, legumes, field vegetables) as preceding crops before cereals effectively reduce the pathogen inoculum from the agricultural soil (Bernhoft et al., 2012). N mineralization accelerates *fusarium* infection and mycotoxin contamination in wheat by generating a denser crop canopy along with a favorable microclimate for DON-producing *fusarium* species. However, a different result was found

for barley in Denmark, were low N input increased infection as a result they suggested higher use of N fertilizer as a potential strategy to minimize the infection (Yang et al., 2010). Fungicide treatment could be a potential strategy to control contamination but eventually, the result was not satisfactory (Shah et al., 2017). The studies from Germany and the USA refer to about 50% reduction of FHB and *DON* after combining the use of triazole, a commonly used fungicide. Also, multiple applications of azoles could reduce FHB, but not cost-effective for commercial cereal production (Beyer et al., 2006). However, fungicide use is not an effective treatment as it leads to reduction of competition from other commensal or pathogenic fungal species ultimately leads to increased *Fusarium* infection and mycotoxin contamination. Also, the use of herbicides might induce changes in the structure of the fungal community which increases the infection. Deep tillage is an effective preventive strategy, but it is not significant for *fusarium* control (Bernhoft et al., 2022).

1.1.5. Mycotoxins and climate change

Climate change (temperature and humidity) increases the risk of mycotoxin contamination in crops due to various factors that create more favorable conditions for mycotoxigenic fungi (Peterson et al., 2010). In areas affected by rising temperatures and increased humidity due to climate change, like certain regions in the southern United States, there has been a noticeable rise in aflatoxin contamination in corn crops. The conducive warm and moist conditions in these regions promote the growth of aflatoxin-producing fungi such as *Aspergillus flavus* (cotty et al., 2007), resulting in elevated levels of aflatoxin in harvested corn (Peterson et al., 2010). The warm and moist conditions can favor the growth of mycotoxigenic fungi on crops, leading to pre-harvest contamination. And in the case of post-harvest contamination different factors such as the influence of temperature, water availability, and gas composition on fungal spoilage and mycotoxin production in stored grain ecosystems included (Peterson et al., 2010).

The grape-growing regions (North and South of the Portuguese, Spane, France) can impact the growth of fungi like *Aspergillus ochraceus*, which produces ochratoxin A. Warmer temperatures and increased moisture can create ideal conditions for the development of ochratoxin A contamination in grapes (Serra et al., 2006), posing a risk to wine production and food safety (Clouvel et al., 2008). *Fusarium* fungi, responsible for producing DON mycotoxin, are influenced by temperature and humidity changes (Isebaert et al., 2009). In regions like Canada, where climate change is altering traditional weather patterns, there have been reports of increased *Fusarium* head blight in wheat crops, leading to higher levels of DON contamination due to the conducive environmental conditions (Baer et al., 2009, Peterson et al., 2010). The coffee-growing regions are also globally affected by climate change, which affects the growth and quality of coffee beans. The change of climate also creates susceptible

conditions for mycotoxigenic fungi to proliferate on coffee plants, resulting in mycotoxin contamination in coffee beans (Noonim et al., 2009).

1.2. *Alternaria* species and their toxins

Approximately 300 species of *Alternaria* (Surai and Mezes, 2005) have been identified worldwide, including *Alternaria alternata*, *Alternaria tenuissima*, *Alternaria arborescense*, *Alternaria brassicicola*, *Alternaria infectoria*, and *Alternaria solani*. These species have been reported to cause diseases in nearly 400 plant species (Meena et al., 2017), with *A. alternata* alone infecting almost 100 plant species (Sajad et al., 2017). *Alternaria* species are responsible for post-harvest diseases in various crops, leading to economic losses (Woudenberg et al., 2015, Meena et al., 2017). *Alternaria* mycotoxins have been discovered in a variety of fruits and vegetables, including tomatoes, citrus fruits, Japanese pears, prune nectar, red currant, carrots, barley, oats, olives, mandarins, melons, peppers, apples, raspberries, cranberries, grapes, sunflower seeds, oilseed rape meal, flax seed, linseed, pecans, melon, lentils, wheat, and other grains. These mycotoxin findings have been reported regularly (Sajad et al., 2017, Woudenberg et al., 2015, Meena et al., 2017).

Alternaria is a genus of fungi that produces a variety of toxins, including host-specific toxins (HSTs) and non-host specific toxins (nHSTs). HSTs are highly specific to certain plant varieties or genotypes and play a role in determining the host range of specificity of plant pathogens. Some of the commonly known HSTs produced by *Alternaria* include *Alternaria alternata lycopersici* (AAL)-, *Alternaria alternata kikuchiana* (AK)-, *Alternaria alternata mali* (AM)-, *Alternaria alternata fragariae* (AF)-, and *Alternaria alternata citri* (ACT)- toxins (Tsuge et al., 2013). These toxins have different modes of action, biochemical reactions, and signaling mechanisms to cause diseases. On the other hand, nHSTs are secondary metabolites that are not specific to any particular host and can affect a broad range of plant species, animals, insects and humans (Meena et al., 2017).

The pathogenicity of *Alternaria* species poses challenges for crop management and disease prevention, highlighting the need for effective strategies to mitigate the impact of these pathogens on agricultural and human health. This is a complex process involving the secretion of hydrolytic enzymes during the penetration process to enter plant tissues. The fungus also secretes chemical compounds that elicit broad host-range defense responses, which can slow pathogen ingress (Jackson et al., 1996). Certain species of *Alternaria* suppress defense responses by manipulating plant signaling pathways. Fungal infection can suppress the host's immune system and encourage disease progression by meddling with plant hormone signaling molecules. To prevent disease invasion, Plants depend upon immune system to activate signal transduction by recognizing pathogen. As defense mechanism plants develop

physical barriers like thicker cell walls or layers of cuticle. Meanwhile, plants use chemical substances to strengthen their defenses by generating phytoalexins and secondary metabolites that inhibit the growth of pathogens. Plants also recognize pathogens through signaling molecules and activate induced resistance, which enhances their defenses. A systemic acquired resistance (SAR) response also strengthens the plant's resistance to infection by triggering defense genes and producing antimicrobial chemicals. *Alternaria* species have developed strategies to suppress these responses or avoid the host's potential defenses by changing surface molecules to conceal pathogen-associated molecular patterns (PAMPs), allowing them to cause disease in susceptible hosts (Meena et al., 2017).

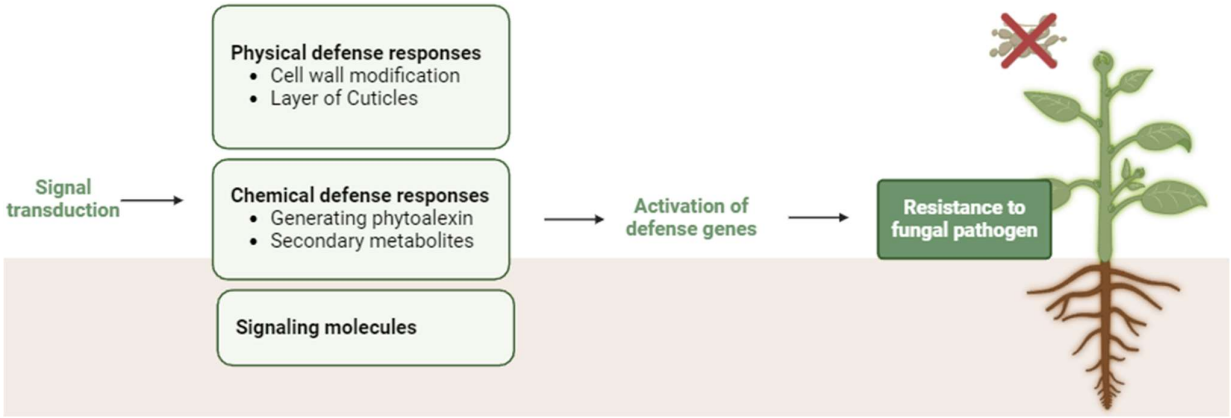

Figure 1.3: How plant resistance mechanism response to fungal pathogens (Biorender.com).

Some of the known nHSTs produced by *Alternaria* include alternariol (AOH), altenuene (ALT), tenuazonic acid (TeA), Alternariol monomethyl ether (AME), tentoxin (TEN), Altertoxin I-IV (ATX-I-IV) etc. (Andersen et al., 2015). These toxins can cause a variety of symptoms in plants, including leaf necrosis, cell fragmentation, inhibition of protein synthesis and causing disassembly of the Golgi complex (Meena et al., 2017). *Alternaria* toxins have also been found to cause asthma and infection of the upper respiratory tract in humans (Meena et al., 2017). According to the European Food Safety Authority (EFSA), several *Alternaria* toxins may pose health hazards to humans, including tentoxin (TEN), alternariol (AOH), alternariol monomethyl ether (AME), tenuazonic acid (TeA), and altenuene (ALT) (EFSA, 2011). Since this study is primarily focused on AOH and AME, more information will be provided about these *Alternaria* toxins.

1.2.1. Alternariol (AOH)

AOH, is produced by various species of the *Alternaria* genus. It is known for its cytotoxic and genotoxic effects such as induction of apoptosis in various cell lines, DNA damage, cell cycle disruption, and mutagenicity (Schmutz et al., 2019). Toxicological studies of AOH have led the European Food Safety Authority (EFSA) to establish a toxicological threshold of concern (TTC) for

AOH based on chemical structure using a decision trees (EFSA, 2011). Additionally, AOH has been found to co-occur with other mycotoxins such as AME in various food commodities, raising concerns about potential synergistic and additive effects at high concentrations, and antagonistic effects at low concentrations (Lin et al., 2023). Lin et al., 2023 tried combined toxicity analysis of AOH, AME and TeA. Their combination induces apoptosis and activated caspase-3 cleavage, indicating apoptotic cell death.

A study by Hollander et al., (2022) demonstrates a dose-dependent toxicity of AOH on the human hepatoma cell line, HepG2 and the human epithelial cell line, Caco-2. HepG2 derived from human hepatocellular carcinoma (liver cancer) which used as a model for human liver cells to study the effects of drugs and toxins on the liver (Donato et al., 2014). Caco-2 derived from human colorectal adenocarcinoma (colon cancer), used as a model of the intestinal epithelial barrier (Lea, 2015) Cytotoxicity is attributed to AOH's ability to generate reactive oxygen species (ROS) and interact with DNA topoisomerase, resulting in the induction of both single and double strand breaks in DNA. This molecular damage leads to a significant reduction in cell proliferation, as evidenced by cell cycle arrest in the G2/M-phase. Notably, AOH's cytotoxic effects are found to be less pronounced in metabolically active human hepatocytes (HepaRG), with no observed cytotoxicity at concentrations up to 100 µM (Hollander et al., 2022).

Schmutz et al., (2019) studied the impact of AOH on inflammation-related signaling at the gastrointestinal barrier, utilizing differentiated Caco-2 cells as a model. Here, AOH exhibited immunomodulatory properties in non-immune cells of the intestinal epithelium, as evidenced by its impact on cytokine transcription and secretion following co exposure to IL-1β stimulation. Specifically, AOH in combination with IL-1β stimulation reduced the transcription and secretion of cytokines such as IL-8, IL-6, and IL-1β These findings suggest that AOH may interfere with both lipopolysaccharide (LPS) and IL-1β-related pathways (Schmutz et al., 2019).

1.2.2. Alternariol monomethyl ether (AME)

Structurally, AME, or alternariol monomethyl ether, is a methylated derivative of alternariol and shares similar toxicological properties with its parent compound (Aichinger et al.2021). It is known for its cytotoxic and genotoxic effects, and it has been shown to induce apoptosis in various cell lines. AME has also been implicated in DNA damage, cell cycle disruption, and mutagenicity. In a comparative study of the cytotoxicity of various mycotoxins on the human gastric epithelial cell line (GES-1), AME was found to have a half-maximal inhibitory concentration, IC50, value of 10.21 µM, which was between those of ochratoxin A (OTA) and zearalenone (ZEN), indicating its moderate cytotoxicity

(Balazs et al., 2021). Additionally, AME has been found to co-occur with other mycotoxins such as AOH and TeA in various food commodities, raising concerns about potential combined toxic effects (Lin et al., 2023).

In a study on the combined toxicity of binary mixtures of AOH and AME, it was found that the toxicity potential was significantly increased, and in an additive manner affecting the cell viability of colon cancer cells. Furthermore, in a combined toxicity analysis of the three binary and ternary compounds, AME and AOH at ratios of 1:2, 1:3, and 1:5 showed some antagonistic effects at low cytostatic concentrations and synergistic and additive effects at high cytotoxic concentrations (Lin et al., 2023).

The study of Hollander et al., (2022) in HepG2 and Caco-2 cell lines also included AME with similar results as seen for AOH. Notably, in lower metabolically active HepG2 cells, AME exhibited stronger cytotoxic effects compared to its counterpart, AOH (Hollander et al., 2022). Grover et al., (2017) studied human bronchial epithelial cells (BEAS-2B) and mouse macrophage cells (RAW264.7) to assess the impact of the *Alternaria* mycotoxins alternariol (AOH) and alternariol monomethyl ether (AME) on innate immunity. Both AOH and AME suppressed LPS-induced immune responses in dose-response manner. Also, the aryl hydrocarbon receptor (AhR) did not appear to play a significant role in the immunosuppressive properties of AOH and AME, it seemed to contribute to the observed low levels of cell death in BEAS-2B cells, which indicates potential impact of AOH and AME on respiratory health (Grover et al., 2017)

1.3. Mycotoxins and the (innate) immune system

The immune system is a complex network of specialized cells, tissues, and organs that work together to defend the body against invading pathogens. The immune system is broadly categorized in innate immune system and adaptive immune system. The innate immune system is the first line of defense, which offers non-specific and immediate response against foreign invaders (Marshall et al., 2018). On the other hand, the adaptive immune system provides specific, long-lasting protection against pathogens by generating antigen-specific lymphocytes (B and T cells) that produce antibodies or directly target infected cells, with subsequent development of immunological memory, as exemplified by the robust secondary antibody response following vaccination (Alberts et al., 2002).

1.3.1. TLR activation

In mammals' immune system is highly complex, where Toll-like receptors (TLRs) are significant family of receptors that constitute the first line of defense system against pathogens and part of the innate immune system. TLRs can recognize PAMPs (pathogen-associated molecular patterns) which

includes lipopolysaccharides (LPS), lipoteichoic acid (LTA), and double- or single-stranded RNA (ds/ssRNA). These molecules are derived from microbes. TLR receptors can be found on the cell membrane, but also within intracellular vesicles or other cell compartments (El-Zayat et al., 2019). The binding of ligands to TLR stimulates specific intracellular downstream signaling cascades that initiate host defense reactions (Figure 1.4) (Wang et al., 2016).

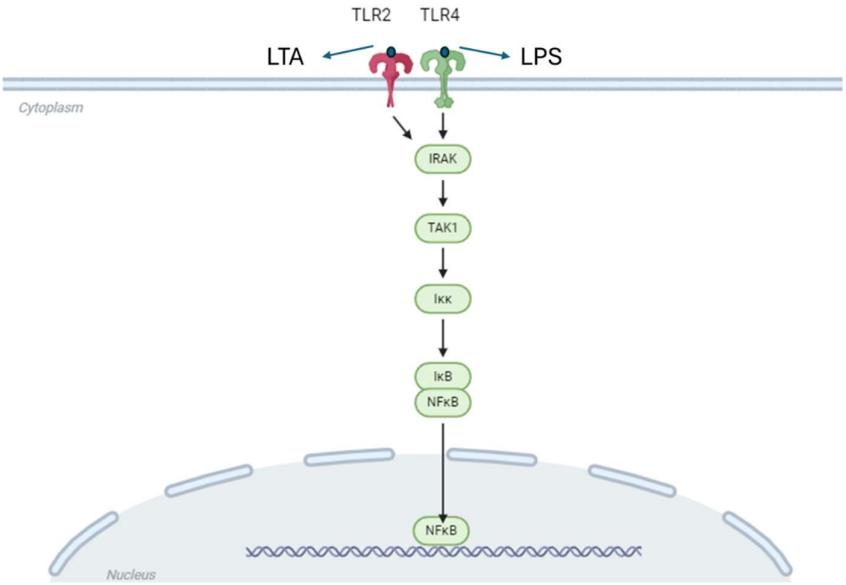

Figure 1.4: ***TLR signaling pathway; NF-κB activation*** *(BioRender.com). LTA and LPS binds to TLR2 and TLR4, respectivly which initiate the signal pathway activation cascade through IRAK: interleukin (IL)-1 receptor-associated kinases, TAK1: Transforming growth factor β-activated kinase 1, Ikk: inhibitor of nuclear factor-κB kinase, IkB: inhibitor of nuclear factor-κB and ultimatly NF-κB: nuclear factor kappa-B which in turn lead to transcription of different pro-inflammatory cytokines (IL -1β) (BioRender.com).*

All TLR family members, except TLR3, signal through myeloid differentiation primary-response gene 88 (MyD88) to activate downstream signaling pathways (Wang et al., 2011). Upon activation, MyD88 recruits interleukin (IL)-1 receptor-associated kinases (IRAKs) and tumor necrosis factor (TNF)-receptor associated factor 6 (TRAF6) (Takeda et al., 2004, Wang et al., 2011). This leads to the formation of the IRAK complex, phosphorylation of IKKα/β, and activation of transcription factors such as nuclear factor kappa B (NF-κB), interferon-β promoter-binding protein (IRF)1, and IRF7. Subsequently, this cascade results in the production of pro-inflammatory cytokines including interleukin (IL)-1β and IL-6 and tumor necrosis factor-alpha (TNF-α). (El-Zayat et al., 2019, Akira et al., 2004, Wang et al., 2011).

1.3.2. Inflammasome activation

The inflammasome is a crucial multiprotein complex that helps the innate immune system respond to danger signals like PAMPs and damage-associated molecular patterns (DAMPs) (Gu et al., 2023). Upon activation, it triggers inflammation by releasing cytokines like interleukin-1 beta (IL-1β) and interleukin-18 (IL-18) while inducing pyroptosis, an inflammatory form of cell death. This two-step activation process involves priming, where pattern recognition receptors (PRRs) like TLRs recognize danger signals, leading to the upregulation of components like pro-IL-1β (Li et al., 2021). In the second step, the inflammasome assembles with a sensor protein (e.g., NLRP3 or NLRC4), an adaptor (ASC), and pro-caspase-1. Active caspase-1 processes pro-IL-1β and pro-IL-18 into mature forms, while also triggering pyroptosis via gasdermin-D (Shi et al., 2015).

NF-κB plays a central role in this process by regulating pro-inflammatory cytokine expression (Li et al., 2021). NF-κB primes the cell for inflammasome activation, boosting the transcription of components like pro-IL-1β and NLRP3. Its activation often follows early pathogen detection by PRRs, thus providing essential groundwork for subsequent inflammasome assembly and immune response (McDaniel et al., 2020).

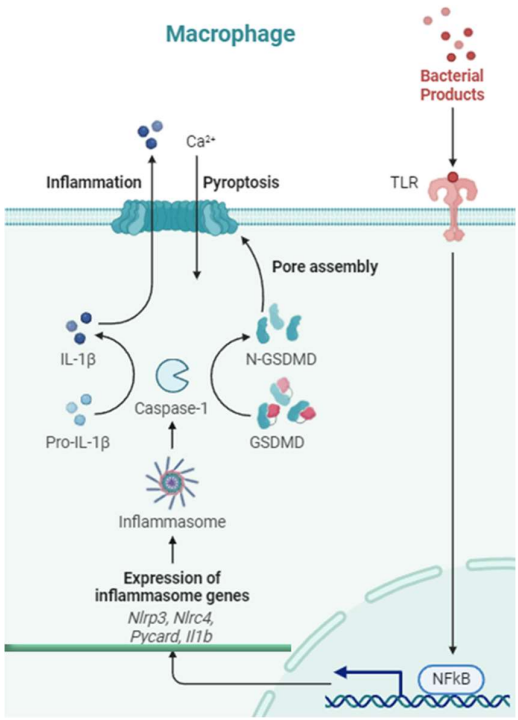

Figure 1.5: Inflammasome activation in macrophages, where NF-κB regulates pro-inflammatory cytokine expression. (BioRender.com).

1.4. Aim of the Study

1.4.1. Objective of the study

This research aim is to shed light on some of the intricate details of how Alternaria toxins may affect innate immune responses, focusing on receptor activation, inflammation induction, and signal transduction pathways. The primary objective is to evaluate the dose-dependent effects of AOH and AME on immune receptor signaling and inflammasome assembly in human cell models. The study's approach involves exposing LPS-stimulated HEK-293 TLR reporter cells and THP-1 immune cells to varying concentrations of mycotoxins. Understanding the nature and effects of *Alternaria* toxins is crucial for developing strategies to mitigate their impact on food safety and human health. The exploration of their diverse biological activities provides a foundation for assessing the risks associated with *Alternaria* toxin exposure.

1.4.1.1. Specific objectives of the study

- To elucidate the impact of AOH and AME mycotoxins on the Toll-like receptors (TLRs) signaling pathway, particularly focusing on their effects on the downstream NF-κB pathway.
- To characterize IL-1β response induced by AOH and AME in THP-1 immune cells.

1.4.2. Null hypotheses

- *Alternaria* toxins do not affect the signaling of immune receptors in human cell models.
- *Alternaria* toxins do not impact the activation of inflammasomes in human cell models.
- *Alternaria* toxins affect cell viability.

2. Materials and Methods

2.1. Model consideration

2.1.1. Cell lines

HEK-293 TLR reporter cell model was employed to explore the innate immune responses to *Alternaria* toxin exposure. This cellular model offers a versatile platform with the possibility to study different receptors, including TLR2 and TLR4. The HEK-293 reporter cells have transfected upregulation of specific TLRs, and intact downstream signaling pathways leading to NF-κB activation. In that way activation and modulation of the receptor and its signal pathway can be explored with minimal confounding factors, typically present in primary cells, allowing for the investigation of dose-dependent effects of toxins on TLR activation, and downstream response.

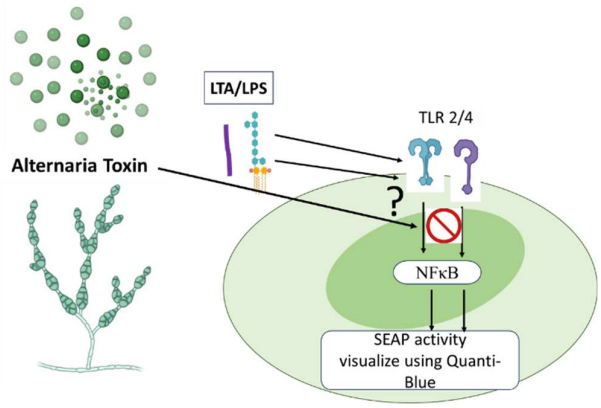

Figure 2.1: Possible toxins effecting on TLR activation (BioRender.com).

HEK null cells were used in the experiment to distinguish between specific and non-specific responses to the ligands. Null cells have endogen receptors, if no signals got from null cells mean that there is no signal from the endogen receptors. But HEK TLR4 and TLR2 cells are genetically modified to express TLR4 and TLR2, respectively. These receptors ligands like bacterial lipopolysaccharide (LPS) or Lipoteichoic acid (LTA) and respond by activating the NF-κB signaling pathway, leading to reporter gene expression (e.g., SEAP production). HEK-Blue Null cells are genetically similar to HEK TLR4 and TLR2 cells but lack the TLR4 and TLR2 gene. Therefore, they cannot respond directly to the ligand and will not activate the NF-κB pathway or induce the reporter gene even when exposed to the ligand. As a result, it is acceptable that there is no non-specific response due to the ligand interacting with other receptors or pathways which are not related to TLR4/TLR2.

The differentiated THP-1 cells were employed to investigate the effect of mycotoxin exposure on the inflammatory response, including the induction of cytokine production. This monocytic cells mimic key features of primary monocytes and macrophages, which are crucial players in the innate immune response and certain key immune functions like phagocytosis (Chanput, 2014) and cytokine production which make them suitable for studying inflammatory responses.

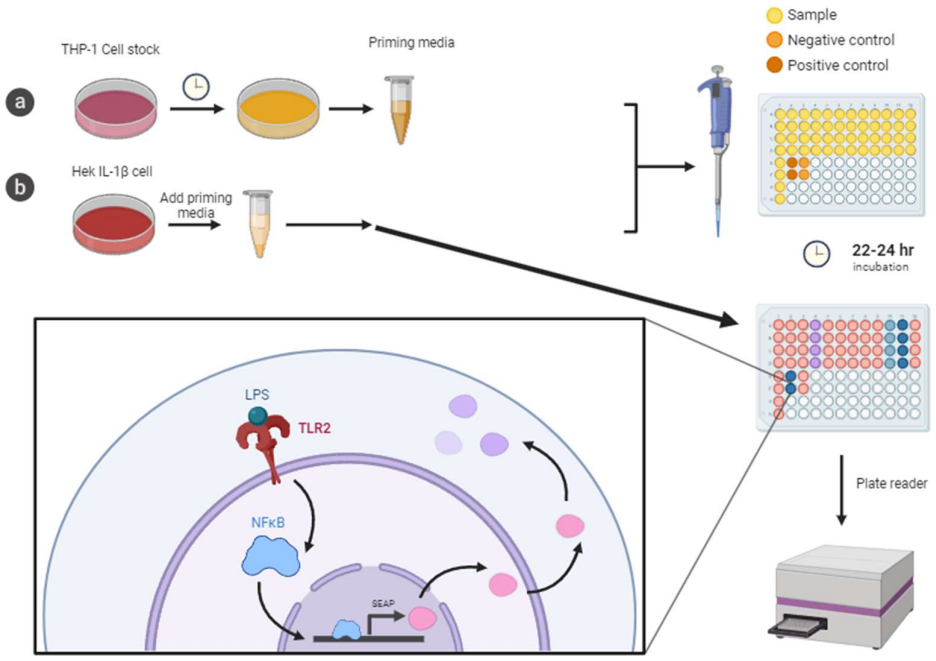

Figure 2.2: Two-step Assay; (a) THP-1 cell seeded for collecting priming media, (b) HEK IL-1β seeded for quantify IL-1β level in THP-1 inflammasome activation (BioRender.com).

The HEK-Blue™ IL-1β cells were used to quantify IL-1β level in THP-1 inflammasome activation assay. While THP-1 cells are valuable for studying inflammasome activation due to their ability to differentiate into macrophage-like cells and express inflammasome components, they might not be ideal for specifically measuring IL-1β production. Inflammasome activation can lead to the secretion of other cytokines besides IL-1β. On the other hand, HEK IL-1β cell is a specific tool for quantifying IL-1β levels. These cells are genetically modified to express a SEAP reporter gene under the control of an NF-κB responsive promoter. The THP-1 cells stimulated and secreted IL-1β, which binds to receptors on the HEK IL-1β cells and activate the NF-κB pathway. This activation triggers the expression of the SEAP reporter gene which enzyme activity can be measured by using QuantiBlue assay.

Both cell lines offer a comprehensive approach with HEK-293 cells providing specific insights into TLR activation and THP-1 cells providing a broader picture of the inflammatory response in a relevant cell type with the help of HEK IL-1β cells.

2.1.2. Assays

The experimental design incorporates various assays to dissect the impacts of *Alternaria* toxins on immune responses. alamar-Blue, a reliable indicator of cellular viability and proliferation, is employed to assess the cytotoxic effects of mycotoxin exposure. almar-Blue uses colorimetric or fluorescent reading to quantify cell viability. This cell viability indicator functions by utilizing resazurin, a non-fluorescent blue compound, which readily permeates living cells (Rampersaud, 2012). Metabolically active cells possess reductases, particularly within the mitochondria and cytoplasm (O'Brien et al., 2000). These enzymes accept electrons generated through cellular respiration and reduce resazurin to resorufin, a pink and highly fluorescent molecule. The quantity of resorufin produced directly correlates with the number of viable and metabolically active cells present within the culture (Longhin et al., 2022).

QuantiBlue assays are utilized for the detection and quantification of SEAP (secreted embryonic alkaline phosphatase) activity which in the mentioned HEK blue receptor cells serves as a reporter for TLR signaling and NF-κB (nuclear factor kappa-light-chain-enhancer of activated B cells) activation (Figure 1.4). NF-κB is a key transcription factor involved in inflammatory gene expression.

In general, ELISA is used for detecting and quantifying specific substances such as peptides, proteins, antibodies, and hormones. Here we used the sandwich ELISA to measure the levels of specific pro-inflammatory cytokines secretion. Here we looked at the change in (IL-1β) secretion by THP-1 cells upon exposure with AOH and AME. This will provide a more detailed picture of the effect of these mycotoxins on the inflammatory response triggered by selected microbial components (LPS and LTA). Also, Two-Step Inflammasome Activation Assay with HEK IL-1β cells is used to specifically measure the secretion of bioactive IL-1β, a hallmark of inflammasome activation. This will help determine how *Alternaria* toxins impact on the role of the inflammasome. In Sandwich ELISA involves adhering a capture antibody to microtiter plate, which selectively captures the target antigen from the sample. A detection antibody conjugated with biotin is introduced then which binds to another epitope on the antigen, forming a “sandwich” with capture antibodies. Streptavidin-HRP then binds with biotin. This enzyme then acts on a chromogenic substrate, producing a color change that directly correlates with the antigen's concentration in the sample (Optofluidic Bioassay, 2021).

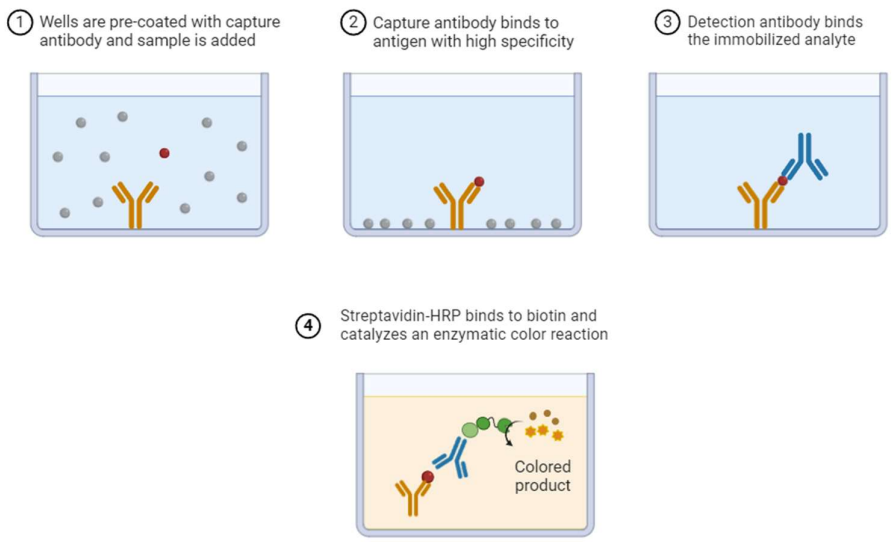

Figure 2.3: Steps of Sandwich ELISA (BioRender.com).

Quantitative Polymerase Chain Reaction (qPCR) is a significant tool used for quantifying gene expression. qPCR is sensitive, specific and with accurate quantification capabilities as well as reproducible. In this study cytokines IL-1β quantified as gene expression using fluorescent dye-Based qPCR. As the expression of cytokines in cells is often low under basal conditions, that is why qPCR is used here because of its high sensitivity. Even small changes in mRNA abundance can be detected and quantified with qPCR. In the fluorescent dye-Based qPCR, SYBR Green is used as DNA binding fluorescent dye. The Dye exhibits minimal background fluorescent prior to binding with DNA. During the amplification, this dye binds to the Double –stranded DNA products in the samples, which lead to a measurable increase in fluorescence. This increase correlates directly with the amount of PCR amplicons generated during each cycle. Fluorescence levels are assessed following each cycle of PCR. The quantification cycle (Cq), also known as the threshold cycle (Ct), signifies the cycle at which the fluorescence due to the dye binding surpasses the background levels. The Ct value is crucial for determining the quantity of target DNA in the sample; a lower Ct value indicates a higher initial concentration of target DNA (Solis BioDyne, 2023).

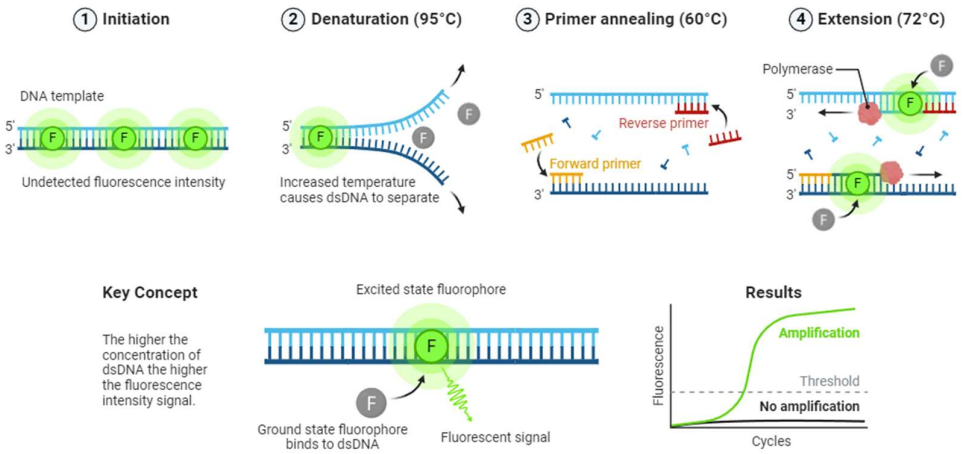

Figure 2.4: Fluorescent Dye-Based qPCR (BioRender.com).

2.2. Study set-up

2.2.1. Cell cultures

The HEK cell lines used in these experiments were procured from Invivogen Toulouse, France. The THP-1 cell line was from ATCC. These cells (Table 2.1) were expanded and cryopreserved at the National Institute of Occupational Health (STAMI) in Norway. The cells are stored at -195.8°C in a nitrogen vapor phase freezer, following the specified protocols for freezing.

Table 2.1: Cell lines used in this study and their specificity.

Cell line	Specificity	Assay used	Endpoint
HEK-Blue Null 1 (Invivogen #hkb-null1)	Parental cell used for TLR2 and TLR4	QuantiBlue alamar-Blue	NF-κB activation, Viability
HEK-Blue hTLR2 (Invivogen #hkb-htlr2)	Responds to TLR2 stimulation by activating the NF-κB signaling pathway	QuantiBlue alamar-Blue	NF-κB activation, Viability
HEK-Blue hTLR4 (Invivogen #hkb-htlr4)	Responds to TLR4 stimulation by activating the NF-κB signaling pathway	QuantiBlue alamar-Blue	NF-κB activation, Viability
HEK-Blue hIL-1β (Invivogen #hkb-il1bv2)	Responds to IL-1β stimulation by activating the NF-κB signaling pathway	QuantiBlue alamar-Blue	NF-κB activation, Viability
HEK-Blue Null-1v (Invivogen #hkb-null1v)	Parental cell used for Hek IL-1β	QuantiBlue alamar-Blue	NF-κB activation, Viability
THP-1	Differentiate into macrophage-like cells; mimic the behavior of primary human monocytes and macrophages, for studying immune responses, cytokine production.	alamar-Blue ELISA qPCR	Viability Cytokine secretion Gene expression

For all cell cultures, a foundational medium composed of Modified Eagle Medium (DMEM; Fisher Scientific #31966-021), for HEK-293 cells, or Roswell Park Memorial Institute 1640 Medium (RPMI; Gibco #21875-034), for THP-1, was used along with 10% ultra-low endotoxin fetal bovine serum (FBS; Biowest #S1860). The FBS was heat-inactivated (see 2.1.1) before added to the medium DMEM/RPMI. This supplemented medium will from now on be referred to as the complete cell medium (CCM). In the case of HEK-293 cells, they were cultured in DMEM-CCM supplemented with antibiotics and for THP-1 cells cultured in PRMI-CCM supplemented with antibiotics (Table 2.2).

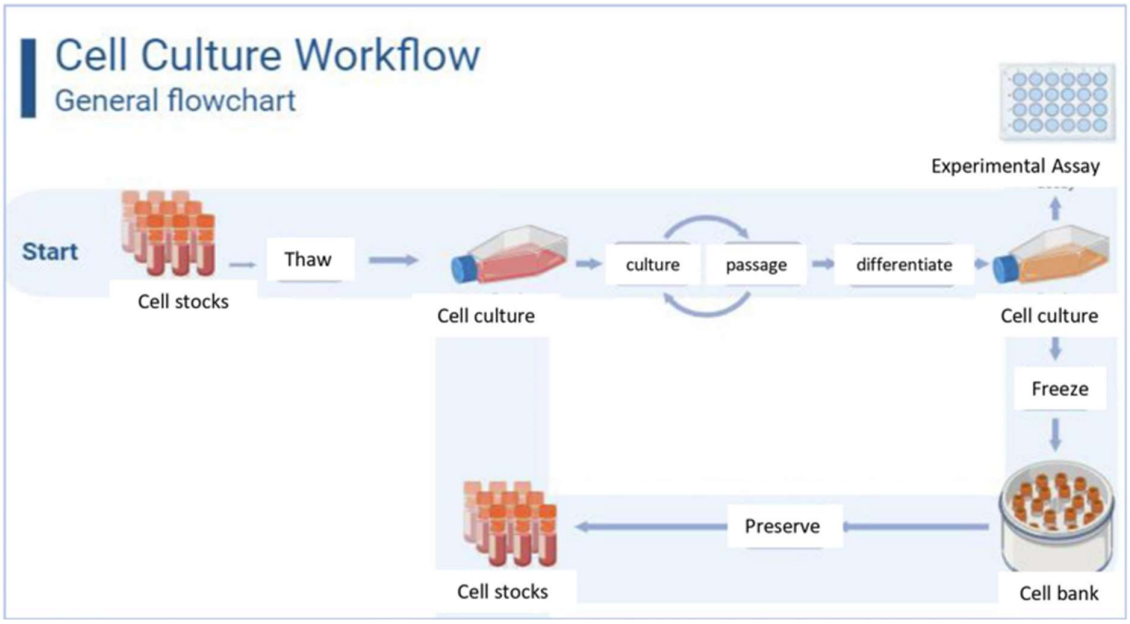

Figure 2.5: Flowchart of Cell Culture (adopted from biorender.com).

2.2.1.1. Heat inactivated FBS

Heat inactivated FBS is a common reagent in cell culture lab to provide essential nutrients, growth factors, and hormones to support cell growth. It is used in cell culture media to supplement basal media to provide suitable environment for cell growth. This heat inactivation process is necessary to reduce the biological activity of complement proteins, which can otherwise cause cell lysis. This is particularly important when working with cell lines or primary cells that are sensitive to complement-mediated cytotoxicity. FBS is heated in water bath at 56℃ ± 2℃ for 45 minutes along with another flask only containing water with a thermometer to control the temperature in the liquid. After heat inactivation, the FBS is sterile filtered to remove any potential contaminants and transferred into 50 ml vials for further use.

2.2.1.2. HEK-293 TLR reporter cell and HEK-Blue IL-1β cell culture

HEK-293 (HEK) reporter cells, specifically Null 1 (Invivogen #hkb-null1), hTLR2 (Invivogen #hkb-htlr2), hTLR4 (Invivogen #hkb-htlr4), and HEK-Blue hIL-1β (Invivogen #hkb-il1bv2), HEK-Blue Null-1v (Invivogen #hkb-null1v) purchased from Toulouse, France were initially expanded and stored in nitrogen freezer as per manufacturer's instructions. For experiment initiation an ampoule was derived from the nitrogen freezer at STAMI. These cells underwent rapid defrosting, were diluted in warm supplemented DMEM, and subsequently centrifuged at 1.2 rpm for 5 minutes. The resulting pellet was resuspended in 2 mL of complete fresh medium, and the cell suspension was transferred to a culture flask containing 10 mL complete fresh medium.

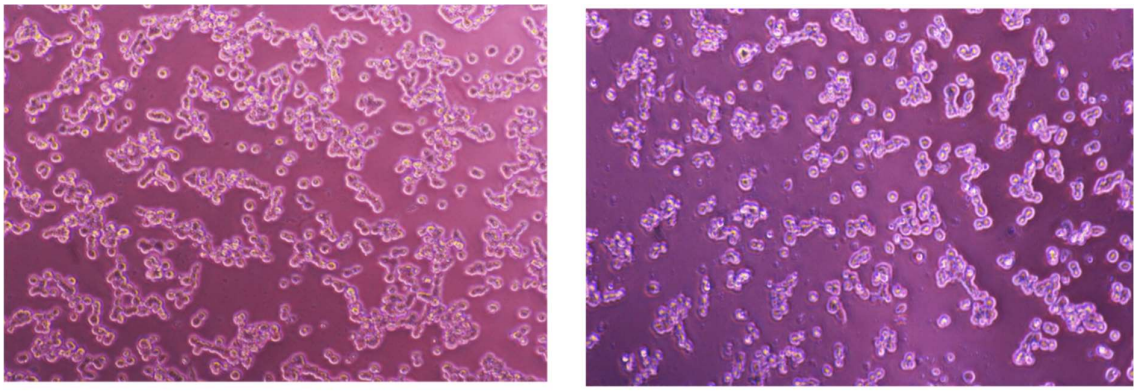

Figure 2.6: Cultures of HEK-293 TLR reporter cell (a) HEK TLR 2 cells and (b) HEK TLR 4 Cells.

HEK cells were passaged when 70-80% confluence, approximately every 2-3 days of growth, the cells were rinsed in PBS 2-3 times followed by dissociation 1 ml PBS by gentle tapping the side of the flask. The detachment of cells was consistently confirmed using a light microscope (Echo Inc., San Diego, USA). Once cells were detached, 5 mL supplemented DMEM was added. Cell viability, concentration, and diameter were documented using an automated cell counter (NucleoCounter NC-200^{TM}, Gydevang, Denmark) further described under point 2.1.4. During subculturing, the cells were seeded at a dilution ranging from 1:2 to 1:5 for HEK, depending on confluence and variant. Assays were initiated by seeding cells at a concentration of 5.6×10^5 viable cells/ml (~50×10^3 cells/well) in 96-well plates. Each dilution of the culture was counted as one passage, with a maximum limit of 20 passages used for the experiment.

Table 2.2: Antibiotics supplements used for HEK variants medium.

HEK- 293 null	HEK- 293 hTLR2/hTLR4	HEK- hIL-1β/ HEK- Null-1v
100 U/mL Penicillin 100 µg/mL Streptomycin 100 µg/mL Normocin		
100 µg/mL Zeocin	1x HEK-Blue selection	100 µg/mL Zeocin

2.2.1.3. THP-1 cell culture

THP-1 monocyte cells were initially derived from an ampoule stored in a nitrogen freezer at STAMI. The cell ampoule was quickly thawed by gentle agitation in the water bath at 37°C. As soon as the content was thawed, it was transferred to a larger tube containing 5ml of pre-warmed complete growth medium (PRMI-1640 + 10 % FBS and 1 % penicillin-streptomycin). Then cells were centrifuged at 1.1 rpm for 5 minutes. Remove the supernatant containing the freezing agent and resuspend the cell pellet in 2ml fresh complete medium. Then cell suspension was transferred to a culture flask (Corning® T-75 flasks arstedt #83.3911.502) containing 10 mL supplemented RPMI.

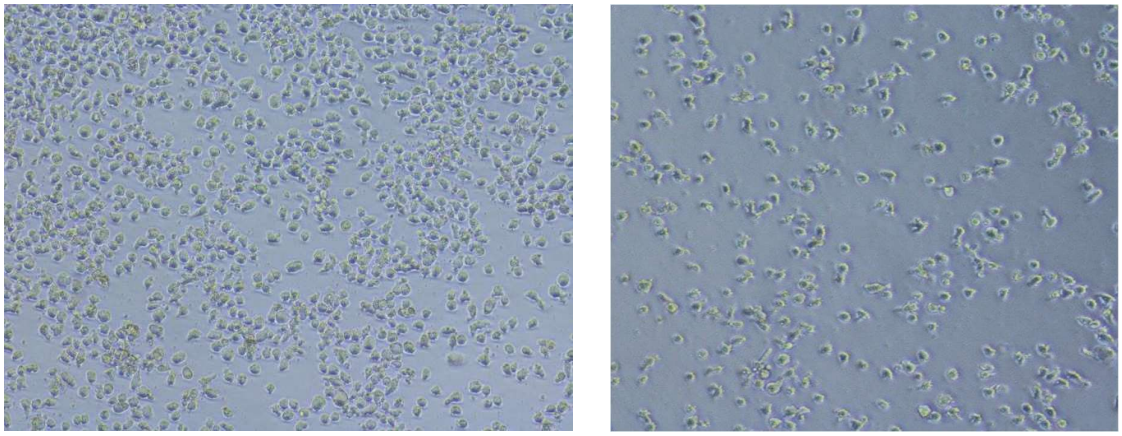

(a) (b)

Figure 2.7: THP-1 Cells (a) before differentiation and (b) after differentiation (magnification 10x).

THP-1 cells are grown as suspension and cultures can be maintained by introducing new media or exchanging the existing media within 2 or 3 days. Subculturing was done when the cell concentration reached 8×10^5 cells/mL, with caution against allowing the cell concentration to surpass 1×10^6 cells/ml. Corning® T-75 flasks (Sarstedt #83.3911.502, Nümbrecht, Germany) flasks were used for subculturing.

For differentiation of THP-1 cells, cells were firstly spun down 1.1 x 1000 rpm for 5 minutes, counted and 800 000 cells/ml were seeded in a T-75 flask (Sarstedt #83.3911.002) together with a final

concentration of 50 ng/ml PMA for 72 h. After the differentiation period the cells become adherent, and the media was easily changed for new fresh media without PMA for a 24 h rest period before seeding for experiment. Assays were initiated by seeding cells at a concentration of 250000 cells/well in 24-well plates.

Table 2.3: Antibiotics supplements used for THP-1 variants medium.

THP-1 Cell
RPMI-1640
10% FBS
1% Penicillin-Streptomycin

2.2.1.4. Cell count

Cell viability, concentration, and diameter of HEK and THP cell lines were assessed using an automated cell counter (NucleoCounter NC-200^{TM}). For HEK-293 reporter cells sample, 20 µL cell suspension was diluted with 380 µL PBS while for THP-1 cells 200 µL cell sample was taken. Then 60 µL of diluted sample was loaded into disposable counting slide, Cassette (Via1-Cassette^{TM}, Chemometec #941-0011) and inserted into the cell counter. The cell counter captured high-resolution images of the cells in the chamber. Then a state-of-the-art image cytometry cell counter was used to identify individual cells by factors such as size, shape, and viability. Each cassette carries an individual dot-code indicating the exact volume of its counting chamber, which is read by the NucleoCounter® to calculate the exact cell concentration. The total volume of analysis within the counting chamber is approximately 1.4 µl.

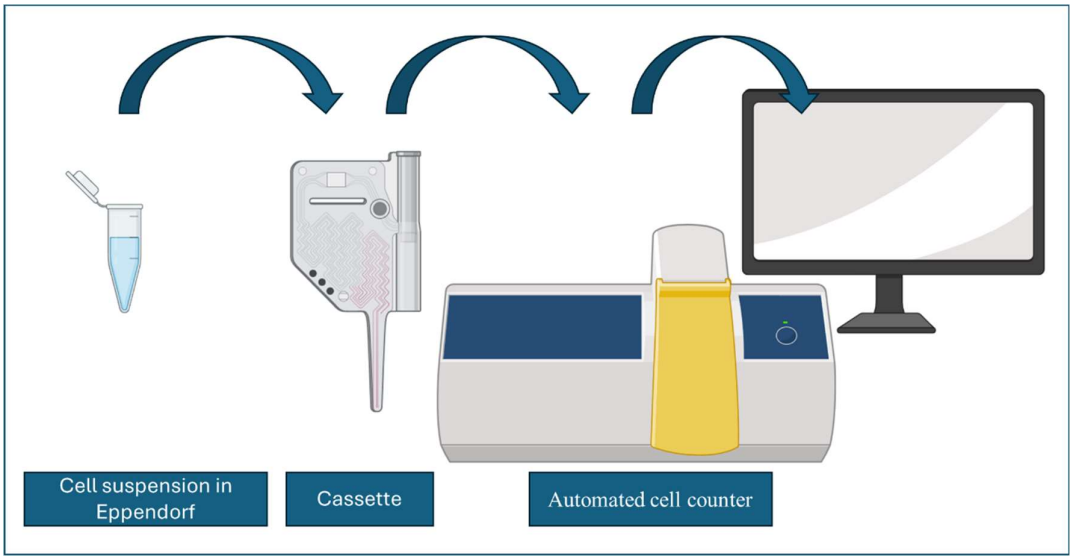

Figure 2.8: Visual representation of cell counting method (BioRender.com).

2.2.2. Mycotoxin preparation

To dilute the received amount of AOH, AME 5 mg of each, 645.5 µL and 1.836 ml DMSO was added respectively, to reach a stock dilution of 7.75 mg/ml = 30µM (AOH) and 2.72 = 10µM (AME) (Table 2.4). The stock solution was vortex for 1 minute followed by sonication in water bath for 15 min, to ensure homogenous solution.

Table 2.4: Calculation for mycotoxin (AOH and AME) preparation.

Name	**Mw**	**UNIVIE stock (mM)**	**UNIVE stock (mg/ml)**	**Amount received**	**DMSO to add for UNIVIE stock suggestion (calculation)** $\frac{g}{g/mol} = \frac{mol}{mol/l}$
Alternariol (AOH)	258.2	30µM	7.75	5	0.005g/258.2 (g/mol) = 0.01936x 10^-3 (mol) 0.01936x 10^-3 (mol)/0.03(mol/l) = 0.64549 x 10^-3(l)= 645.5µl
Alternariol monomethyl ether (AME)	272.3	10µM	2.72	5	0.005g/272.3 (g/mol) = 0.01836x 10^-3 (mol) 0.01836x 10^-3 (mol)/ 0.01(mol/l) =1.836 x 10^-3(l)= 1.836ml

After sonication, the solutions were aliquoted into sterile tubes wrapped in tinfoil to prevent light, with the necessary information such as mycotoxin name, concentration and date. Based on the experimental set ups a working stock volume of 20µL for each was chosen. Then the aliquots were stored in -20°C for further use.

2.2.3. Test sample preparation

For all calculations of sample preparation, equation 1 was used

$$C_1xV_1 = C_2xV_2 \quad (1)$$

$$V_1= (C_2xV_2)/ C_1 \qquad (2)$$

Here:

C_1= Initial concentration

C_2= Final concentration

V_1= Initial volume (volume take out of substance)

V_2= Final volume (volume using for experiment)

2.2.3.1. Preparation of 0.1% DMSO in cell media

As described in section 2.2. *mycotoxin preparation*, the mycotoxins are diluted in 100% DMSO. Different concentrations of DMSO were tested in HEK cells (0.05%, 0.1%, 0.2%, 0.4%, 0.8%, 10 %) to test the toxicity of DMSO on cell viability. After this viability test, it was decided to consider 0.1% DMSO as an acceptable concentration, also supported by literature. For the preparation of media with the chosen DMSO concentration equation 1 was used.

2.2.3.2. Preparation of mycotoxin in cell media

The mix of mycotoxin (AOH or AME) and cell media was prepared by pipetting cell media suspension and different concentrations of mycotoxins, using equation 1. The highest concentration was prepared, and then it was gradually diluted to the lowest concentration. The highest concentration of AOH is 30µM and then the other concentrations (6µM, 1.2µM, 0.24µM) were prepared by 1:5 serial dilution.

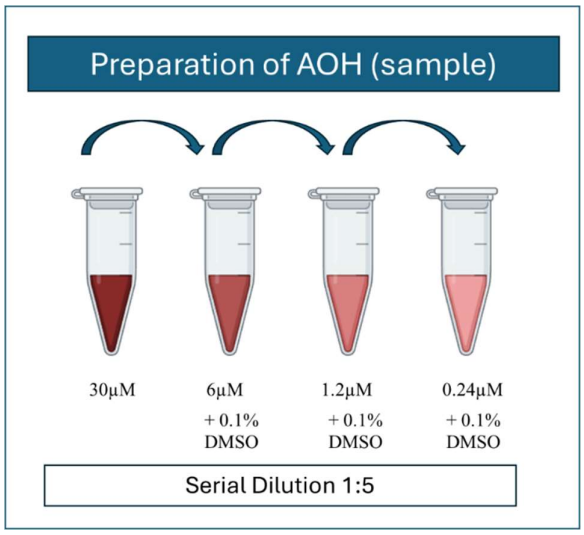

Figure 2.9: Visual representation of AOH preparation as samples (BioRender.com).

Alongside, the highest concentration of AME is 10µM and then the other concentrations (2.5µM, 0.625µM, 0.156µM) were prepared by 1:4 serial dilution. DMSO 0.1% media was used to dilute and make the required concentrations. Addition of DMSO to reach a concentration of 0.1% in each dilution was used to maintain equivalency of each test sample.

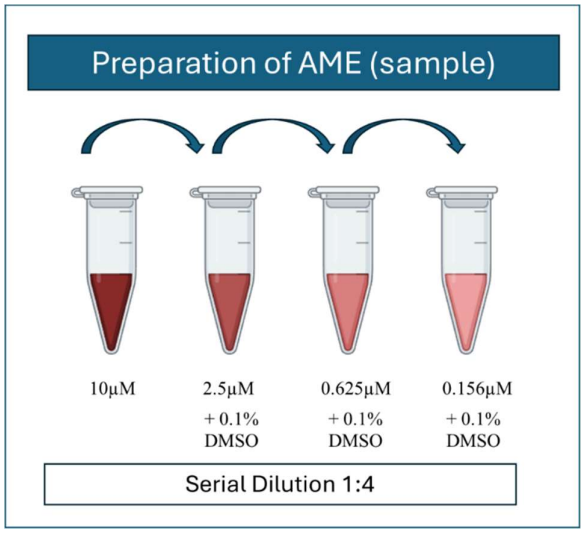

Figure 2.10: Visual representation of AME preparation as samples (BioRender.com).

2.2.3.3. Addition of TLR2 and TLR4 agonist LTA and LPS respectively

For each concentration of mycotoxin, as seen in Figure 2.5 and 2.6 a small aliquot of the diluted sample was taken into two separate test tubes. Subsequently, LTA or LPS were added to the tubes, resulting in final concentrations of 100 ng/ml and 10 ng/ml, respectively, in the samples.

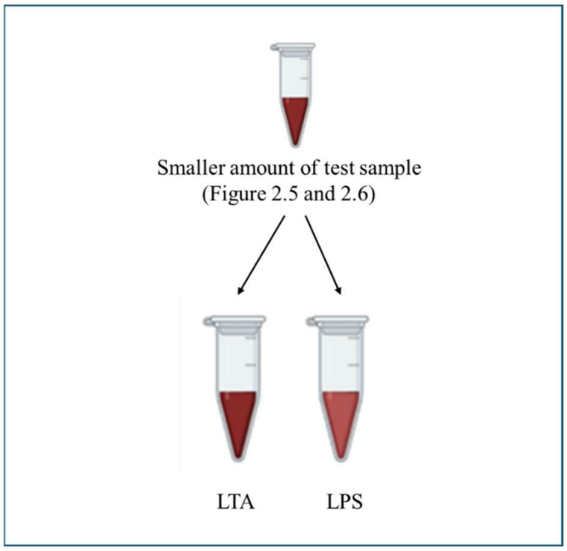

Figure 2.11: Visual representation of addition of TLR2 and TLR4 agonist LTA and LPS, respectively, as samples (BioRender.com).

In all the alarmarBlue™ cell viability assay, 10% DMSO was used as negative control.

Table 2.5: Summary of test compounds, their concentration and endpoint measured.

Test Compound	**Concentrations of mycotoxins (µM)**	**LPS/LTA**	**Endpoint**
AOH + media	30, 6, 1.2, 0.24	---	NF-κB activation, Viability
AME + media	10, 2.5, 0.625, 0.156	---	NF-κB activation, Viability
AOH + media + LTA	30, 6, 1.2, 0.24	100ng/ml	NF-κB activation, Viability
AME + media + LTA	10, 2.5, 0.625, 0.156	100ng/ml	NF-κB activation, Viability
AOH + media + LPS	30, 6, 1.2, 0.24	10ng/ml	NF-κB activation, Viability
AME + media + LPS	10, 2.5, 0.625, 0.156	10ng/ml	NF-κB activation, Viability
DMSO 0.1% + media	---	---	NF-κB activation, Viability
0.1% DMSO + media + LTA	---	100ng/ml	NF-κB activation, Viability
DMSO 0.1% + media + LPS	---	10ng/ml	NF-κB activation, Viability
DMSO 10% + media	---	----	Viability

2.2.4. Cell viability assay

alamar-Blue was employed to assess the potential impact of the test compounds on cellular viability by gauging alterations in metabolic activity. This assay utilizes resazurin dye to assess the metabolic activity of the living cells, where living cells reduce the blue nonfluorescent to pink, fluorescent resorufin. The experimental protocol, developed following literature and manufacture protocol, involves seeding 90 microliters of cell suspension at a concentration of 5.6×10^5 cells/ml into each well of a standard 96-well plate. Before the exposure of test materials, cell cultures were incubated in a 5% CO2 humidified atmosphere at 37°C for 24 hours.

10% DMSO was prepared from the 100% DMSO as a test sample (negative control) in the alarmarBlue^{TM} viability assay. The total amount of media for each well was calculated, according to this calculation 10% DMSO was prepared. As instance the calculated media was 90µL in each well, then 10µL of DMSO was added from 100% FBS to make 10% DMSO. The viability assay was used for HEK cells (HEK-Blue Null, TLR2 and TLR4) and THP1 cells. The viability assay was conducted slightly differently in the two cell types, as detailed below.

2.2.4.1. HEK cells

Following the first 24 hours incubation period, each well received 10 µL of samples, controls, or blanks. Subsequently, the plate underwent an additional 24-hour incubation at 37°C in a humidified atmosphere with 5% CO2. After this incubation, 10 µL of alamar-Blue (Fisher Scientific #DAL1025) was added to each well, and the plates were further incubated in a 5% CO2 humidified atmosphere at 37°C for 4 hours. Before fluorescence measurements, 100 µL of supernatant was transferred into a black 96-well plate (Sarstedt #1969002). Fluorescence intensity was then measured in the supernatant using a microplate reader at 560 nm excitation and 590 nm emission.

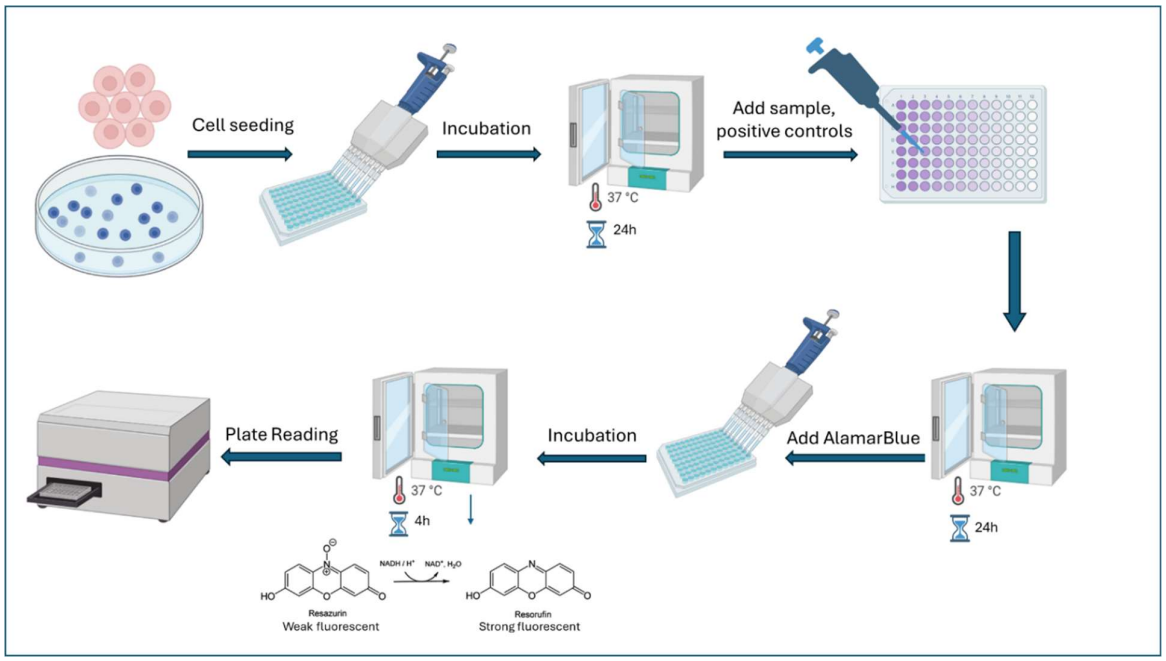

Figure 2.12: Visual representation of Cell Viability assay in HEK cells (BioRender.com).

To enhance reliability, the entire experiment was conducted three times (biological replicates), and each treatment was repeated three times in each biological replicate. The fluorescence data were meticulously adjusted for background and subsequently normalized to the untreated cell controls (Positive Control; DMSO 0.1%).

2.2.4.2. THP-1 cells

For THP-1 cells 300 microliters of cell suspension at a concentration of 200 000 cells/well into a 48-well plate (thermoscientific #136101, Waltham, USA). Before exposure to test materials THP-1 cell cultures were incubated in a 5% CO2 humidified atmosphere at 37℃ for 24 hours. After 24 hours of incubation, the suspended media from each well were aspirated, and then the cells received 300 µL of samples or controls with media and were incubated for additional 24-hours. Following the incubation period, the cell media was collected and stored in ampules at -80℃ for further experiments (for ELISA and two-step assays) and 10% of alamar-Blue(Fisher Scientific #DAL1025) was added with new media to each well. The plates were further incubated for 4 hours. Fluorescence intensity was measured using a microplate reader at 560 nm excitation and 590 nm emission, but before that 100 µL of supernatant was transferred into a white 96-well plate (thermoscientific #136101) to read the signal in microplate reader.

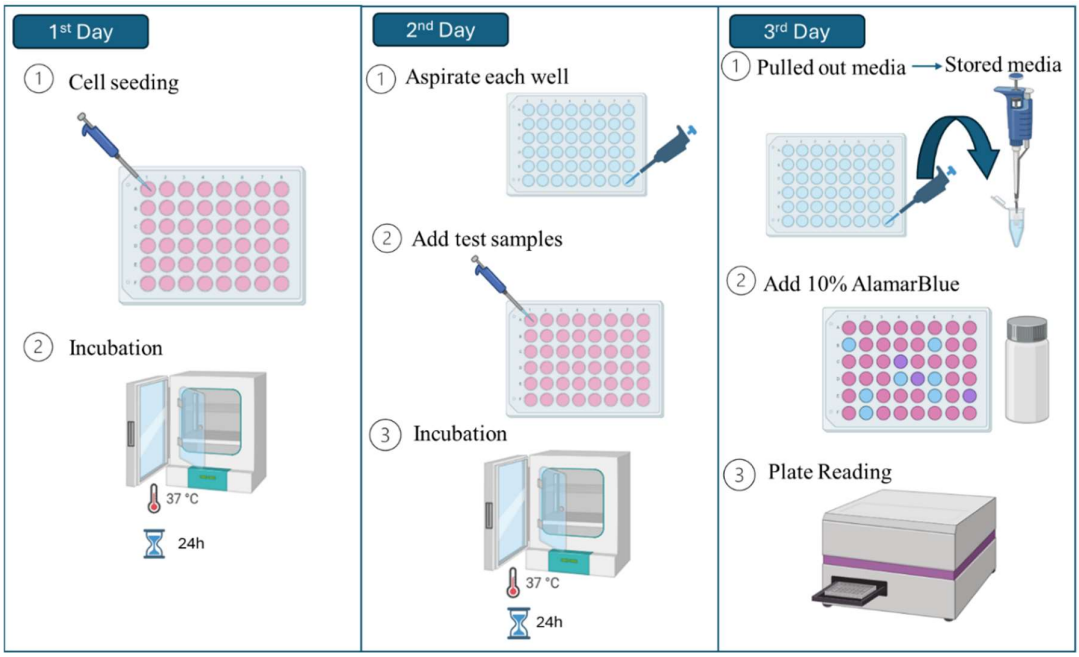

Figure 2.13: ***Visual representation of Cell Viability assay in THP-1 cells****; 1st day: 1; cells were seeded, 2; incubated for 24h, 2nd day: 1; aspirated each well, 2; exposure agents were added 3; incubation of cells with exposure material, 3rd day: 1; The supernatant was pulled out and stored for further use, 2; media with 10% alamar-Blueadded and incubated for 4 hours, 3; before read signal in supernatant. (BioRender.com).*

2.2.5. Detect and quantify SEAP activity to see NF-κB pathway activated

QuantiBlue was utilized to detect SEAP activation for its high sensitivity and convenience. This assay incubates the sample with a ligand specific for the activated state of the enzyme and then detects the enzyme-ligand complex formation using a labeled reagent that binds to the ligand. So, When TLR2/TLR4 ligands are present in the samples exposed to cells, the development of a blue color in the plate after adding Quantiblue indicates the activation of NF-κB and AP-1 pathways, leading to the induction of the SEAP gene. This color change occurs as a result of SEAP activation, reflecting the activation of NF-κB through TLR signaling. SEAP serves as a reporter gene demonstrating TLR activation, while Quantiblue acts as a detection reagent for SEAP activity, providing a functional readout of TLR binding and activation. The intensity of the blue color correlates with the amount of TLR ligands present, illustrating the level of TLR activation in the samples (Stierschneider et al., 2023).

The current methodology outlined in this thesis is adjusted from the procedure detailed by Brummelman et al. in 2015. Ninety microliters of HEK-Blue cells (Null, hTLR2, and hTLR4) at a concentration of 5.6×10^5 cells/ml suspended in CCM with antibiotics, were dispensed into each well of a standard 96-well plate. The plate was then incubated for 24 hours in a humidified atmosphere with 5% CO2 at 37℃. Subsequently, the cells were exposed to 10 µL of samples, positive controls, and

blanks. The positive control included a TLR4 ligand, ultra-pure Lipopolysaccharides from *Escherichia coli* K12 (LPS; Invivogen #tlrl-peklps), and a TLR2 ligand, purified Lipoteichoic Acid from *Staphylococcus aureus* (LTA; Invivogen #tlrl-pslta). The plate underwent an additional 24-hour incubation at 37°C in a humidified atmosphere with 5% CO2.

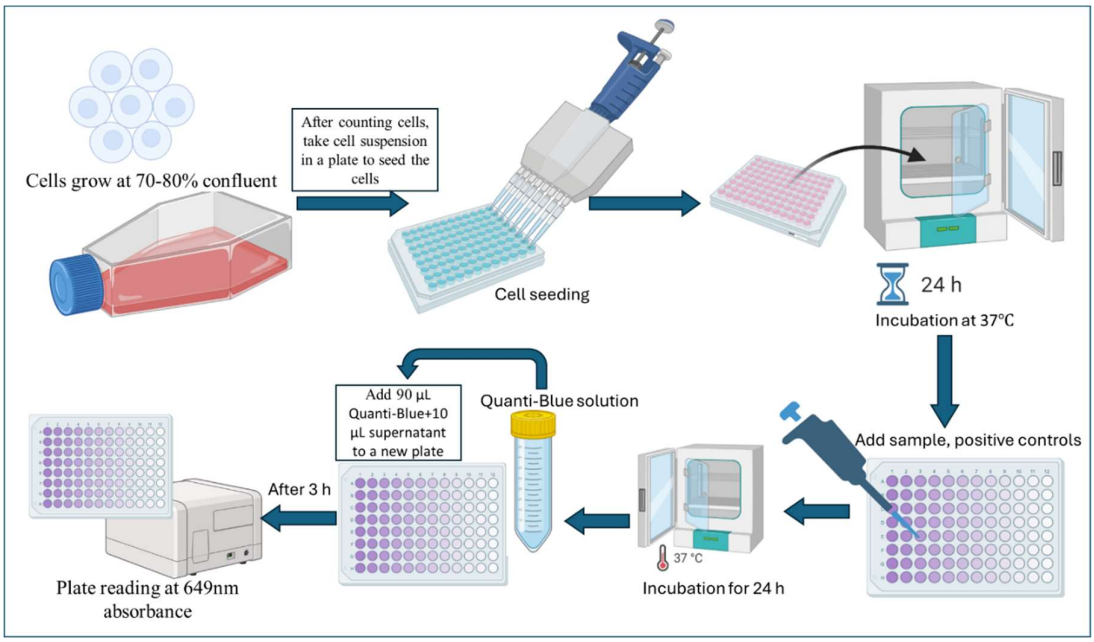

Figure 2.14: Visual representation of SEAP activity method (BioRender.com).

Following the incubation period, 10 µL of supernatant from the exposed cells was transferred to a new 96-well plate (Sarstedt #83.3924), and 90 µL of QuantiBlue solution (Invivogen #rep-qbs2) was added. After 3 hours of further incubation at 37°C in a humidified atmosphere with 5% CO2, the plate was read using absorbance at 649 nm in a microplate reader (Agilent, BioTek Gen5, Santa Clara, USA). Each treatment in the experiment had 3 replicates (technical replicates) and the entire experiment was independently conducted three times (biological replicates). For data analysis, absorbance values were normalized to untreated cell controls (Positive Control; DMSO 0.1%). The entire experiment was repeated thrice for robustness and consistency.

2.2.6. THP-1/HEK-Blue IL-1β inflammasome activation assay

THP-1 cells are commonly used in inflammation activation experiments/assays as it can be differentiated into macrophage-like cells and express functional inflammasome components, including NLRP3 (NOD-like receptor family, pyrin domain-containing 3), ASC (apoptosis-associated speck-like protein containing a CARD), and caspase-1. Also, Inflammasome inducers like Nigericin, MSU crystals, Alum Hydroxide, Poly(dA:dT), LPS, and E. coli OMVs stimulate these cells to produce IL-1β (Schmid-Burgk, 2015). The inflammasome activation assay is a two-step activation model, where

the 1st step is priming, and the other step is activation. In this experimental set up priming has been done before (see 2.5.2).

150 microliters of Hek IL-1β cell suspension were seeded at a concentration of 3.33×10^5 cells/ml into each well of a standard 96-well plate. Then 50 µl supernatant from prime and activated THP-1 cells (THP-1 supernatant mentioned in 2.5.2) was added in each well as test sample and the recombinant human IL-1β at 0.25 µg/ml (50 µl) was added as positive control. Then the cell cultures were incubated in a 5% CO2 humidified atmosphere at 37°C for 24 hours.

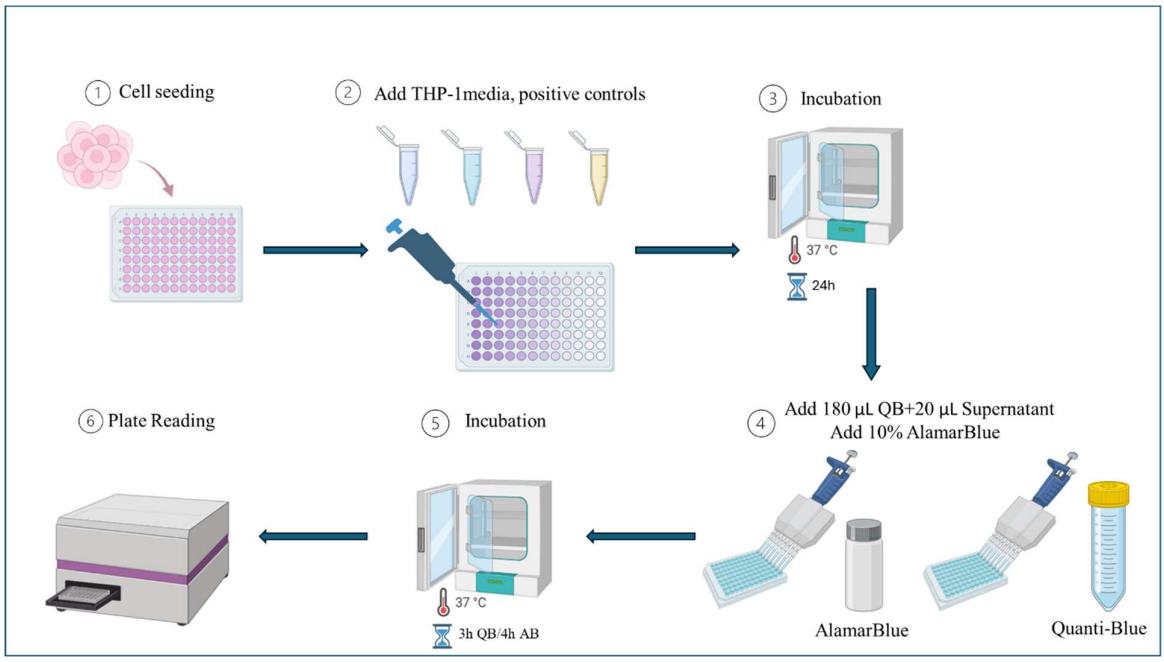

Figure 2.15: ***Visual representation of THP-1/HEK IL-1β inflammasome activation assay.*** *1; HEK IL-1β sensor cells were seeded, 2; supernatant from THP-1 were added, 3; incubation of cells with exposure material, 4; 20 µl media was transferred for QuantiBlue assay, 10% alamar-Bluewas added to the remaining cell media, 5; both assays were incubated for 3 h, 6; before results were collected. (activation) (BioRender.com).*

Following the incubation period, 20 µL of supernatant from the exposed HEK cells was transferred to a new 96-well plate (Sarstedt #83.3924), and 180 µL of QuantiBlue solution (Invivogen #rep-qbs2) was added. After 3 hours of further incubation at 37°C in a humidified atmosphere with 5% CO2, the plate was read using absorbance at 649 nm in a microplate reader (Agilent, BioTek Gen5, Santa Clara, USA). Alongside 10 µL of alamar-Blue (Fisher Scientific #DAL1025) was added to each well, and the plates were further incubated in a 5% CO2 humidified atmosphere at 37°C for 4 hours. Before fluorescence measurements, 100 µL of supernatant was transferred into a white 96-well plate (thermoscientific #136101). Fluorescence intensity was then measured using a microplate reader at

560 nm excitation and 590 nm emission. Each treatment in the experiment had 3 replicates (technical replicates) and the entire experiment was independently conducted three times (biological replicates).

2.2.7. ELISA for quantification of IL-1β

ELISA (Enzyme-linked immunosorbent assay) is used for quantifying IL-1β, due to its sensitivity and ability to detect small amounts, such as picogram (pg) per ml range. ELISA is suitable for quantifying low-level expressions or changes in response to stimuli. For quantifying IL-1β, Human IL-1β DuoSet ELISA kit (Biotech (R & D) #5 DY201) was used. The DuoSet ELISA Ancillary Reagent Kit 2 (Biotech # DY008B) was used for microplates, buffers, and substrates. The wash buffer, substrate solution, reagent diluent, and other components were prepared by diluting as per the kit's instruction (Table 2.6 and Table 2.7).

Table 2.6: Overview of preparations of Reagent diluent and wash buffer.

Reagent	**Preparation (reagent:deionized water)**
Reagent Diluent	1:10
Wash buffer	1:24

Table 2.7: Overview over target concentration of each antibody and standard.

Reagent	**Vial concentration**	**Preparation**	**Working concentration**
Capture Antibody	240 µg	0.5ml PBS	4 µg/ml
Detection Antibody	4.50µg	1ml Reagent Diluent	75ng/ml
Streptavidin-HRP	2ml	-	40 fold dilution
Standard	45ng	0.5ml Deionized water	3.91-250 pg/ml

1. Capture antibodies were diluted to working concentration with PBS without carrier protein (see Table 2.5). The capture antibody was added to each well in an ELISA plate, which was sealed and left at room temperature overnight.
2. The following day A standard curve was prepared from the recommended concentration (see Table 2.5). It was prepared by serial dilution using a 2-fold factor, diluted in diluent consistent of deionized water.

3. The coated plate was aspirated after 24 hours and washed with wash buffer, repeating the process two times for a total three washes (400 µL wash buffer in each well in each time) using a plate washer (BioTek ELx405 HT Microplate Washe**r**, Winooski, USA).

4. Each well in the plate was blocked using 300 µL block buffer (1% BSA in PBS) for 1 hour and repeat the wash 3 times as previously.

5. Then 100 µL sample, standard and blank were added to the coated and blocked plate. The samples were diluted 40 times. In this step plate needs top incubate for 2 hours and then aspirate and wash the plate as in step 3.

6. Diluent diluted detection antibody was added at the recommended concentration (see Table 2.5) for 2 hours at room temperature.

7. After the aspiration and wash, 100 µL detection antibody was added to each well and incubated for additional 2 hours in room temperature.

8. Then 100 µL of the working dilution of streptavidin-HRP added to each well and incubated for 20 minutes at room temperature and avoiding direct light, after repeating the aspiration and wash.

9. Again, the aspiration/wash were repeated and 100 µL substrate solution were added to each well. The plate was incubated at room temperature and avoided direct light for 20 minutes.

10. Finally, 50 µL stop solution was added to each well and the plate gently tapped to ensure thorough mixing. At this point the color development was observed. The plate was read immediately using a microplate reader (Agilent, BioTek Gen5, Santa Clara, USA) using absorbance at 450 nm, wavelength corrected subtract reading at 540 nm or 570 nm. For a more detailed protocol, see the manufacturer protocol.

2.2.8. Cells and supernatant for gene expression analysis of the IL-1β gene

THP-1 cells were differentiated into macrophage-like cells, for this cell were seeded in 500 microliters of cell suspension at a concentration of 8×10^5 cells/ml into T-25 flasks (Corning® T-25 flasks Sarstedt #83.3910.002) together with a final concentration of 50 ng/ml PMA for 72 h. After differentiation period the cells become adherent, and the media was easily changed for new fresh media without PMA for a 24 h rest period before exposed to sample and controls. RNA was harvested after 24 h of treatment. For cells collection, THP-1 cells supernatant media was aspirated, and cells were rinsed with cold PBS. After aspirating the PBS, 600 µL RL-buffer (Norgen #48300) were used to lyse cells. The cells were

scraped using a cell scraper and the lysate was transferred into a 1.5 ml microcentrifuge tube. The cell lysate was frozen at -80°C until downstream analysis.

2.2.9. Gene Expression of IL-1β

As immune modulators, cytokines play a vital role in controlling and defining an infection's immune response. RNA was extracted from treated THP-1 cells to quantify these cytokines genetic expression. This RNA is then reversely transcribed into complementary DNA (cDNA), which serves as the template for quantification by quantitative polymerase chain reaction (qPCR).

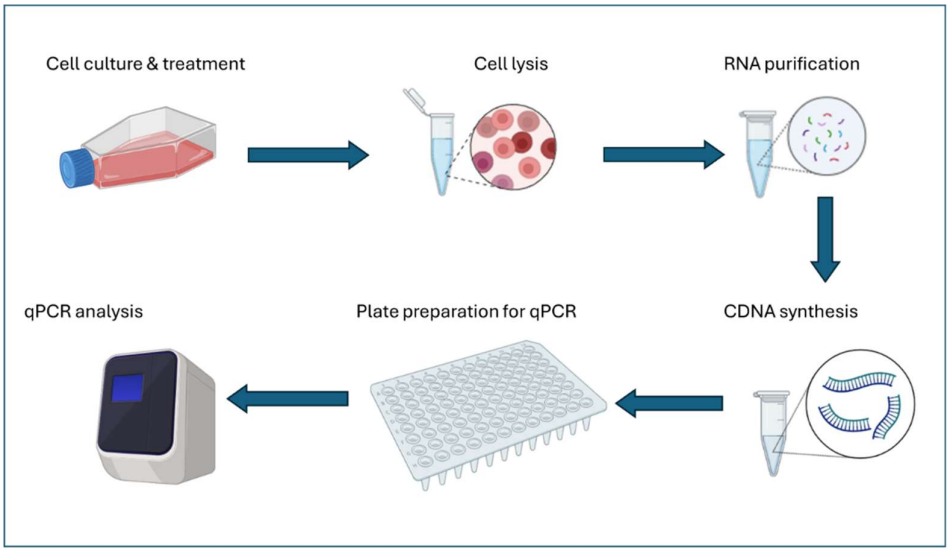

Figure 2.16: Visual representation of gene expression method (BioRender.com).

2.2.9.1. RNA isolation

The RNA Purification Kit (Norgen #48300) was used to isolate RNA. The RNA samples were collected and stored as described in section 2.8., using the accompanied protocol following the kit for extraction of RNA from mammalian cells. After rapid thawing from -80°C, each sample's entire lysate was loaded onto a single column. Flowthrough was diluted with absolute ethanol with ratio suggested by the kit. RNA was eluted with 30 µL of elution buffer A. To enhance the yield of extracted RNA, the flowthrough of purified RNA was transferred back onto the column once. See the protocol provided by the kit manufacturer for more information.

2.2.9.2. RNA quantification

The RNA concentration and purity of the samples were quantified by using NanoDrop 2000 (Invitrogen, Waltham, USA). The Nanodrop was blanked with 1 µL elution buffer prior to quantification. After that, 1µL of purified RNA was loaded for quantification and characterization.

The RNA concentration and purity (A230/A260-ratio, A260/A280-ratio) was recorded. The nanodrop was washed with lint free paper with water in between readings.

2.2.9.3. Reverse transcription

cDNA was synthesized using cDNA synthesis kit (Quanta-qScript #95047) from the purified RNA sample. The samples were processed following the standard protocol included with the kit. A master mix containing reverse transcriptase and buffer was prepared.

Table 2.8: Overview over reaction content and amount for cDNA synthesis.

Component	**Volume (µL)**	**Notes**
qScript RT-enzyme	1	
qScript Reaction mix	4	
N-Water	variable	
RNA	variable	1000 ng RNA
Total	20	

All reactions consisted of master mix and 1000 ng RNA in a 20 µL reaction (See Table 2.6). All reactions were transferred to a thermal cycler (Eppendorf, Mastercycler nexus, Hamburg, Germany). The thermal cycler was set at one cycle [Annealing: 22℃ 5 min, Elongation: 42℃ 30 min, Enzyme deactivation: 85℃ 5 min]. The final cDNA was diluted 3-fold by adding 54 µL of Nuclease-free water (Sigma-Aldrich #W4502), resulting in a final concentration of 10 ng μL^{-1} per tube. See the protocol provided by the kit manufacturer for more information.

2.2.9.4. Quantitative polymerase chain reaction

Quantitative polymerase chain reaction (qPCR) was based on the SYBR Green (Quantabio #95073) kit using the accompanying protocol. With a master mix consistent of 50% SYBR Green and 304 nM forward and reverse primers diluted in nuclease-free water, 10 µL reactions were setup. Based on testing, Actin was chosen as reference controls, and IL-1β, was normalized to this gene by geometric mean, using ΔΔCq analysis.

Table 2.9: Overview of reaction content and concentration for qPCR.

Component	Volume (µL)	Notes
dH_2O	17.82	
SYBR Green master mix	34.5	
Forward primer	0.84	25 pmol/µL initial concentration 14 pmol/µL working concentration
Reverse primer	0.84	25 pmol/µL initial concentration 14 pmol/µL working concentration
cDNA	15	10 ng/µL input concentration
Total	69	

10 ng cDNA were added to each reaction, then mixed (Table 2.7). Using a QuantStudio 5 thermal cycler (Applied Biosystems, Waltham, USA), the plate was read with Design and Analysis software 1.5.2 (Applied Biosystems, Waltham, USA). The heat curves parameters are mentioned in Figure: 2.12. See the protocol recommended by the manufacturer for more information.

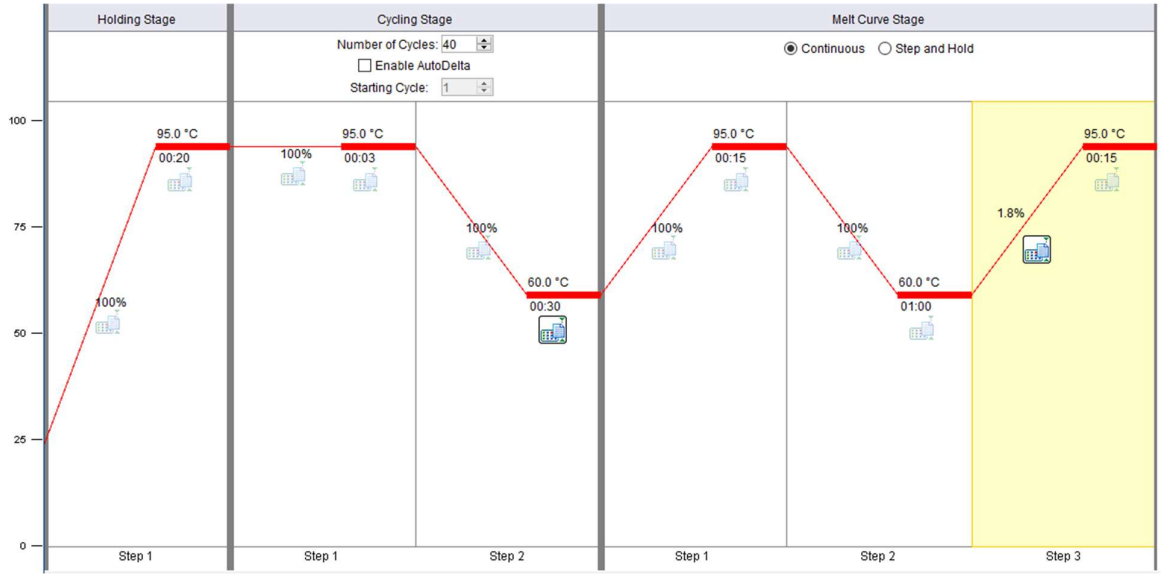

Figure 2.17: qPCR thermal cycle and Melt curve settings.

2.3. Data analysis and statistics

All data processing was performed using Excel v2402 (Microsoft, Redmond, United states). Statistics and data analysis and presentation was performed using GraphPad Prism 10 (Dotmatics, Boston, United states).

3. Result

3.1. Seeding with different amounts of media

To decide the optimal amount of media for seeding ~ 50,000 HEK TLR2 and TLR4 cells /well we're seeded in different amounts of media; 90 µL, 135 µL, and 180 µL. (Figure 3.8). The cells were subjected to control conditions (only media), LTA (TLR2)/LPS (TLR4), DMSO at 0.1%, and DMSO at 10% concentration. The fold change in cell response was measured to evaluate the effect of the seeding density on cell activity. However, the results indicate no significant changes in the fold change in cell response across different seeding densities for both cell lines (TLR2 and TLR4) (Figure 3.1). From the experiment, it was determined to use 90 µL cell media for cell seeding.

Cell viability after seeding with different amounts of media for TL2 and TL4

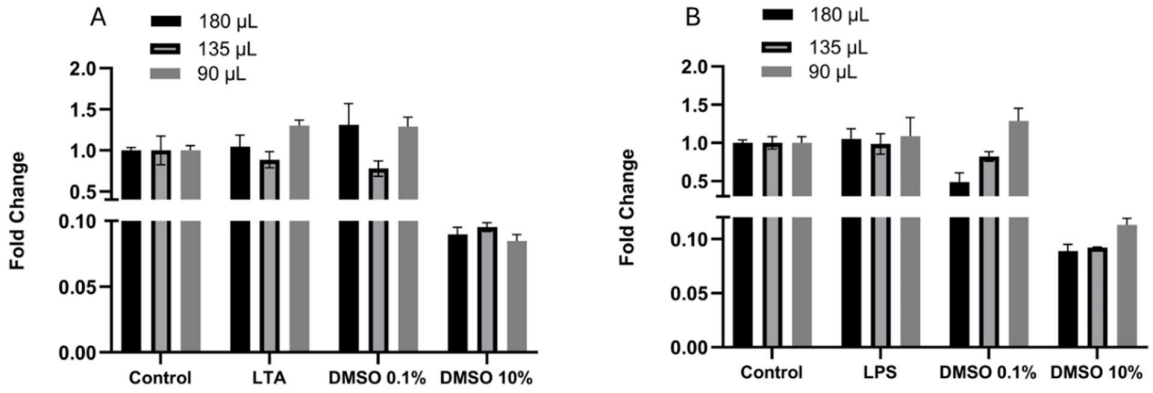

Figure 3.1: ***Relative activation of TLR2 and TLR4 by LTA/LPS and DMSO treatment with different amount of media when seeding.*** *HEK TLR2 and TLR4 were seeded at 50 000 cells pr well in a 96 well plate with 90, 135 and 180 µl media. One day after seeding cells were exposed to 1000 ng/ml LTA/LPS, 0.1 % or 10 % DMSO for 24 h before alamar-Blue analysis was performed. (A) HEK TLR2 Cells (B) HEK TLR4 cells. Control is DMSO 0.1%, and the results represent mean values ± SEM of 3 independent experiments.*

3.2. DMSO test on HEK cells for deciding test concentration

DMSO is toxic to the cells and can lead to cell death. To find a DMSO concentration with acceptable toxicity a dose-response experiment was performed on the HEK cells (Figure 3.2). HEK cells were treated with increasing concentrations of DMSO, ranging from 0.05% to 0.8 % and 10% DMSO as positive control. The HEK cells exhibit increasing variability and uncertainty in the results with increasing DMSO concentration up to 0.8%. Test concentration was determined to DMSO 0.1% as finding from the experiment suggest minimal effect on cell viability.

Effect of DMSO on cell viability

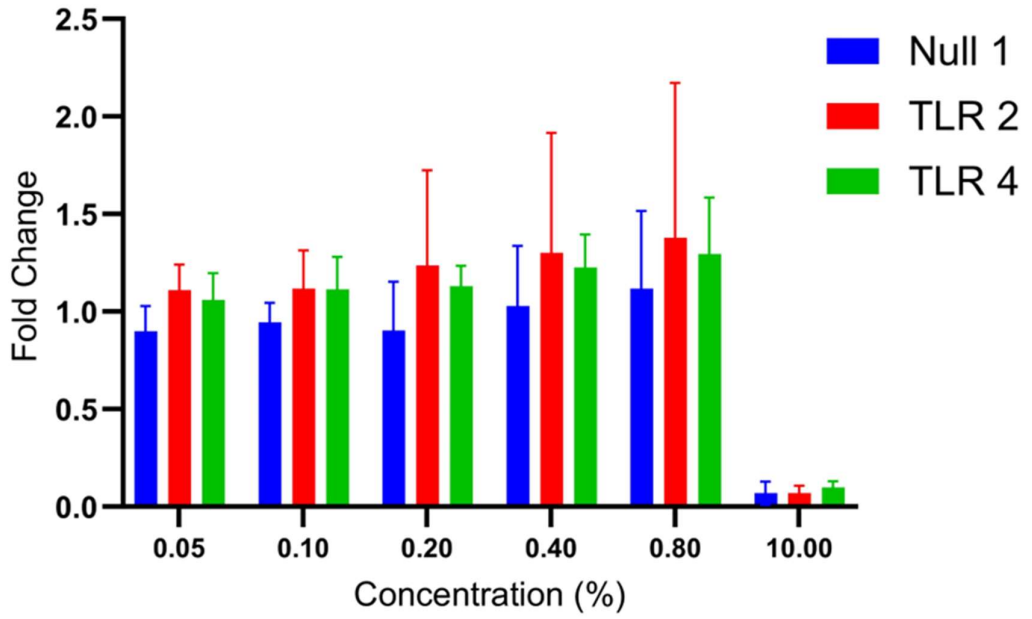

Figure 3.2: ***Dose-response curve of HEK Cell (Null 1, TLR2, TLR4) viability at different DMSO concentrations (0.05% to 10%).*** *The results represent mean values ± SEM of 3 independent experiments.*

3.3. Positive control test (LTA/LPS) for deciding test concentration

Before LTA and LPS could be used as positive controls in the TLR2 and TLR4 activation experiments, respectively, their ability to activate NF-κB was determined using a broad range of concentrations from 0.001 and up to 100 ng/ml for LPS and up to 5000 ng/ml for LTA. (Figure 3.3) to find the exponential area. A concentration of 100 ng/ml for LTA and 10 ng/ml for LPS was within the exponential part of the curve and determined to be used in the following experiments.

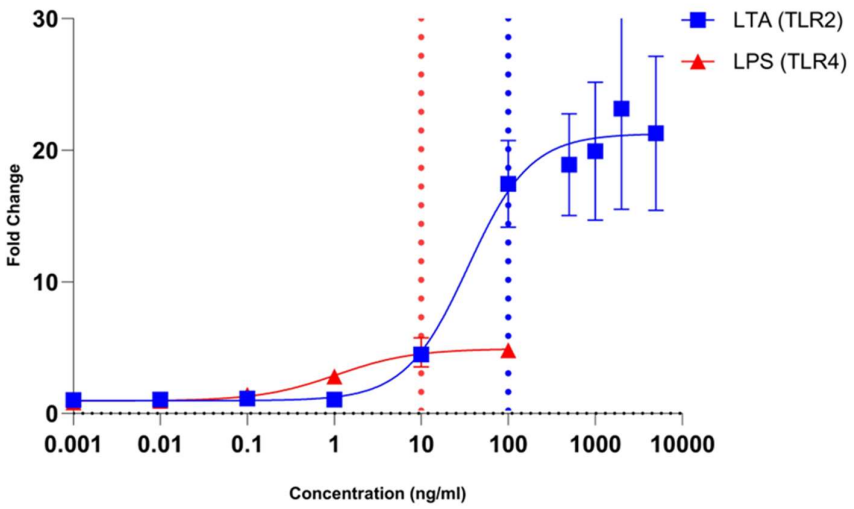

Figure 3.3: ***Positive Control Test (LTA and LPS).*** *HEK TLR2 and TLR4 were seeded at 50 000 cells pr well in a 96 well plate with 90 µl media. One day after seeding cells were exposed upto 5000 ng/ml LTA and 100 ng/ml LPS for 24 h before QuantiBlue analysis was performed. The results represent mean values ± SEM of 3 independent experiments.*

3.4. Cell morphology

In order to evaluate the effect of the tested mycotoxins on the different HEK cells and THP-1 cells morphology cells were treated with AOH (30µM) or AME (10µM) in combination with LTA (100 ng/ml) (TLR2) or LPS (10 ng/ml) (TLR4, IL1β, and THP-1) for 24 h before cell appearance was studied in the microscope (Echo Inc., San Diego, USA).

Figure 3.4 shows HEK Blue TLR2 cells; before exposure Figure 3.4 a, when exposed to AOH 30µM for 24 h Figure 3.4 b and when exposed to AOH combined with LTA Figure 3.4 c.

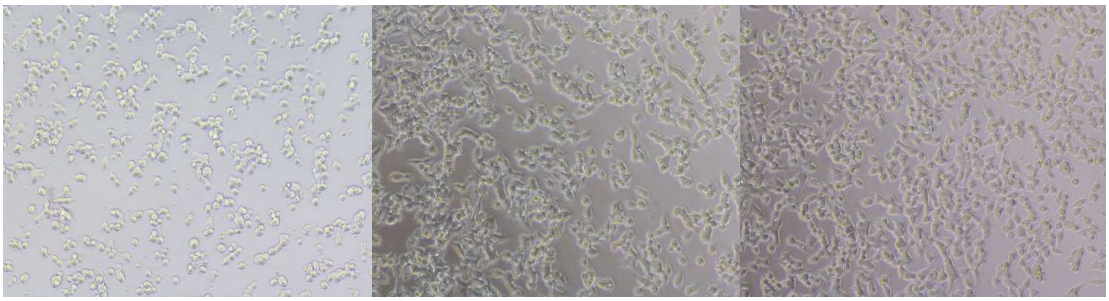

(a) (b) (c)

Figure 3.4: Cell morphology of Hek Blue TLR2 cells (a) before exposure (b) after exposure to AOH (c) after exposure to AOH combined with LTA.

Below in Figure 3.5, HEK Blue TLR 4 cells; before exposure Figure 3.5 a, when exposed to AOH 30µM for 24 h Figure 3.5 b and when exposed to AOH combined with LPS Figure 3.5 c.

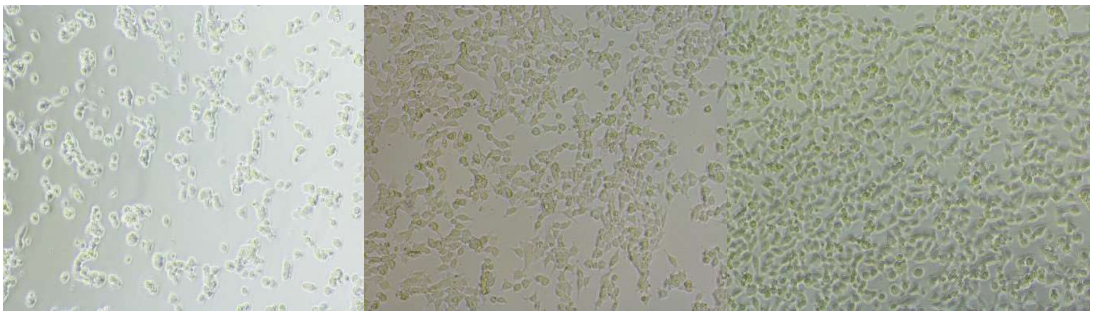

(a) (b) (c)

Figure 3.5: Cell morphology of Hek Blue TLR4 cells (a) before exposure (b) after exposure to AOH (c) after exposure to AOH combined with LPS.

HEK Blue TLR2 cells (Figure 3.6); before exposure Figure 3.6 a, exposed to AME 10µM for 24 h Figure 3.6 b and exposed to AME combined with LTA Figure 3.6 c. The shape was different in both cases according to our observation through microscope.

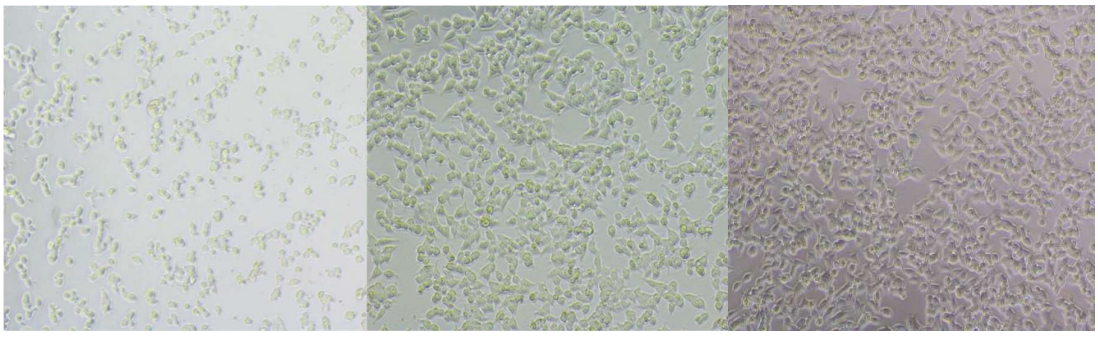

(a) (b) (c)

Figure 3.6: Cell morphology of Hek Blue TLR2 cells (a) before exposure (b) after exposure to AME (c) after exposure to AME combined with LTA.

Similarly, in Figure 3.7 Hek-Blue TLR4 cells; before exposure Figure 3.7 a, exposed to AME 10µM for 24 h Figure 3.7 b and exposed to AME combined with LPS Figure 3.7 c.

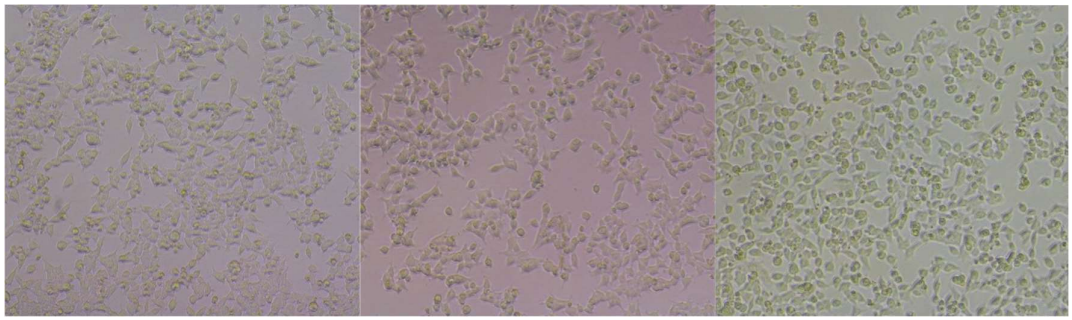

(a) (b) (c)

Figure 3.7: Cell morphology of Hek Blue TLR4 cells (a) before exposure (b) after exposure to AME (c) after exposure to AME combined with LPS.

THP-1 cells are shown in Figure 3.8 and 3.9. In Figure 3.8 THP-1 cells; before exposure, Figure 3.8 a, exposed to AOH 30µM for 24 h Figure 3.8 b and exposed to AOH combined with LPS Figure 3.8 c.

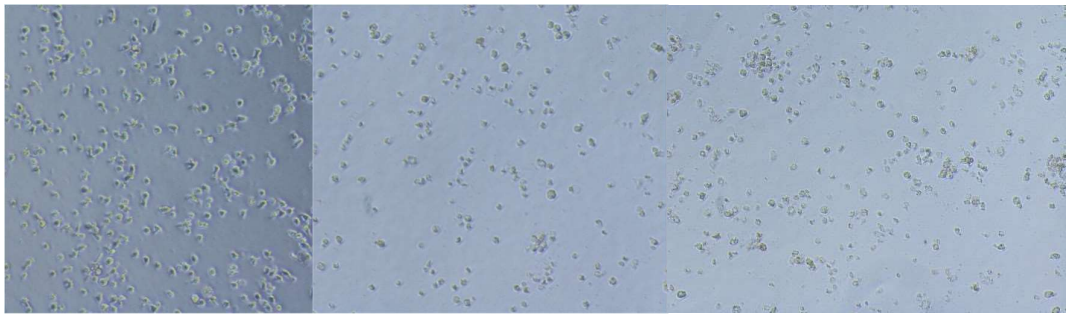

(a) (b) (c)

Figure 3.8: Cell morphology of THP-1 cells (a) before exposure (b) after exposure to AOH (c) after exposure to AOH combined with LPS.

On the other hand, In Figure 3.9 THP-1 cells; before exposure Figure 3.9 a, exposed to AME 10µM for 24 h Figure 3.9 b and exposed to AOH combined with LPS Figure 3.9 c. The combined exposure to AME and LPS seems to have some visible impact on the cells.

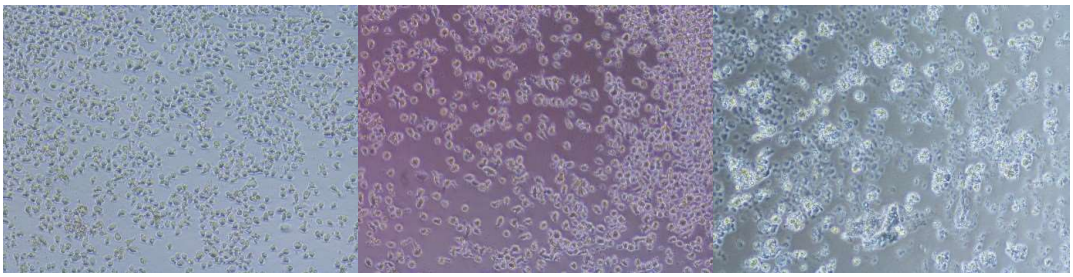

(a) (b) (c)

Figure 3.9: Cell morphology of THP-1 cells (a) before exposure (b) after exposure to AME (c) after exposure to AME combined with LPS.

Below in Figure 3.10, HEK IL-1β cells are pictured. HEK IL-1β before exposure Figure 3.10 a, exposed to AOH 30µM for 24 h Figure 3.10 b and exposed to AOH combined with LPS Figure 3.10 c, exposed to AME 10µM for 24 h Figure 3.10 d and exposed to AOH combined with LPS Figure 3.10 e.

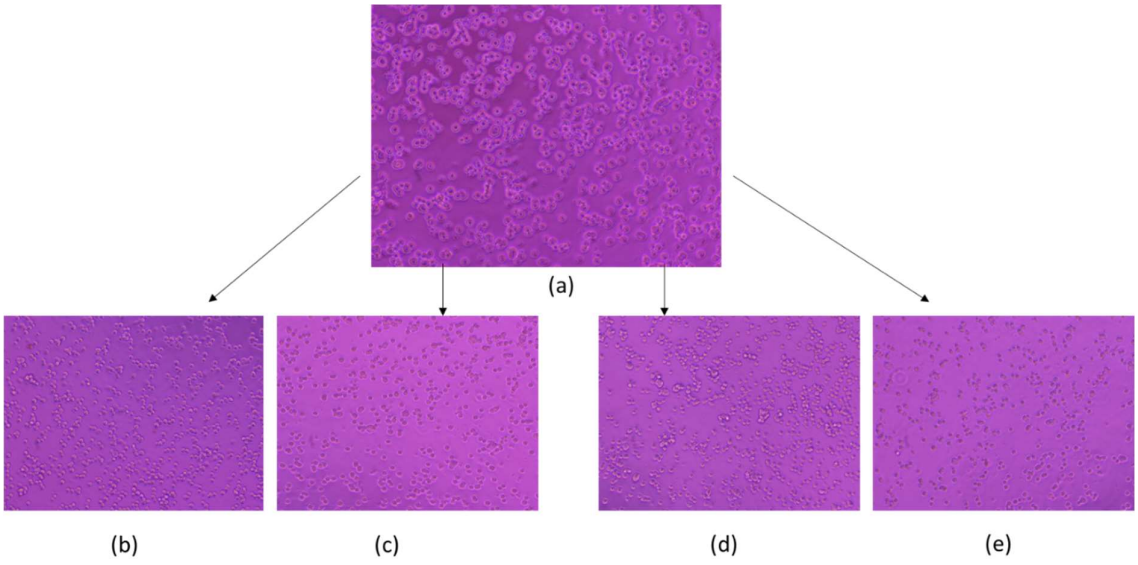

Figure 3.10: Cell morphology of HEK IL-1β cells before exposure (a) after exposure to AOH (b) after exposure to AOH combined with LPS (c) after exposure to AME (d) after exposure to AME combined with LPS(e).

3.5. THP-1 cells

The cytotoxic effects of AOH and AME on THP-1 cells were evaluated both with and without LPS to simulate an inflammatory condition. Viability was assessed by comparing the fold change in cell number relative to the control (DMSO 0.1%). The viability of the THP-1 cells was significantly reduced by AOH and AME in the presence of LPS and tended to be reduced in the absence of LPS as well. There was no dose-response (Figure 3.11).

Relative Cytotoxic Effects of AOH and AME on THP-1

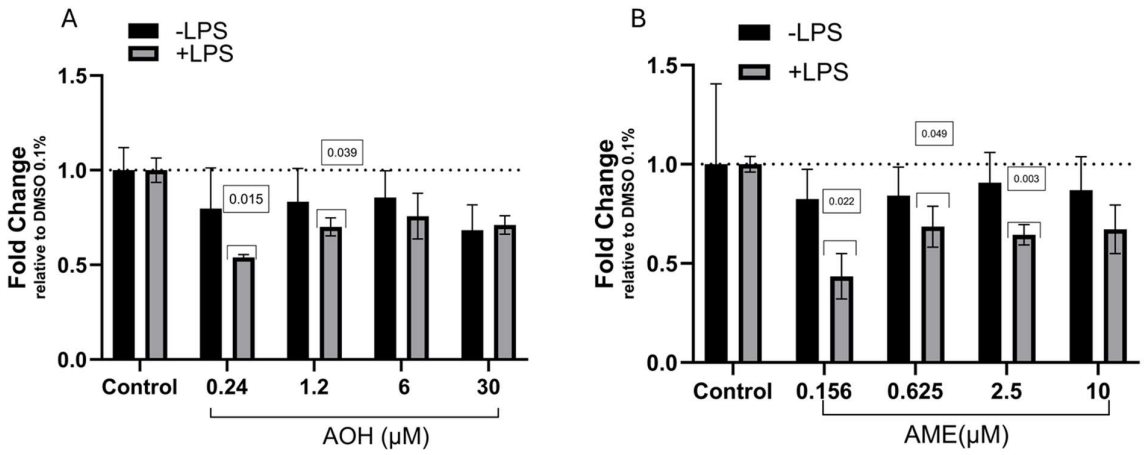

Figure 3.11: ***Relative cytotoxic effects of AOH and AME on THP-1.*** *Differentiate THP-1 were seeded at 200000 cells pr well in a 48 well plate with 300 µl media. One day after suspended media aspirated and seeding cells were exposed to 300 µl samples and controls for 24 h before alamar-Blue analysis was performed. (A) THP-1 cells exposure to AOH (B) THP-1 cells exposure to AME. Control is DMSO 0.1%, and the results represent mean values ± SEM of 3 independent experiments. For significant difference P values mentioned in the box, p< 0.05 paired t-test.*

3.6. HEK-Blue TLR2 and TLR4 cells

To check the TLR activity on HEK-Blue TLR2 and TLR4 cells, different concentrations of toxin (AOH and AME) were exposed to the cells with or without TLR ligands (LTA/LPS) (Figure 3.12 to 3.15). Cell viability was also observed to check the cytotoxicity. TLR activity then adjusted to toxicity to see the impact of cell viability in the NF-κB signal. This adjustment was done to ensure that activation of NF-κB is triggered by the activation of TLR receptor, not because of cytotoxicity.

The effects of AOH on HEK TLR2 cells were examined through SEAP activation (which initiate NF-κB activation) using a QuantBlue assay (Figure 3.12 A) and cell viability using an alamar-Blue assay (Figure 3.12 B). Then, NF-κB activation adjusted to cell viability to recognize true signaling changes from effects due to cytotoxicity (Figure 3.12 C). The presence of LTA and LPS lead to activation of TLR receptors which led to an increase in NF-κB signal. But in the absence of LTA, AOH has no impact on NF-κB signal in TLR2 receptor cell lines (Figure 3.12 A). The cell viability is significantly lower in DMSO 10% but no significant difference in the presence of LTA was observed (Figure 3.12 B). There is no dose-dependent relationship observed particularly for cell viability. NF-κB activation adjusted to cell viability to ensure that NF-κB activation is not merely a consequence of cell death (Figure 3.12 C).

HEK Blue TLR2 cells Exposed to AOH

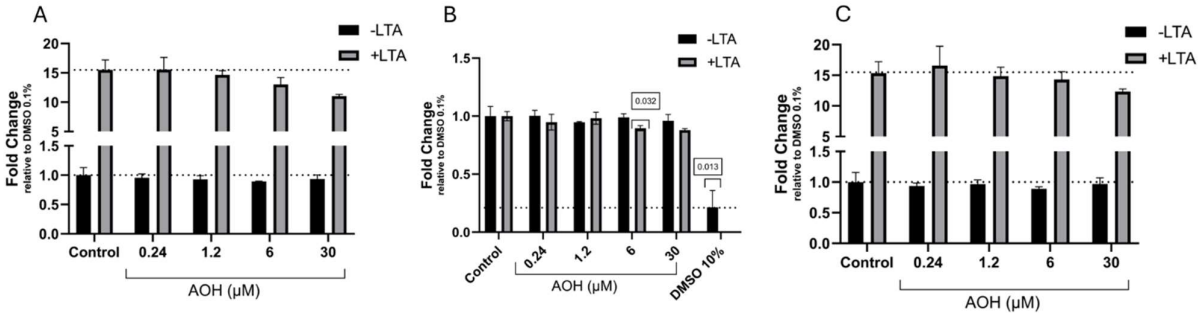

Figure 3.12: ***HEK Blue TLR2 Cells Exposed to AOH****, (A) Relative activation of HEK TLR2 to AOH (QuantiBlue assay) (B) Relative cytotoxic effects of AOH on HEK TLR2 Cells (alamar-Blue assay) (C) NF-κB activation adjusted for toxicity. HEK TLR2 were seeded at 50 000 cells pr well in a 96 well plate with 90 µl media. One day after seeding cells were exposed to 20 µl of test samples and controls for 24 h before QuantiBlue analysis was performed. Control is DMSO 0.1%, and the results represent mean values ± SEM of 3 independent experiments. For significant difference P values mentioned in the box, p< 0.05 paired t-test.*

The effects of AOH on HEK TLR4 cells were examined (Figure 3.13). The AOH alone has no impact on TLR- NF-κB signal pathway. But combination exposure to LPS with mycotoxins reduced the increased NF-κB signal in TLR4 receptor cell lines. The NF-κB signal was significantly decreased in the HEK-TLR4 cells at the highest AOH concentration (Figure 3.13 A). The cell viability is significantly lower in DMSO 10%, with some unspecific significant reduction observed in the presence of LPS (Figure 3.13 B). NF-κB activation adjusted to cell viability, to elucidate if reduction of NF-κB signaling is not merely a consequence of cell death (Figure 3.13 C).

HEK Blue TLR4 cells Exposed to AOH

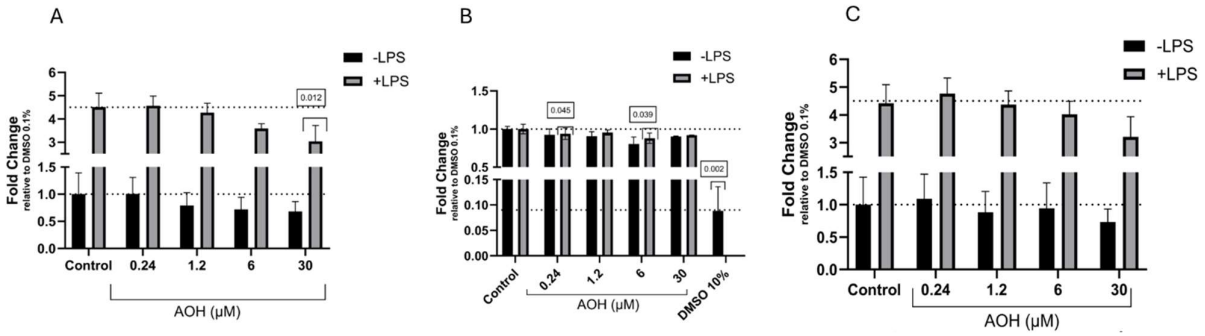

Figure 3.13: ***HEK Blue TLR4 Cells Exposed to AOH****, (A) Relative activation of HEK TLR4 to AOH (QuantiBlue assay) (B) Relative cytotoxic effects of AOH on HEK TLR4 Cells (alamar-Blue assay) (C) NF-κB activation adjusted for toxicity. HEK TLR4 were seeded at 50 000 cells pr well in a 96 well plate with 90 µl media. One day after seeding cells were exposed to 20 µl of test samples and controls for 24 h before QuantiBlue analysis was performed. Control is DMSO 0.1%, and the results represent mean values ± SEM of 3 independent experiments. For significant difference P values mentioned in the box, p< 0.05 paired t-test.*

Figure 3.14 A shows no significant change in NF-κB signal in TLR2 cells in the presence of AME. But the presence of TLR2 ligands (LTA) lead to activation of TLR receptors which led to an increase in NF-κB signal. The combination exposure of LTA with AME reduced the increased NF-κB signal in TLR2 receptor cell line, significant decreased observed at the highest concentration of AME (Figure 3.14 A). The cell viability was significantly lower in the negative control (DMSO 10%) but no significant difference from positive control was observed (Figure 3.14 B). NF-κB activation adjusted to cell viability to recognize true signaling changes from effects due to cytotoxicity which refers NF-κB activation is not merely a consequence of cell death (Figure 3.14 C). After adjusting for toxicity, a significant decrease was observed in NF-κB signal in TLR2 cell lines at the two highest concentrations of AME in the presence of LTA.

HEK Blue TLR2 cells Exposed to AME

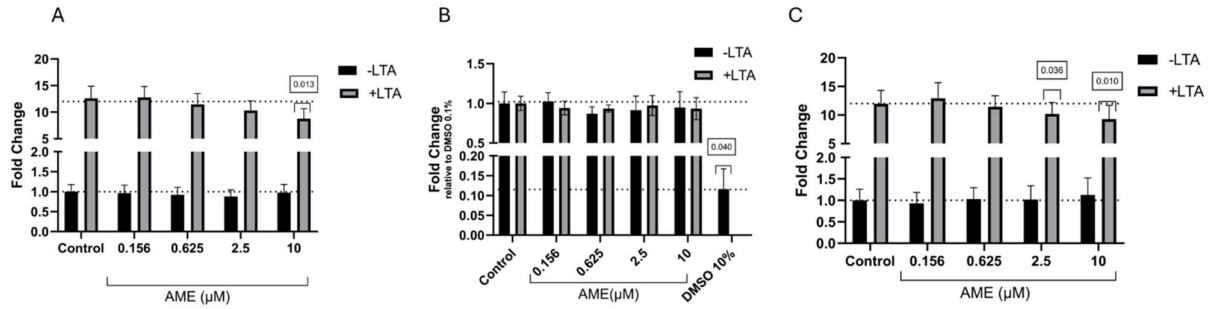

Figure 3.14: ***HEK Blue TLR2 Cells Exposed to AME****, (A) Relative activation of HEK TLR2 to AME (QuantiBlue assay) (B) Relative cytotoxic effects of AME on HEK TL2 Cells (alamar-Blueassay) (C) NF-κB activation adjusted for toxicity. HEK TLR2 were seeded at 50 000 cells pr well in a 96 well plate with 90 µl media. One day after seeding cells were exposed to 20 µl of test samples and controls for 24 h before QuantiBlue analysis was performed. Control is DMSO 0.1%, and the results represent mean values ± SEM of 3 independent experiments. For significant difference P values mentioned in the box, p< 0.05 paired t-test.*

The effects of AME on HEK TLR4 cells were examined (Figure 3.15). There is no significant change in NF-κB signal in TLR4 cells in the presence of AME. But along with LPS, AME reduced the increased NF-κB signal in TLR4 receptor cell lines. The NF-κB signal was significantly decreased in the HEK-TLR4 cells at the concentration of 0.625 and 10µM (Figure 3.15 A). The cell viability is significantly lower in positive control, DMSO 10%, but no significant difference observed in the presence of LPS (Figure 3.15 B). There is no dose-dependent relationship observed particularly for cell viability. NF-κB activation adjusted to cell viability to ensure that NF-κB activation is not merely a consequence of cell death (Figure 3.15 C). The NF-κB signal was significantly decreased in the HEK-TLR4 cells at the concentration of 0.625 to 10µM after adjusting toxicity (Figure 3.15 C).

HEK Blue TLR4 cells Exposed to AME

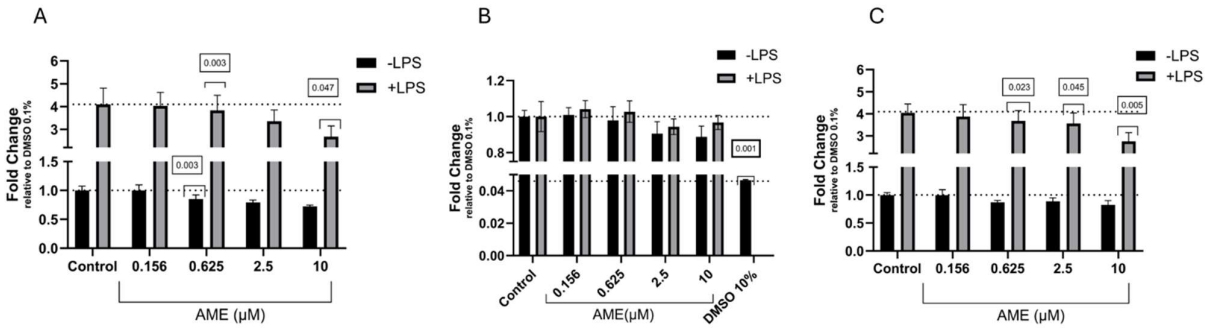

Figure 3.15: ***HEK Blue TLR4 Cells Exposed to AME****, (A) Relative activation of HEK TLR4 to AME (QuantiBlue assay) (B) Relative cytotoxic effects of AME on HEK TLR4 Cells (alamar-Blue assay) (C) NF-κB activation adjusted for toxicity. HEK TLR4 were seeded at 50 000 cells pr well in a 96 well plate with 90 µl media. One day after seeding cells were exposed to 20 µl of test samples and controls for 24 h before QuantiBlue analysis was performed. Control is DMSO 0.1%, and the results represent mean values ± SEM of 3 independent experiments. For significant difference P values mentioned in the box, p< 0.05 paired t-test.*

3.6.1. HEK-Blue Null 1 cells

To examine the TLR activity on HEK-Blue Null 1 cells, different concentrations of toxin (AOH or AME) were exposed to the cells with or without positive control (LTA or LPS). HEK-Blue Null 1 cells treated with AOH displayed no significant alteration in TLR activity across all tested concentrations, regardless of LPS or LTA absence or presence (Figure 3.16, A and B). Similarly, AME showed no significant modulation of TLR activity as well in any conditions (with or without LTA/LPS) (Figure 3.16, C and D).

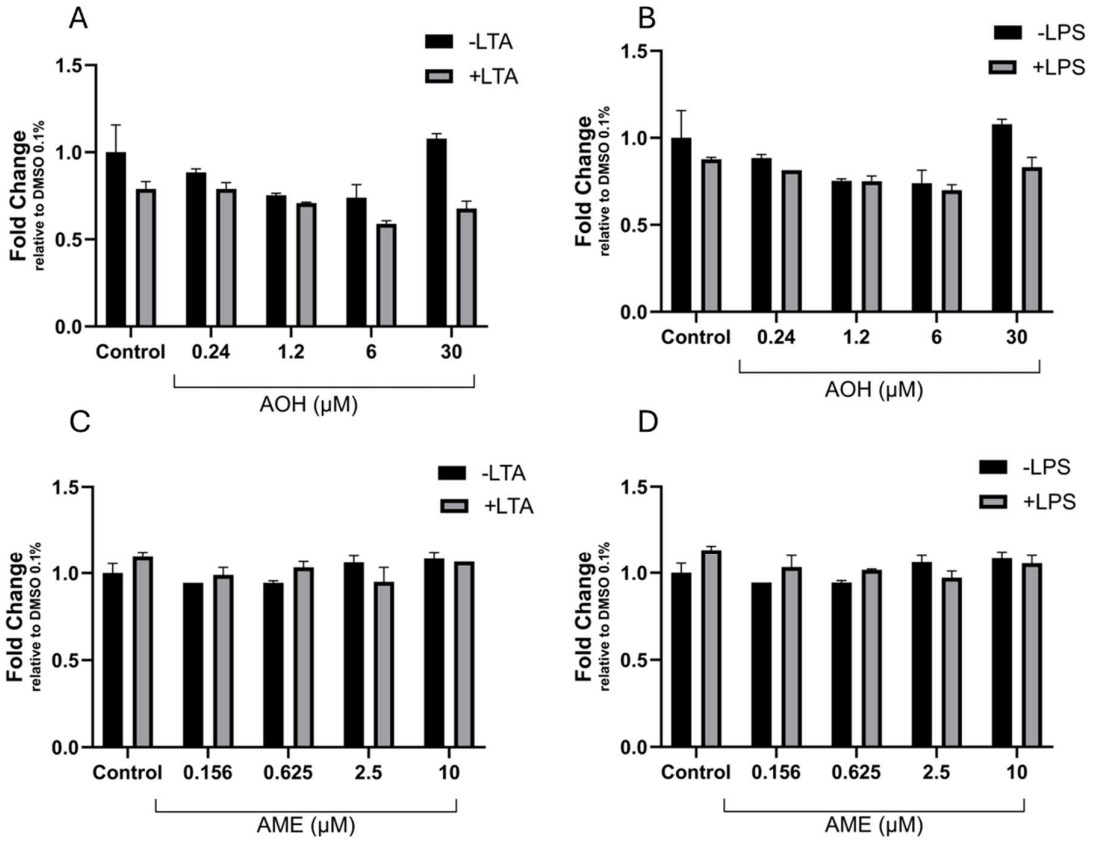

Figure 3.16: ***Relative activation of HEK Null 1v Cells Exposed to AOH and AME.*** *HEK Null 1 cells were seeded at 50 000 cells pr well in a 96 well plate with 90 µl media. One day after seeding cells were exposed to 20 µl of test samples and controls for 24 h before QuantiBlue analysis was performed. (A) HEK-Null 1 cells after treatment with AOH (–LTA/+LTA), (B) HEK-Null 1 cells after treatment with AOH (–LPS/+LPS), (C) HEK-Null 1 cells after treatment with AME (-LTA/+LTA), (D) HEK-Null 1 cells after treatment with AME (–LPS/+LPS). Control is DMSO 0.1%, and the results represent mean values ± SEM of 2 independent experiments.*

To investigate the effects of AOH and AME on HEK Null 1 cell viability, the cells were treated with different concentrations of AOH and AME in the presence or absence of LTA or LPS. No significant difference in viability was observed compared to positive control across all tested conditions, but the viability was significantly reduced in the negative control (DMSO 10%) (Figure 3.17).

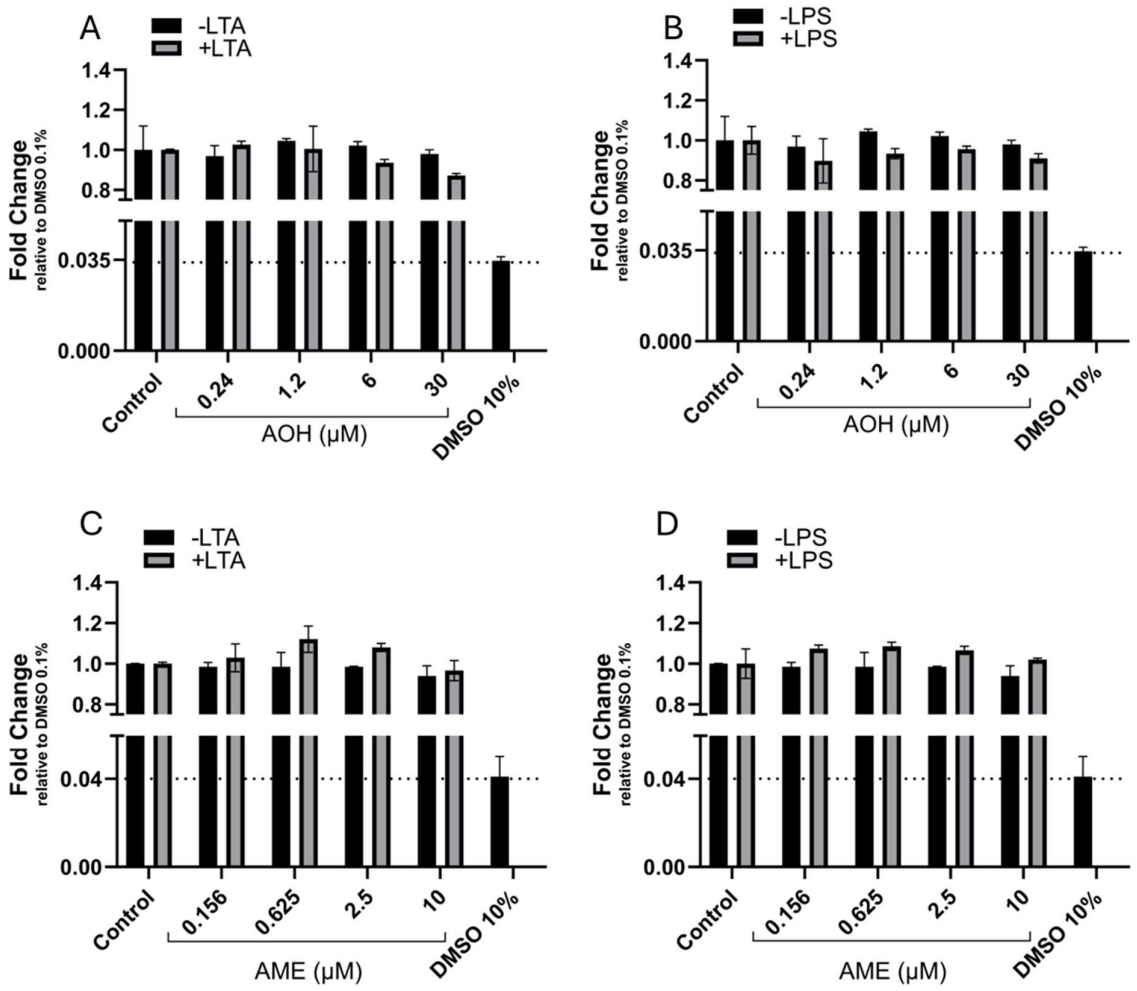

Figure 3.17: ***Relative cytotoxic effects of AOH and AME on HEK Null 1 cells.*** *HEK Null 1 cells were seeded at 50 000 cells pr well in a 96 well plate with 90 µl media. One day after seeding cells were exposed to 20 µl of test samples and controls for 24 h before alamar-Blue analysis was performed. (A) HEK-Null 1 cells after treatment with AOH (–LTA/+LTA), (B) HEK-Null 1 cells after treatment with AOH (–LPS/+LPS), (C) HEK-Null 1 cells after treatment with AME (-LTA/+LTA), (D) HEK-Null 1 cells after treatment with AME (–LPS/+LPS). Control is DMSO 0.1%, and the results represent mean values ± SEM of 2 independent experiments.*

3.7. Effect of mycotoxin on THP-1 / HEK IL-1β inflammasome activation

To functionally explore the effect of AOH and AME mycotoxins in combination with known ligands a two-step assay was used. HEK-IL-1β cells were conditioned with media from AOH and AME exposed THP-1 cells to measure inflammasome activation and release of functional IL-1β.

The treatment of HEK IL-1β with conditioned media from THP-1 cells exposed AOH in the absence of LPS did not significantly affect NF-κB activity at any concentration tested. However, conditioned media from LPS exposed THP-1 cells induced an increased response compared to control. When, the

AOH exposure was in combination with LPS, the LPS induced increase of the NF-κB signal was decrease significantly at 6 µM AOH concentration (Figure 3.18 A). Cell viability assays revealed that AOH does not significantly affect the viability of HEK IL-1β cells up to a concentration of 30 µM, regardless of LPS presence (Figure 3.18 B). A negative control with 10% DMSO confirmed the assay's capability to detect cell viability loss. When the graph was adjusted for viability also AOH 30µM in combination with LPS reduced the LPS induced signal (Figure 3.18 C). Recombinant IL-1β served as a positive control, confirming the assay's sensitivity to NF-κB pathway activation.

HEK IL-1β Exposed to AOH

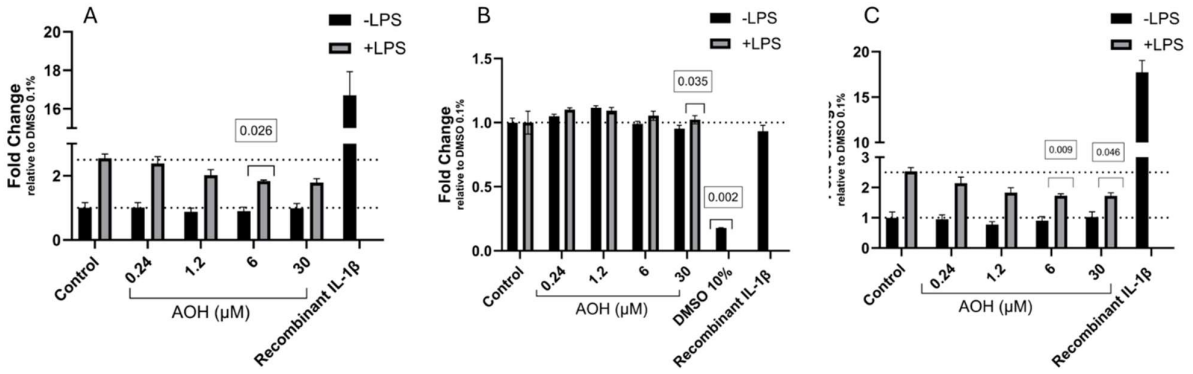

Figure 3.18: ***HEK IL-1β Cells Exposed to AOH (THP-1 conditioned media)****, (A) Relative activation of HEK IL-1β to AOH (QuantiBlue assay) (B) Relative cytotoxic effects of AOH on HEK IL-1β Cells (alamar-Blueassay) (C) NF-κB activation adjusted for toxicity. HEK IL-1β were seeded at 3.33×10^5 cells/ml in a 96 well plate with 150 µl media and exposed to 50 µl THP-1 conditioned media (AOH). After 24 h QuantiBlue and alamar-Blueanalysis was performed. Control is DMSO 0.1%, and the results represent mean values ± SEM of 3 independent experiments. For significant difference P values mentioned in the box, p< 0.05 paired t-test.*

The effects of AME on HEK IL-1β cells were examined through NF-κB activation using a QuantiBlue assay and cell viability using an alamar-Blue assay. Then, NF-κB activation adjusted to cell viability to recognize true signaling changes from effects due to cytotoxicity (Figure 3.19 C). AME treatment did not significantly affect NF-κB activation at concentrations without LPS; but with LPS, a significant increase in NF-κB activation was observed. But the NF-κB signal was significantly decreased in the HEK IL-1β cells at the concentration of 2.5µM (Figure 3.19 A).
No significant cell viability observed with or without LPS. However, in the presence of LPS, an unspecific significant decreased in cell viability observed at 10 µM AME (Figure 3.19 B).

Adjusting the NF-κB activation data for the corresponding cell viability measurements allowed to confirm if NF-κB activation is merely a consequence of cell death, a non-significant decrease was observed (Figure 3.19 C).

HEK IL-1β Exposed to AME

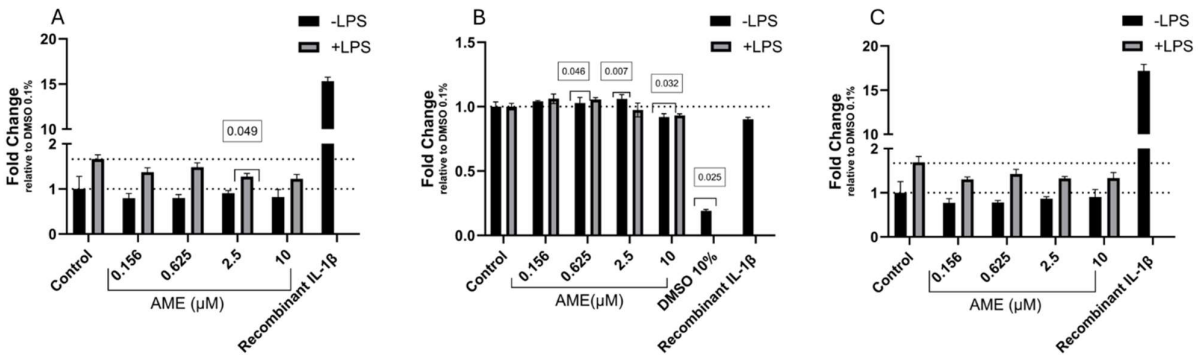

Figure 3.19: ***HEK IL-1β Cells Exposed to AME (THP-1 conditioned media)****, (A) Relative activation of HEK IL-1β to AME (QuantiBlue assay) (B) Relative cytotoxic effects of AME on HEK IL-1β Cells (alamar-Blue assay) (C) NF-κB activation adjusted for toxicity. HEK IL-1β were seeded at 3.33×10^5 cells/ml in a 96 well plate with 150 µl media and exposed to 50 µl THP-1 conditioned media (AME). After 24 h QuantiBlue and alamar-Blueanalysis was performed. Control is DMSO 0.1%, and the results represent mean values ± SEM of 3 independent experiments. For significant difference P values mentioned in the box, p< 0.05 paired t-test.*

3.7.1. HEK-Blue Null 1v

The responsiveness of HEK-Blue Null 1v cells exposed to conditioned media from THP-1, which were priorly exposed to AOH and AME with and without LPS was assessed in terms of cellular activity, as determined by a fold change in signal relative to a control with 0.1% DMSO. This analysis was performed both in the absence and presence of LPS to investigate the compounds' effects under inflammatory conditions. When the AOH exposure was in combination with LPS, the LPS-induced increase of the NF-κB signal was observed. This LPS-induced NF-κB signal decreased dose-dependently from the lowest concentration (0.24 µM) to the highest (30 µM). (Figure 3.20 a).

HEK NULL 1v Exposed to AOH and AME

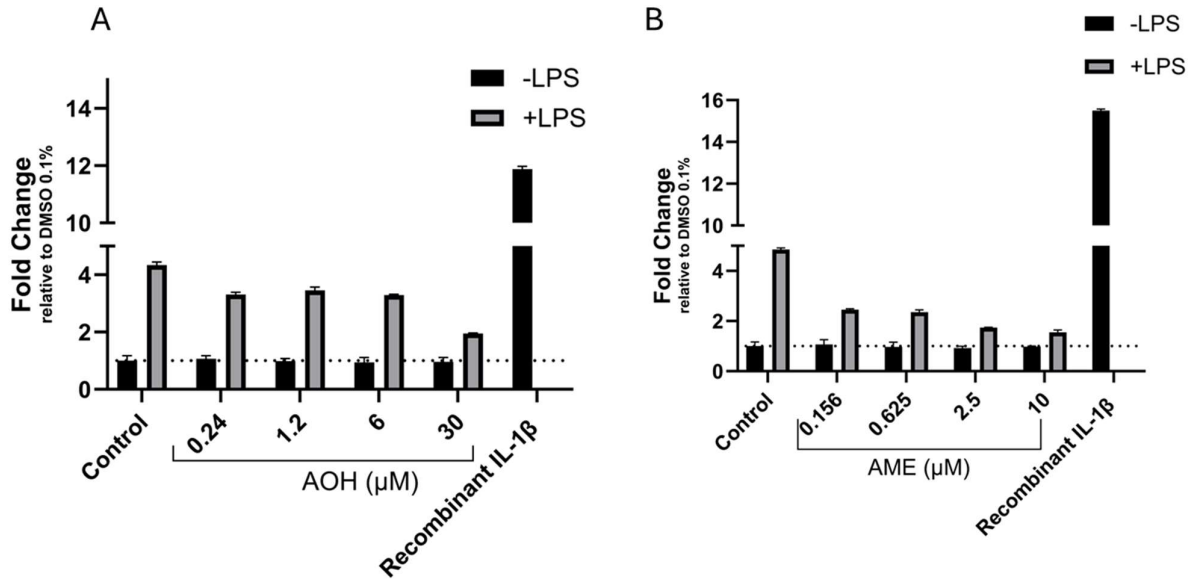

Figure 3.20: ***Relative activation of HEK Null 1v Cells Exposed to AOH and AME (THP-1 conditioned media).*** *HEK Null 1v were seeded at 3.33×10^5 cells/ml in a 96 well plate with 150 µl media and exposed to 50 µl THP-1 conditioned media. After 24 h QuantiBlue analysis was performed. (A) HEK Null 1v exposed to AOH (THP-1 conditioned media) (B) HEK Null 1v cells exposed to AME (THP-1 conditioned media). Control is DMSO 0.1%, and the results represent mean values ± SEM of 2 independent experiments.*

Similar to AOH, AME did not significantly affect NF-κB activation without LPS; but with LPS, a significant increase in NF-κB activation was observed. But the NF-κB signal was significantly decreased in dose dependent fashion like (Figure 3.20 b) which suggest about cells' response to AME suppressed NF-κB signals under inflammatory conditions.

The potential cytotoxicity (cell viability) of AOH and AME was investigated in HEK-Blue Null 1v cells. AOH didn't show any significant impact on cell viability in any concentrations in either condition (-LPS/+LPS) (Figure 3.19). However, like AOH, AME also showed no significant cell viability (Figure 3.21).

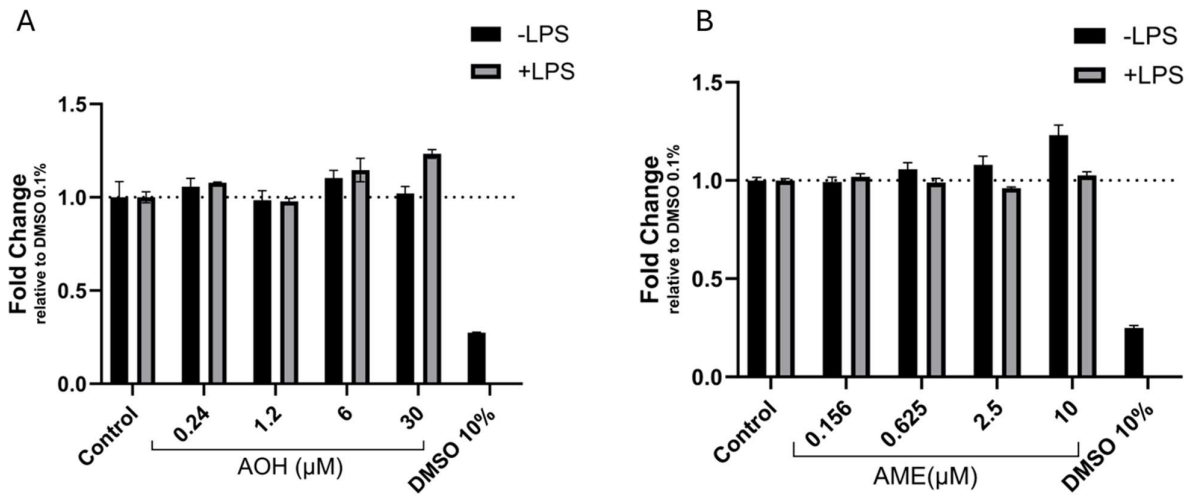

Figure 3.21: ***Relative cytotoxic effects of AOH and AME on HEK Null 1v.*** *HEK Null 1v were seeded at 3.33×10^5 cells/ml in a 96 well plate with 150 µl media and exposed to 50 µl THP-1 conditioned media. After 24 h alamar-Blueanalysis was performed. (A) HEK Null 1v exposed to AOH (THP-1 conditioned media) (B) HEK Null 1v cells exposed to AME (THP-1 conditioned media). Control is DMSO 0.1%, and the results represent mean values ± SEM of 2 independent experiments.*

3.8. THP-1 inflammasome activation by toxins (ELISA)

The activation of THP-1 inflammasome by LPS can regulate IL-1β secretion. To examine whether AOH and AME affect this regulation, ELISA was performed. The concentration (pg/ml) of IL-1β secretion was calculated based on the standard curve and normalized to Control (DMSO 0.1%). The conditioned media from THP-1 cells exposed to AOH or AME alone did not affect IL-1β secretion. Our experiment result suggests that conditioned media from THP-1 cells co-exposed to LPS increase the secretion of IL-1β, which was reduced significantly at the highest concentrations of AOH (30 µM) and AME (10 µM). A dose-dependent increase of IL- 1β level was observed in figure 3.22 A, at the lowest concentration of AOH. But in figure 3.22 B a dose-dependent IL-1β reduction was observed, except at the second lowest concentration of AME (0.625 µM).

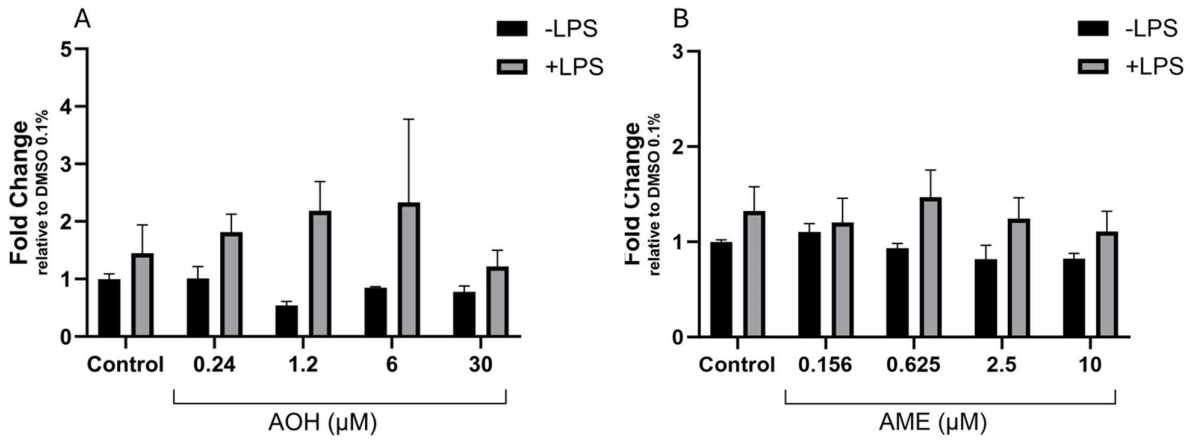

Figure *3.22:* ***The amount of IL-1β secreted by THP-1 cell media after exposure to AOH and AME with or without LPS for 24 hours.*** *(A) IL-1β secreted by THP-1 after exposed to AOH (B) IL-1β secreted by THP-1 after exposed to AME. Control is DMSO 0.1%, and the results represent mean values ± SEM of 3 independent experiments.*

3.9. Gene expression (qPCR)

The impact of LPS, AOH, and AME on the gene expression of IL-1β in THP-1 cells was quantitatively assessed using qPCR (Figure 3.23). The cells were subjected to the following treatments: 0.1%DMSO, AOH, AME with or without LPS. The gene expression levels of IL-1β were normalized to the expression of a housekeeping gene (actin) and are presented as fold change relative to the control. The results demonstrate that LPS significantly upregulates the expression of IL-1β, with a fold increase surpassing 60 times that of the control; but alone AOH and AME didn't show statistically significant increase in IL-1β expression compared to the control (Figure 3.23).

Gene Expression of IL-1β

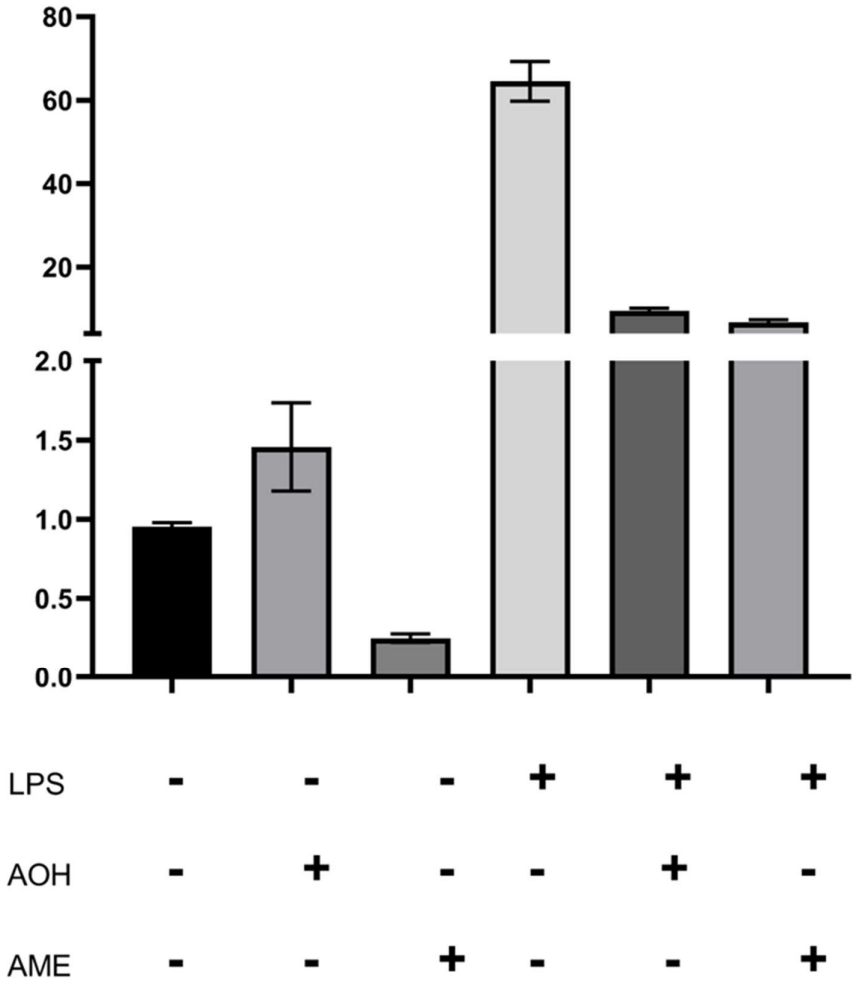

Figure 3.23: ***Gene expression for THP-1 cells after 24 hours treatment with AOH (30*** μM***) and AME (10*** μM***).***
Normalized using ΔΔCq to the geometric mean of Actin. The mean±SEM of three technical replicates is shown.

4. Discussion

Both farmers, people working in the food industry and consumers may be exposed to mycotoxins from contaminated food, e.g. cereal grains and fruits contaminated by these toxins. This study sheds light on how mycotoxins such AOH and AME might impact the immune response in human cells, specifically the TLR's signaling pathway in transfected HEK 293 cells and IL-1β production in THP1 cell.

4.1. Methodological consideration

4.1.1. Cell culture as an *in vitro* model

In vitro cell culture is a technique that allows scientists to study human and animal cells in a controlled setting, away from natural variation. It a good tool for studying drugs and chemicals interactions with cells or effect on cells (Arango et al., 2013). Mostly 2D cell culture models are used in this type of study, but recently 3D models have become famous for advanced settings which stimulate the function of cells in culture close to *in vivo* models. Despite the improvements it is sometimes hard to mimic real life physiological function *in vitro* models, as actual human and animal tissue is more complex in some ways (Wang et al., 2024). However, the US National Research Council's 2007 strategic plan significantly influenced the shift in testing environmental toxicants by promoting the identification of molecular targets and pathways related to toxic effects and advocating for the development of new, high-throughput methods to quantitatively assess these disturbances in cellular pathways and biomarkers for predicting health outcomes (Natural Resource Council 2007, Hirsch et al., 2019). However, the field of toxicology and pharmacology greatly benefited from advancement in understanding cellular stress pathways and molecular processes, despite having limitations (Hirsch et al, 2019). This makes the system a good and effective way of studying the mechanism, however as they do not reflect the behavior of immune cells in a physiological environment; the transferability to actual immune responses in vivo is limited (El-Zayat et al., 2019).

4.1.2. Methods for studying immune response.

In this study, we used HEK 293 cells with transfected upregulation of either TLR 2, TLR4 or IL-1β immune receptors. These cells are not immune cells, they are immortalized human embryonic kidney cells, which allows specifically study the activation and signal pathway of the upregulated receptor (El-Zayat et al., 2019). These cells allow for detection and respond to pathogens or damage without

needing direct involvement from primary immune tissues which most likely exaggerate the cellular activity or response due to increased receptor activity. TLR2 frequently forms heterodimers with TLR1 or TLR6, potentially altering the signaling cascade depending on the ligand and the co-receptor involved (Kawai et al., 2011). However, to get around the issue with potential activation of endogenous receptors a null cell was used as a control in this experiment. The null cells are the parental cell of their transfected counterpart however missing the specific receptor (TLR2, TLR4 or IL-1 β) and therefore is an excellent way to ensure that the signal monitored is due to activation of the receptor studied.

4.1.3. Methods for gene/protein measurements

Sandwich ELISA is used for its effectiveness to measure protein content. Here the antigen is detected between two layers of antibodies- capture antibody and detection antibody (Optofluidic Bioassay, 2021). The sandwich ELISA doesn't require purified samples to analysis and is able to detect small amounts of antigens as it depends on antigen-antibody reaction. However, false positives or negatives due to technical error, sample contamination and low quality of reagents are an issue that can occur (Thermo Fisher Scientific, 2024).

For gene quantification, qPCR is a common method. Dye-based quantitative PCR (qPCR) is used in this study which uses SYBR Green as the dye, to track DNA. When the SYBR Green binds to dsDNA, its background fluorescence substantially increases. As a result, when the target sequence is amplified, the amount of dsDNA present during each PCR cycle is closely correlated with the increase in fluorescence (Solis BioDyne, 2023). This makes it easy to measure DNA amounts in real-time with just two specific primers, making this method fast and cost-effective for analyzing many samples. However, the fact that intercalating dye-based techniques identify any dsDNA generated during the reaction is one of its drawbacks. This comprises primer-dimers and off-target amplification products, which lead to imprecise measurement. Therefore, to make sure the right DNA is measured, a melting curve analysis is done after the PCR to check the specificity of the reaction. Unlike probe qPCR methods, dye-based qPCR can only measure one DNA target per experiment (New England Biolabs, 2024).

4.2. Initial experiments for deciding experimental set-up

4.2.1. Initial experiment

Cell density is important to immune modulation and toxicity testing experiments as too high cell density could affect cell behavior due to overcrowding. However, low cell density, on the other hand, might slow cell growth due to a lack of interaction between cells. As a result, optimal cell density is

required for desired experimental outcome (Opentros, 2024). Therefore, in Section 3.1., various seeding densities of HEK TLR2 and TLR4 cells were evaluated to determine the optimal cell density for the experiments. This was done with the aim of minimizing the consumption of cell media and mycotoxins, thereby enhancing cost-effectiveness. As the cells didn't show any significant fold change in different concentration, so for the experiments optimal seeding density was decided to be 90µL (5.6×10^5 cells/ml). The seeding density of THP-1 and PMA concentration for THP-1 differentiation was decided by reviewing the existing literature. Phuangbubpha et al., (2023) suggested a common protocol in which THP-1 cells require a PMA concentration ranging from 5 to 200 ng/ml for differentiation, with a treatment duration of 24 to 72 hours. The PMA concentration is important to consider because too low concentration leads to insufficient differentiation, and a high concentration would have a toxic effect on cells (Liu et al, 2023).g

The seeding density for HEK IL-1β cells was maintained as specified in the Invivogen catalog for IL-1β receptor cells (Invivogen, 2024). DMSO is toxic to the cells, from literature we can read that Hollander et al., (2022) found the final concentration of 1.2-2.4% DMSO non-cytotoxic in preliminary experiments. Schmutz et al., 2019 used a final concentration of 1% DMSO with the necessary concentrations of test substances. Therefore, we tested DMSO concentration (0.05% to 0.8%) on HEK TLR2 and TLR4 cells in section 3.2. for the two lowest concentrations tested, 0.05% and 0.1% DMSO, there was little change in viability. For the higher concentrations, 0.2 and up, there is no significant difference in viability however, the variation in the results increased substantially suggesting an undesired change in viability. Based on these experiments a test concentration of DMSO was set to 0.1%, which was then used for all the cell lines in this study. Though higher concentrations have been proven safe for many cell lines, a concentration of 0.1% DMSO is commonly considered safe for about all cell lines and used as solvent control in a similar study to ours (Solhaug et al., 2015).

From literature we expected a reduction of LPS induced signal when co exposing to mycotoxins AOH and AME (kollarova et al., 2018). To see this reduction in our experiments, it was important that the dose of LPS/LTA chosen for the experiments was within the exponential phase. Therefore, we conducted an experiment exposing the HEK- TLR2, -TLR4 cells to 0.001 – 100 ng/ml LPS and 500ng/ml LTA to find the exponential area. Based on these experiments we found that 10 ng/ml LPS and 100ng/ml LTA was within the exponential part of the curve and was therefore chosen as concentrations for our studies (Figure 3.3). To our best knowledge it is the first time LTA has been used in cell stimulation.

For THP-1, various LPS concentrations have been used in previous studies. Kallorova et al. exposed their THP-1 cells to LPS and AOH, where 10 ng/ml LPS was used (kallorova et al., 2018). Del Favero et al., (2020) used 100 ng/ml LPS in THP-1 Lucia NF-κB monocytes cell and Solhaug et al., (2016) used 0.1 ng/ml LPS in THP-1 macrophage cells.

4.2.2. Impact of mycotoxin on cell morphology

The cells were monitored using a light microscope throughout the process of seeding, proliferating and exposure to ensure consistency in cell growth and if there were any visual effects of exposure on cells. Existing research shows that mycotoxins can significantly alter cell shape (Schulz et al., 2018). Previous studies have demonstrated the cytotoxic effects of *Alternaria* toxins on various cell lines, affecting cell morphology and viability, potentially leading to cellular apoptosis (Hollander et al., 2022). Meena et al., (2017) mentioned that toxin-induced Golgi vesicle fusion could contribute to membrane damage, potentially explaining the observed morphological changes. These alterations might be indicative of underlying cellular stress or damage mechanisms triggered by the mycotoxins. Furthermore, *Alternaria* toxins are known to disrupt cellular signaling pathways and induce oxidative stress (Archinger et al., 2021), which could contribute to the changes in cell morphology. Our study could not confirm these previous observations as we did not observe any noticeable changes in morphology in our cells after mycotoxin exposure. This, however, does not mean changes did not occur but might be more down to the tool used for detection. The light microscope (Echo Inc., San Diego, USA) used in our study is a good tool for monitoring the cell growth during experiments, however, is not adequate to monitor small changes in morphology.

4.2.3. Viability

Cell viability assays are used to determine if the exposure has large impact on the cell growth or death and thereof could lead to skewed or biased interpretation of results if not taken into consideration. No specific significance on cell viability was observed in any of the cell types used (HEK-TLR2, TLR4, THP-1 and HEK- IL-1 β cells) when exposed to AOH or AME alone (Figure 3.11-3.15 and 3.18-3.19). However, when the cells were co-exposed to LPS and mycotoxins some reduction in viability was seen in both HEK-TLR2 (Figure 3.12 B and Figure 3.14 B), TLR4 (Figure 3.13 B and Figure 3.15 B) and THP-1 (Figure 3.11) cells however, not in a dose-dependent fashion. A higher concentration of LPS (5-20µg/ml) has previously been shown to be significantly toxic in THP-1 cells (Liu et al., 2018). Similar result has also been found in a study on human umbilical cord mesenchymal stem cells, which found higher doses of LPS (40-50µg/ml) to be cytotoxic while lower doses (up to 1µg/ml) appeared to enhance cell viability (Hou et al., 2015). Schmutz et al., (2019) also observed no cytotoxic effect

induced by AOH in Caco-2 cells (neither IL-1β simulated or non-simulated cells). Similarly, Grover et al., (2017) observed less than 10% cell death in BEAS-2B Cells in the presence of AOH compared to control cells.

Kollarova et al., (2018) observed that AOH was cytotoxic only for THP-1 macrophage at the highest concentration (20µM) when cells were stimulated by LPS. AOH and AME were marginally cytotoxic for human tumor cells (colon HT29, liver HepG2 and esophagus KYSE510) up to 50 µM concentration according to Pahlke et al., (2016). The cytotoxic effect of AOH and AME in the human colon adenocarcinoma cell line (HT29) was marginal at the highest concentration 50 µM according to the study of Tiessen et al., (2013). In our experiments, lower doses of LPS (10ng/ml) in combination with up to 30µM AOH and 10µM AME were used (Figure 3.11-3.15 and 3.18-3.19). There was little evidence of these concentrations having much impact on the cell viability and we believe the significant reduction seen in viability is due to coincidental reasons.

4.3. Impact of mycotoxins on immune response

4.3.1. TLR- NF-κB pathway modulation by mycotoxins

Activation and induction of the TLR-NF-κB pathway is an important innate immune response. Cell surface TLRs recognize microbial membrane components such as LPS/LTA to induce inflammatory response (Kawai et al., 2011). By exposing the HEK-TLR2 and TLR4 cells to AOH or AME with or without LTA/LPS, we can get an understanding of how these mycotoxins may impact the immune response. As can be seen from the result in section 3.6. (Figure 3.11-3.14 A) the *Alternaria* toxins (AOH and AME) had no significant impact on TLR- NF-κB signal pathway in TLR2 and TLR4 cells when exposed to the mycotoxins alone. However, when co-exposed with LTA (TLR2) or LPS (TLR4) they significantly reduced the LTA/LPS induced NF-κB signal in a dose-dependent matter. This led to a weaker TLR- NF-κB signal from co-exposure of AOH and AME and LTA/LPS than the signal produced by LTA/LPS alone. This observed reduction of LPS activated NF-κB pathway by AOH has previously been shown by Kollarova et al., (2018) who saw reduced secretion of several pro-inflammatory cytokines including IL-8, IL-6 and TNF-α from differentiated THP-1 cells after combined AOH and LPS exposure. In the same study it was also observed that mycotoxin somehow targets the NF-κB pathway, reducing the inflammation signal (Kollarova et al., 2018). Similar findings have been seen by Schmutz et al., (2019), who reported that AOH could repress immune response in an inflamed environment in epithelial Caco-2 cells. During the differentiation process of THP-1 (monocytes to macrophage), AOH reduced the gene expression of TNF-α and IL-1β, which are early regulators of inflammation and immune responses (Schmutz et al., 2019). It was observed that both

AOH and AME have immunosuppressive properties in the human bronchial epithelial cell line (BEAS-2B) by Grover et al., (2017), where a dose-dependent immunosuppressive effect of these mycotoxins was found. Although, as previous studies suggest that mycotoxin can decrease the LPS induced responses, which aligns with our results, we believe to be the first to show that AOH and AME also reduce the LTA induced TLR- NF-κB responses.

Due to some unspecific reduced viability seen for some of the concentrations (results section 3.5., which is discussed in section 4.2.3.) we wanted to adjust for the toxicity in our experiments. The results were adjusted in respect of toxicity to ensure that cell death is not responsible for the ability to suppress LPS induced response (Grover et al., 2017). Solhaug et al., (2016) reported AOH induced immunosuppression is the effect of cell cycle arrest rather than cell death. However, adjusting for toxicity had no large impact on the results (Figure 3.11-3.14 C).

Section 3.6.1. mentioned the result of mycotoxins impact on HEK Null 1 cells (Figure 3.15). No significant difference observed on TLR- NF-κB signal pathway, which confirming that the result was seen in section 3.5. was triggered by TLR2 and TLR4 respectively in HEK TLR2 and HEK TLR4 cell line. Also, no significant impact on cell viability observed in HEK Null 1 cells (Figure 3.16) which refers to all the existing studies about no impact of mycotoxins on cell viability (Grover et al., 2017, Solhaug et al., 2016, Schmutz et al., 2019).

4.3.2. Modulation of inflammasome activation by mycotoxins in THP-1/IL- 1β-assay

To functionally explore the effect of AOH and AME mycotoxins in combination with immunoreceptor ligands, an inflammasome activation assay with THP-1 cells was used. From the result section 3.7. it was observed that the effect of conditioned media from THP-1 cells exposed to AOH or AME did not lead to an activation of the NF-κB signal pathway of HEK IL-1β alone (Figure 3.18 A and Figure 3.19 A), indicating that exposure to AOH or AME did not activate the IL-1β production in THP-1 cells. However, conditioned media from LPS exposed THP-1 cells induced a response in the HEK IL-1β cells. When HEK IL-1β cells were exposed to conditioned media from THP-1 cells exposed to AOH or AME in combination with LPS, the LPS induced increase of the NF-κB signal was reduced in a dose-dependent manner.

The pro-inflammatory properties of the cells decreased significantly when exposed to mycotoxins (Schmutz et al., 2019). Solhaug et al., (2016) reported downregulation of LPS induced responses by AOH, seen by reduction in LPS induced release of TNF-α as well as suppression of gene expression of proinflammatory cytokines in THP-1 derived macrophage cells (Kollarova et al., 2018). This activation of innate immunity is consistent with the known interactions of recognizing molecular

patterns of microorganisms through toll like receptor (cellular signaling pathway) that mediate inflammatory responses, as detailed by Akira et al., (2004). The major feature of TLR activation is the secretion of proinflammatory cytokines such as TNF-α, IL-1β, IL-6 which can inhibit by small molecule inhibitors (El-Zayat et al., 2019).

The inhibition of IL-1β activity by AOH and AME might occur through direct or indirect interactions with components of the NF-κB signaling pathway, which is crucial for the transcription of inflammatory cytokines. The mycotoxins might act as small molecule inhibitors which inhibit TLR signaling, thereby leading to reduce NF-κB signal (El-Zayat et al., 2019).

It was observed from section 3.7. that cell viability is not significantly affected by AOH and AME (Figure 3.18 B and Figure 3.19 B). In some cases, unspecific significance was observed. But the result observed from section 3.7. align with the discussion in section 4.3.1., it was discussed that cell viability was not significantly affected by AOH and AME. Schmutz et al., (2019) tried different concentrations of AOH (0.02-40μM) which showed no effect on IL-1β stimulated cell viability.

Alternaria toxins (AOH and AME) had no significant impact on TLR- NF-κB signal pathway in Null 1v cells when exposed to the mycotoxins alone (Figure 3.20). But when co-exposed with LPS they significantly reduced the LTA/LPS induced the NF-κB signal in a dose-dependent matter, which didn't serve the purpose of this study. The Null 1v cell line is used as control in this study to ensure that the signal isn't coming from other receptors. The observed signal could be from TNF-α, produced by the THP-1 cells and released in the media alongside IL- 1β. TNFα is suggested as a positive control in the HEK-Null1v cells. No significant change in cell viability was observed in Null 1v cells (Figure 3.21) supporting the previous statements (section 4.3.1.).

4.3.2.1. THP-1 inflammasome activation and IL- 1β release after mycotoxin and LPS exposure (ELISA)

ELISA is an immunological assay commonly used, which can measure protein content in a sample. Unlike the functional study of THP-1-HEK IL-1β described in (section 3.8.) the ELISA method is a quantitative method. Exposing THP-1 cells to LPS leads to inflammasome activation, and secretion of IL-1β in media. ELISA is used to quantify IL-1β level in THP-1 conditioned media (section 3.8.). As seen from figure 3.22, exposure of THP-1 to AOH and AME didn't affect the level of IL-1β secretion, but LPS stimulated THP-1 cells increased the secretion level of IL-1β, which significantly reduced at the highest concentration of AOH and AME. This finding aligns with previous studies on cytokine release after mycotoxin exposure Schmutz et al., (2019); observed reduced secretion of IL-8 (IL-1β-induced) in Caco-2 cells at the highest concentration of AOH (20–40 μM). But slight induction was

observed in the secretion of IL-6 and IL-8 (Schmutz et al., 2019) at the lowest concentration of AOH, which is similar to our result (Figure 3.22 A). The study of Lee et al., (2021) observed that ZEA suppressed the LPS induced IL- 1β secretion. This resulted in weakening the innate immune response and blocking LPS triggered signaling pathways. Another study showed that AOH significantly downregulated the level of LPS induced proinflammatory cytokine secretion (IL-6, IL-8, TNF-α) (Kollarova et al., 2018). According to previous studies, the reduced levels of LPS induced proinflammatory cytokine secretion in stimulated macrophages are caused by NF-κB suppression resulting from mycotoxin exposure (Grover et al., 2017, Kollarova et al., 2018, Lee et al., 2021, Schmutz et al., 2019).

4.3.2.2. Gene expression of inflammatory cytokines in THP-1 cells after AOH, AME and LPS exposure (qPCR)

qPCR is a suitable tool to precisely quantitate changes in gene expression. As shown in part 3.9, the exposure of THP-1 to AOH and AME did not affect the gene expression of IL-1β much, while the LPS stimulated THP-1 cells had a high IL- 1β b expression, which was significantly reduced when exposed in combination with AOH and AME.

This finding suggests that these toxins may suppress their pro-inflammatory effects at the transcriptional level. This observation aligns with previous study by Kollarova et al., (2018) who demonstrated that AOH substantially suppresses transcription of proinflammatory cytokines in dose-dependent manner. According to the study of Solhaug et al., (2016 b) AOH reduced the immune response to LPS by alleviating gene expression of TNF-α. Also, the suspect about reactive oxygen species (ROS) induced NF-κB activation due to AOH has been cleared out. Kollarova et al., (2018) explain that AOH didn't affect the basal NF-κB activity, but the cells stimulated with LPS, AOH reduced the activation of the NF-κB pathway more effectively. This statement aligns with the findings of this study.

The current findings are further supported by the work of Schmutz et al. (2019), who reported pro-inflammatory suppression properties associated with AOH and AME. These mycotoxins were shown to suppress immune function, as significant reduction of transcription levels of IL-1β and TNF-α was observed.

4.8. Study limitation

This study aimed to investigate the impact of AOH and AME mycotoxins on the Toll-like receptors (TLRs) signaling pathway (QuantiBlue assay), to observe the cell viability (alamar-Blueassay), measure the IL-1β as the activity of mycotoxins on THP-1 (ELISA) and as well as measure the gene

expression of IL-1β cytokines (qPCR). However, several limitations were identified in this study. For instance, it could not observe mycotoxin induced morphological changes. Solhaug et al, (2015) used a fluorescence microscope to observe nuclear morphological changes in human cells. Observing the morphological changes helps determine if there are any morphological alterations in cells despite no significant change in cell viability.

Also, the alamar-Blue assay was used to measure metabolic activity of cells, but this assay is not enough to explain cytotoxic effect, rather it explains that cell viability has no impact on immunosuppression properties of these mycotoxins. It would be great if cell cycle also could be examined as it could help to understand the properties of mycotoxins to reduce LTA or LPS induced response. As other studies referred to that cell cycle arrest is responsible for these immunosuppressive properties (Grover et al., 2017).

4.9 Future prospects

In this research, our focus was primarily on IL-1β; however, it would be beneficial to extend this study to include other proinflammatory cytokines such as TNF-α, IL-8, and IL-6 in future work. Due to constraints in time and resources, qPCR was performed only once, but conducting this assay with three biological replicates in future experiments could provide more robust justification for the results. Additionally, further experimentation with the ELISA assay is necessary to optimize dosages and experimental conditions.

One question about signaling cascade is raised during the study, exactly where in the signaling pathway mycotoxins effects. To precisely pinpoint where in the signaling cascade AOH and AME exert their effects, further detailed molecular studies are necessary. Employing techniques such as Western blotting for pathway-specific proteins or advanced imaging techniques could reveal the specific junctures of NF-κB pathway interruption or modulation.

5. Conclusion

This study provides an insight into the modulatory effects of the mycotoxins AOH and AME on the NF-κB signaling pathway and inflammasome activation, particularly in the context of HEK TLR cells (TLR2 and TLR4), THP-1 cells and HEK IL-1β cells. The result demonstrates that AOH and AME can significantly suppress the LPS and LTA induced activation of the NF-κB signaling pathway, reducing the gene expression and secretion of key pro-inflammatory cytokine IL-1β. Also, no significant cell viability was observed in response to exposure to both mycotoxins. The implications of these findings are important in both agricultural and occupational health contexts. In agriculture, the presence of *Alternaria* toxins like AOH and AME is a significant concern due to their potential contamination of crops and subsequent entry into the food supply chain. From an occupational health perspective, individuals working in environments where mold exposure is common—such as farming, food processing, and storage facilities—may be at risk of experiencing altered immune responses due to mycotoxin exposure.

The immunosuppressive effect of these mycotoxins should be considered when developing strategies to mitigate their impact on human health. Agricultural practices that limit fungal growth might be necessary to reduce mycotoxin accumulation in the food supply chain. Implementing better agricultural practices can reduce these risks, safeguarding both the health of plants and the quality of the food, which is good for both public health and workers' health. On the other hand, prolonged exposure to these toxins can weaken workers' immune systems, making them more susceptible to infections, inflammation, and other health problems.

6. References

Aichinger, G., Del Favero, G., Warth, B., & Marko, D. (2021). Alternaria toxins—Still emerging? *Comprehensive Reviews in Food Science and Food Safety*, Advance online publication. https://doi.org/10.1111/1541-4337.12803

Akira, S., Takeda, K. (2004). Toll-like receptor signalling. *Nature Reviews Immunology* 4, 499–511. https://doi.org/10.1038/nri1391

Alberts, B., Johnson, A., Lewis, J., et al. (2002). Molecular Biology of the Cell (4th edition). New York: Garland Science. Chapter 24, The Adaptive Immune System. https://www.ncbi.nlm.nih.gov/books/NBK21070/

Andersen, B., Nielsen, K. F., Fernández Pinto, V., & Patriarca, A. (2015). Characterization of Alternaria strains from Argentinean blueberry, tomato, walnut, and wheat. *International Journal of Food Microbiology*, 196, 1-10. https://doi.org/10.1016/j.ijfoodmicro.2014.11.029

Arango, M. T., Quintero-Ronderos, P., Castiblanco, J., et al. (2013). Cell culture and cell analysis. In J. M. Anaya, Y. Shoenfeld, A. Rojas-Villarraga, et al. (Eds.), *Autoimmunity: From Bench to Bedside* [Internet]. Chapter 45. Bogota (Colombia): El Rosario University Press. Retrieved from: https://www.ncbi.nlm.nih.gov/books/NBK459464/ Accessed on: May 3, 2024.

Balazs, A., Faisal, Z., Csepregi, R., Kőszegi, T., Kriszt, B., Szabó, I., & Poór, M. (2021). In vitro evaluation of the individual and combined cytotoxic and estrogenic effects of zearalenone, its reduced metabolites, alternariol, and genistein. *International Journal of Molecular Sciences*, 22(12), 6281. https://doi.org/10.3390/ijms22126281

Baer, P., & Risbey, J. S. (2009). Uncertainty and assessment of the issues posed by urgent climate change: An editorial comment. *Climatic Change*, 92, 31–36. https://doi.org/10.1007/s10584-008-9529-3

Bennett J. W. (1987). Mycotoxins, mycotoxicoses, mycotoxicology and Mycopathologia. *Mycopathologi*a, 100(1), 3–5. https://doi.org/10.1007/BF00769561

Bennett, J. W., & Klich, M. (2003). Mycotoxins. *Clinical Microbiology Reviews*, 16(3), 497–516. https://doi.org/10.1128/CMR.16.3.497–516.2003

Bernhoft, A., Torp, M., Clasen, P.-E., Løes, A.-K., & Kristoffersen, A. B. (2012). Influence of agronomic and climatic factors on Fusarium infestation and mycotoxin contamination of cereals in Norway. *Food Additives & Contaminants: Part A, 29*(7), 1129-1140. https://doi.org/10.1080/19440049.2012.672476

Bernhoft, A., Wang, J., & Leifert, C. (2022). Effect of organic and conventional cereal production methods on Fusarium head blight and mycotoxin contamination levels. *Agronomy*, 12(4), 797. https://doi.org/10.3390/agronomy12040797

Beyer, M., Klix, M. B., Klink, H., et al. (2006). Quantifying the effects of previous crop, tillage, cultivar and triazole fungicides on the deoxynivalenol content of wheat grain — a review. *Journal of Plant Diseases and Protection*, 113(4), 241–246. https://doi.org/10.1007/BF03356188

Bills, G. F., & Gloer, J. B. (2016). Biologically active secondary metabolites from the fungi. *Microbiol Spectrum*, 4(6), FUNK-0009. https://doi.org/10.1128/microbiolspec.FUNK-0009-2016

Bräse, S., Gläser, F., Kramer, C., Lindner, S., Linsenmeier, A. M., Masters, K.-S., Meister, A. C., Ruff, B. M., & Zhong, S. (2013). *The Chemistry of Mycotoxins*. Springer Verlag, Vienna, Austria. http://dx.doi.org/10.1007/978-3-7091-1312-7

Brummelman, J., Veerman, R. E., Hamstra, H. J., Deuss, A. J., Schuijt, T. J., Sloots, A., Kuipers, B., van Els, C. A., van der Ley, P., Mooi, F. R., Han, W. G., & Pinelli, E. (2015). Bordetella pertussis naturally occurring isolates with altered lipooligosaccharide structure fail to fully mature human dendritic cells. *Infection Immunology*, 83(1), 227-238. https://doi.org/10.1128/IAI.02197-14

Champeil, A., Fourbet, J. F., Doré, T., & Rossignol, L. (2004). Influence of cropping system on Fusarium head blight and mycotoxin levels in winter wheat. *Crop Protection*, 23(6), 531-537. https://doi.org/10.1016/j.cropro.2003.10.011

Chanput, W., Mes, J. J., & Wichers, H. J. (2014). THP-1 cell line: an in vitro cell model for immune modulation approach. *International Immunopharmacology, 23*(1), 37-45. https://doi.org/10.1016/j.intimp.2014.08.002

Clouvel, P., Bonvarlet, L., Martinez, A., Lagouarde, P., Dieng, I., & Martin, P. (2008). Wine contamination by ochratoxin A in relation to vine environment. *International Journal of Food Microbiology*, 123(1-2), 74-80. https://doi.org/10.1016/j.ijfoodmicro.2007.12.003

Cotty, P. J., & Jaime-Garcia, R. (2007). Influences of climate on aflatoxin-producing fungi and aflatoxin contamination. *International Journal of Food Microbiology*, 119(1-2), 109-115. https://doi.org/10.1016/j.ijfoodmicro.2007.07.060

Del Favero, G., Hohenbichler, J., Mayer, R. M., Rychlik, M., & Marko, D. (2020). Mycotoxin Altertoxin II induces lipid peroxidation connecting mitochondrial stress response to NF-κB inhibition in THP-1 macrophages. *Chemical Research in Toxicology*, 33(2), 492-504. https://doi.org/10.1021/acs.chemrestox.9b00378

Donato, M. T., Tolosa, L., & Gómez-Lechón, M. J. (2014). Culture and functional characterization of human hepatoma HepG2 cells. *Protocol. In Methods in Molecular Biology* (Vol. 1250). https://doi.org/10.1007/978-1-4939-2074-7_5

El-Zayat, S. R., Sibaii, H., & Mannaa, F. A. (2019). Toll-like receptors activation, signaling, and targeting: an overview. *Bulletin of the National Research Centre*, 43(1). https://doi.org/10.1186/s42269-019-0227-2

EFSA Panel on Contaminants in the Food Chain (CONTAM). (2011). Scientific Opinion on the risks for animal and public health related to the presence of Alternaria toxins in feed and food. *EFSA Journal*, 9(10), 2407. https://doi.org/10.2903/j.efsa.2011.2407

European Union Commission. (2006). Recommendation on the Presence of Deoxynivalenol, Zearalenone, Ochratoxin A, T-2 and HT-2 and Fumonisins in Products Intended for Animal Feeding. http://eur-lex.europa.eu/LexUriServ/LexUriServ.do?uri=OJ:L:2006:229:0007:0009:EN:PDF

Food and Drug Administration (FDA); Rockville, MD, USA. (Accessed on 2024, February 29). Guidance for Industry and FDA: Advisory Levels for Deoxynivalenol (DON) in Finished Wheat Products for Human Consumption and Grains and Grain By-Products used for Animal Feed.

https://www.fda.gov/regulatory-information/search-fda-guidance-documents/guidance-industry-and-fda-advisory-levels-deoxynivalenol-DON-finished-wheat-products-human

InvivoGen. (2024). HEK-Blue™ IL-1β cells [Catalog code: hkb-il1bv2]. Retrieved from https://www.invivogen.com/sites/default/files/invivogen/products/files/hekblue_il1bv2_tds_0.pdf Accessed on: April 24, 2024

Giménez, I., Escobar, J., Ferruz, E., Lorán, S., Herrera, M., Juan, T., Herrera, A., & Ariño, A. (2012). The effect of weather and agronomic practice on deoxynivalenol mycotoxin in durum wheat. *Journal of Life Sciences*, *49*, 513-517.

Góral, T., Łukanowski, A., Małuszyńska, E., Stuper-Szablewska, K., Buśko, M., & Perkowski, J. (2019). Performance of winter wheat cultivars grown organically and conventionally with focus on Fusarium head blight and Fusarium trichothecene toxins. *Microorganisms*, 7(10), 439. https://doi.org/10.3390/microorganisms7100439

Grover, S., & Lawrence, C. B. (2017). The Alternaria alternata Mycotoxin Alternariol Suppresses Lipopolysaccharide-Induced Inflammation. *International journal of molecular sciences*, *18*(7), 1577. https://doi.org/10.3390/ijms18071577

Gu, Q., Zou, J., Zhou, Y., & Deng, Q. (2023). Mechanism of inflammasomes in cancer and targeted therapies. Frontiers in Oncology, 13, 1133013. https://doi.org/10.3389/fonc.2023.1133013

Halstensen, A. S., Nordby, K.-C., Kristensen, P., & Eduard, W. (2008). Mycotoxins in grain dust. *Stewart Postharvest Review, 4*(6), 1-9. https://doi.org/10.2212/spr.2008.6.6

Hirsch, C., & Schildknecht, S. (2019). *In Vitro* Research Reproducibility: Keeping Up High Standards. *Frontiers in pharmacology*, *10*, 1484. https://doi.org/10.3389/fphar.2019.01484

Hiltunen, M., & Söderhäll, K. (1992). Alternatiol-O-methyltransferase from Alternaria alternata: Partial purification and relation to polyketide synthesis. *Journal of Biotechnology*, 26(2-3), 281-291. https://doi.org/10.1016/0147-5975(92)90040-X

Hollander, D. D., Holvoet, C., Demeyere, K., De Zutter, N., Audenaert, K., Meyer, E., & Croubels, S. (2022). Cytotoxic effects of alternariol, alternariol monomethyl-ether, and tenuazonic acid and their relevant combined mixtures on human enterocytes and hepatocytes. *Frontiers in Microbiology*, 13, 849243. https://doi.org/10.3389/fmicb.2022.849243

Hou, Y. S., Liu, L. Y., Chai, J. K., Yu, Y. H., Duan, H. J., Hu, Q., Yin, H. N., Wang, Y. H., Zhuang, S. B., Fan, J., Chu, W. L., & Ma, L. (2015). Lipopolysaccharide pretreatment inhibits LPS-induced human umbilical cord mesenchymal stem cell apoptosis via upregulating the expression of cellular FLICE-inhibitory protein. *Molecular Medicine Reports*, 12(4), 2521-2528. https://doi.org/10.3892/mmr.2015.3723

Isah, T. (2019). Stress and defense responses in plant secondary metabolites production. *Biological Research*, 52, 39. https://doi.org/10.1186/s40659-019-0246-3

Isebaert, S., De Saeger, S., Devreese, R., Verhoeven, R., Maene, P., Heremans, B., & Haesaert, G. (2009). Mycotoxin-producing Fusarium species occurring in winter wheat in Belgium (Flanders) during 2002–2005. Journal of Phytopathology. *Advance online publication*. https://doi.org/10.1111/j.1439-0434.2008.01443.x

Jackson, A. O., & Taylor, C. B. (1996). Plant-Microbe Interactions: Life and Death at the Interface. *The Plant Cell*, 8(10), 1651–1668. https://doi.org/10.1105/tpc.8.10.1651

Kollarova, J., Cenk, E., Schmutz, C., & Marko, D. (2018). The mycotoxin alternariol suppresses lipopolysaccharide-induced inflammation in THP-1 derived macrophages targeting the NF-kappaB signalling pathway. *Archives of Toxicology*, **92**(11), 3347–3358. https://doi.org/10.1007/s00204-018-2299-4

Kawai, T., & Akira, S. (2011). Toll-like receptors and their crosstalk with other innate receptors in infection and immunity. *Immunity, 34*(5), 637-650. https://doi.org/10.1016/j.immuni.2011.05.006

Lea, T. (2015). The Impact of Food Bioactives on Health: In vitro and ex vivo models. Chapter 10: Caco-2 Cell Line. In K. Verhoeckx, P. Cotter, I. López-Expósito, et al. (Eds.), *Springer*.

Retrieved from https://www.ncbi.nlm.nih.gov/books/NBK500149/ doi: 10.1007/978-3-319-16104-4_10

Lee, P.-Y., Liu, C.-C., Wang, S.-C., Chen, K.-Y., Lin, T.-C., Liu, P.-L., Chiu, C.-C., Chen, I.-C., Lai, Y.-H., Cheng, W.-C., & et al. (2021). Mycotoxin zearalenone attenuates innate immune responses and suppresses NLRP3 inflammasome activation in LPS-activated macrophages. *Toxins*, 13(9), 593. https://doi.org/10.3390/toxins13090593

Lemmens, M., Haim, K., Lew, H., & Ruckenbauer, P. (2004). The effect of nitrogen fertilization on Fusarium head blight development and deoxynivalenol contamination in wheat. *Journal of Phytopathology, 152*(1), 1-8. https://doi.org/10.1046/j.1439-0434.2003.00791.x

Li, Y., Huang, H., Liu, B., Zhang, Y., Pan, X., Yu, X. Y., Shen, Z., & Song, Y. H. (2021). Inflammasomes as therapeutic targets in human diseases. *Signal Transduction and Targeted Therapy*. https://doi.org/10.1038/s41392-021-00650-z

Lin, H., Jia, B., & Wu, A. (2023). Cytotoxicities of co-occurring alternariol, alternariol monomethyl ether, and tenuazonic acid on human gastric epithelial cells. *Food and Chemical Toxicology*, 171, 113524. https://doi.org/10.1016/j.fct.2022.113524

Liu, T., Huang, T., Li, J., Li, A., Li, C., Huang, X., Li, D., Wang, S., & Liang, M. (2023). Optimization of differentiation and transcriptomic profile of THP-1 cells into macrophage by PMA. *PloS one*, *18*(7), e0286056. https://doi.org/10.1371/journal.pone.0286056

Liu, X., Yin, S., Chen, Y., Wu, Y., Zheng, W., Dong, H., Bai, Y., Qin, Y., Li, J., Feng, S., & Zhao, P. (2018). LPS-induced proinflammatory cytokine expression in human airway epithelial cells and macrophages via NF-κB, STAT3 or AP-1 activation. *Molecular Medicine Reports*, 17(4), 5484-5491. https://doi.org/10.3892/mmr.2018.8542

Longhin, E. M., El Yamani, N., Rundén-Pran, E., & Dusinska, M. (2022). The alamar-Blueassay in the context of safety testing of nanomaterials. *Frontiers in Toxicology, 4*, 981701. https://doi.org/10.3389/ftox.2022.981701

Luo, S., Du, H., Kebede, H., Liu, Y., & Xing, F. (2021). Contamination status of major mycotoxins in agricultural products and foodstuffs in Europe. *Food Control*. Advance online publication. https://doi.org/10.1016/j.foodcont.2021.108120

Malik, A., Ali, S., Shahid, M., & Bhargava, R. (2014). Occupational exposure to Aspergillus and aflatoxins among food-grain workers in India. *International Journal of Occupational and Environmental Health, 20*(3), 189-193. http://dx.doi.org/10.1179/2049396714Y.0000000055

Marshall, J. S., Warrington, R., Watson, W., et al. (2018). An introduction to immunology and immunopathology. *Allergy, Asthma & Clinical Immunology, 14*(Suppl 2), 49. https://doi.org/10.1186/s13223-018-0278-1

Mayer, S., Twarużek, M., Błajet-Kosicka, A., & Grajewski, J. (2016). Occupational exposure to mould and microbial metabolites during onion sorting--insights into an overlooked workplace. *Environmental monitoring and assessment*, *188*(3), 154. https://doi.org/10.1007/s10661-016-5150-5

McDaniel, M. M., Kottyan, L. C., Singh, H., & Pasare, C. (2020). Suppression of inflammasome activation by IRF8 and IRF4 in cDCs is critical for T cell priming. *Cell Reports, 31*(5), 107604. https://doi.org/10.1016/j.celrep.2020.107604

Meena, M., Gupta, S. K., Swapnil, P., Zehra, A., Dubey, M. K., & Upadhyay, R. S. (2017). Alternaria toxins: Potential virulence factors and genes related to pathogenesis. *Frontiers in Microbiology*, 8, 1451. https://doi.org/10.3389/fmicb.2017.01451

Munger, H., Vanasse, A., Rioux, S., & Légère, A. (2014). Bread wheat performance, fusarium head blight incidence and weed infestation response to low-input conservation tillage systems in eastern Canada. Canadian *Journal of Plant Science*, 94(2), 193-201. https://doi.org/10.4141/cjps2013-132

National Research Council (NRC). (2007). *Toxicity testing in the 21st century: A vision and a strategy*. Washington, DC: National Academies Press. ISBN: 0-309-10993-0

Retrieved from: https://books.google.no/books?hl=en&lr=&id=3AWfAwAAQBAJ&oi=fnd&pg=PT21&ots=UxnlSBzbzh&sig=vZ-rl_zZnmNhC67ePE8BHCLJfk8&redir_esc=y#v=onepage&q&f=false Accessed on: May 3, 2024.

New England Biolabs. (2024). Dye-based qPCR. Retrieved from https://www.neb.com/en/applications/dna-amplification-pcr-and-qpcr/qpcr-and-rt-qpcr/dye-based-qpcr Accessed on: April 22, 2024.

Noonim, P., Mahakarnchanakul, W., Nielsen, K. F., Frisvad, J. C., & Samson, R. A. (2009). Fumonisin B2 production by Aspergillus niger in Thai coffee beans. *Food Additives & Contaminants: Part A, Chemistry, Analysis, Control, Exposure & Risk Assessment*, 26(1), 94-100. https://doi.org/10.1080/02652030802366090

O'Brien, J., Wilson, I., Orton, T., & Pognan, F. (2000). Investigation of the alamar-Blue(resazurin) fluorescent dye for the assessment of mammalian cell cytotoxicity. *European Journal of Biochemistry, 267*(17), 5421-5426. https://doi.org/10.1046/j.1432-1327.2000.01606.x

Opentros. (2024). *Cell Seeding.* Retrieved from: https://opentrons.com/applications/cell-seeding/ Accessed on: April 24, 2024.

Optofluidic Bioassay. (2021). *Understanding Sandwich ELISA: Its Advantages and Steps*. https://www.optobio.com/understanding-sandwich-ELISA-its-advantages-and-steps/

Pahlke, G., Tiessen, C., Domnanich, K., Kahle, N., Groh, I. A. M., Schreck, I., Weiss, C., & Marko, D. (2016). Impact of Alternaria toxins on CYP1A1 expression in different human tumor cells and relevance for genotoxicity. *Toxicology Letters, 240*(1), 93-104. https://doi.org/10.1016/j.toxlet.2015.10.003.

Paterson, R. R. M., & Lima, N. (2010). How will climate change affect mycotoxins in food? *Food Research International*, 43(7), 1902-1914. https://doi.org/10.1016/j.foodres.2009.07.010

Phuangbubpha, P., Thara, S., Sriboonaied, P., Saetan, P., Tumnoi, W., & Charoenpanich, A. (2023). Optimizing THP-1 Macrophage Culture for an Immune-Responsive Human Intestinal Model. *Cells*, *12*(10), 1427. https://doi.org/10.3390/cells12101427

Pinton, P., & Oswald, I. P. (2014). Effect of Deoxynivalenol and Other Type B Trichothecenes on the Intestine: A Review. *Toxins (Basel)*, 6(5), 1615–1643. https://doi.org/10.3390/toxins6051615

Rampersad S. N. (2012). Multiple applications of Alamar-Blue as an indicator of metabolic function and cellular health in cell viability bioassays. *Sensors (Basel, Switzerland)*, *12*(9), 12347–12360. https://doi.org/10.3390/s120912347

Saad-Hussein, A., Taha, M. M., Beshir, S., Shahy, E. M., Shaheen, W., & Elhamshary, M. (2014). Carcinogenic effects of aflatoxin B1 among wheat handlers. *International Journal of Occupational and Environmental Health, 20*(3), 215-219. https://doi.org/10.1179/2049396714Y.0000000069

Sajad, A. M., & Jamaluddin, Abid, H. Q. (2017). Fungi associated with the spoilage of post-harvest tomato fruits and their frequency of occurrences in different markets of Jabalpur, Madhya Pradesh, India. *International Journal of Current Research and Review*, 9, 12–16. https://ijcrr.com/uploads/118_pdf.pdf

Schmid-Burgk, J. L., Gaidt, M. M., Schmidt, T., Ebert, T. S., Bartok, E., & Hornung, V. (2015). Caspase-4 mediates non-canonical activation of the NLRP3 inflammasome in human myeloid cells. *European Journal of Immunology*, 45(10), 2911-2917. https://doi.org/10.1002/eji.201545523

Schmutz, C., Cenk, E., & Marko, D. (2019). The Alternaria Mycotoxin Alternariol Triggers the Immune Response of IL-1β-stimulated, Differentiated Caco-2 Cells. *Molecular nutrition & food research*, *63*(20), e1900341. https://doi.org/10.1002/mnfr.201900341

Schulz, M.C., Schumann, L., Rottkord, U., Humpf, H.U., Gekle, M., & Schwerdt, G. (2018). Synergistic action of the nephrotoxic mycotoxins ochratoxin A and citrinin at nanomolar concentrations in human proximal tubule-derived cells. Toxicology Letters, 291. https://doi.org/10.1016/j.toxlet.2018.04.014

Shah, L., Ali, A., Yahya, M., Zhu, Y., Wang, S., Si, H., Rahman, H., & Ma, C. (2017). Integrated control of Fusarium head blight and deoxynivalenol mycotoxin in wheat. Plant Pathology, 67(3), 532-548. https://doi.org/10.1111/ppa.12785

Shi, J., Zhao, Y., Wang, K. *et al.* Cleavage of GSDMD by inflammatory caspases determines pyroptotic cell death. *Nature* **526**, 660–665 (2015). https://doi.org/10.1038/nature15514

Sobrova, P., Adam, V., Vasatkova, A., Beklova, M., Zeman, L., & Kizek, R. (2010). Deoxynivalenol and its toxicity. *Interdisciplinary Toxicology*, 3(3), 94–99. https://doi.org/10.2478/v10102-010-0019-x

Solhaug, A., Eriksen, G. S., & Holme, J. A. (2016 a). Mechanisms of action and toxicity of the mycotoxin Alternariol: A review. *Basic & Clinical Pharmacology & Toxicology*, Advance online publication. https://doi.org/10.1111/bcpt.12635

Solhaug, A., Karlsøen, L. M., Holme, J. A., Kristoffersen, A. B., & Eriksen, G. S. (2016 b). Immunomodulatory effects of individual and combined mycotoxins in the THP-1 cell line. *Toxicology in Vitro, 36*, 120-132. https://doi.org/10.1016/j.tiv.2016.07.012

Solhaug, A., Wisbech, C., Christoffersen, T. E., Hult, L. O., Lea, T., Eriksen, G. S., & Holme, J. A. (2015). The mycotoxin alternariol induces DNA damage and modifies macrophage phenotype and inflammatory responses. *Toxicology Letters, 239*(1), 9–21. https://doi.org/10.1016/j.toxlet.2015.08.1107

Solis BioDyne, (2023). *Everything you need to know about dye-based qPCR*. Retrieved from https://solisbiodyne.com/EN/everything-you-need-to-know-about-dye-based-qpcr-/

Stierschneider, A., Neuditschko, B., Colleselli, K., Hundsberger, H., Herzog, F., & Wiesner, C. (2023). Comparative and Temporal Characterization of LPS and Blue-Light-Induced TLR4 Signal Transduction and Gene Expression in Optogenetically Manipulated Endothelial Cells. *Cells*, *12*(5), 697. https://doi.org/10.3390/cells12050697

Stoev, S. D. (2024). Food security, underestimated hazard of joint mycotoxin exposure and management of the risk of mycotoxin contamination. *Food Control*, 159, 110235. https://doi.org/10.1016/j.foodcont.2023.110235

Straumfors, A., Uhlig, S., Eriksen, G.S., Heldal, K.K., Eduard, W., Krska, R., & Sulyok, M. (2015). Mycotoxins and other fungal metabolites in grain dust from Norwegian grain elevators and compound feed mills. *World Mycotoxin Journal*, *8*(3), 361-374. https://doi.org/10.3920/WMJ2014.1799

Surai, P. F., & Mezes, M. (2005). Mycotoxins and immunity: theoretical consideration and practical applications. *Praxis Veterinaria*, 53(1-2), 71-88. https://www.researchgate.net/publication/236660212

Taevernier, L., Veryser, L., Roche, N., et al. (2016). Human skin permeation of emerging mycotoxins (beauvericin and enniatins). *Journal of Exposure Science & Environmental Epidemiology, 26*(3), 277–287. https://doi.org/10.1038/jes.2015.10

Teoh, E. S. (2016). Secondary Metabolites of Plants. In Medicinal Orchids of Asia (pp. 59-73). *Springer*, Cham. https://doi.org/10.1007/978-3-319-24274-3_5

Thermo Fisher Scientific. (2024). Overview of ELISA. Retrieved from https://www.thermofisher.com/no/en/home/life-science/protein-biology/protein-biology-learning-center/protein-biology-resource-library/pierce-protein-methods/overview-ELISA.html icid=bid_cbu_sbu_r01_co_cp1605_pjt10933_blg50608_0so_blg_il_awa_og_s00_C2SELISA BlogELISA Accessed on: April 22, 2024.

Tiessen, C., Fehr, M., Schwarz, C., Baechler, S., Domnanich, K., Böttler, U., Pahlke, G., & Marko, D. (2013). Modulation of the cellular redox status by the Alternaria toxins alternariol and alternariol monomethyl ether. *Toxicology Letters, 216*(1), 23-30. https://doi.org/10.1016/j.toxlet.2012.11.005.

Tsuge, T., Harimoto, Y., Akimitsu, K., Ohtani, K., Kodama, M., Akagi, Y., Egusa, M., Yamamoto, M., & Otani, H. (2013). Host-selective toxins produced by the plant pathogenic fungus Alternaria alternata. *FEMS Microbiology Reviews*, 37(1), 44–66. https://doi.org/10.1111/j.1574-6976.2012.00350.x

Viegas, S., Veiga, L., Almeida, A., dos Santos, M., Carolino, E., & Viegas, C. (2016). Occupational exposure to Aflatoxin B1 in a Portuguese poultry slaughterhouse. *The Annals of Occupational Hygiene, 60*(2), 176–183. https://doi.org/10.1093/annhyg/mev077

Viegas, S., Viegas, C., & Oppliger, A. (2018). Occupational Exposure to Mycotoxins: Current Knowledge and Prospects. *Annals of Work Exposures and Health, 62*(8), 923–941. https://doi.org/10.1093/annweh/wxy070

Wang, L., Hu, D., Xu, J., Hu, J., & Wang, Y. (2023). Complex in vitro Model: A Transformative Model in Drug Development and Precision Medicine. *Clinical and translational science*, *17*(2), e13695. Advance online publication. https://doi.org/10.1111/cts.13695

Wang, YC., Lin, S. & Yang, QW. (2011). Toll-like receptors in cerebral ischemic inflammatory injury. *J Neuroinflammation* **8**, 134. https://doi.org/10.1186/1742-2094-8-134

Wang, Y., Song, E., Bai, B., & Vanhoutte, P. M. (2016). Toll-like receptors mediating vascular malfunction: Lessons from receptor subtypes. *Pharmacology & Therapeutics, 158*, 91-100. https://doi.org/10.1016/j.pharmthera.2015.12.005

Woudenberg, J. H. C., Seidl, M. F., Groenewald, J. Z., de Vries, M., Stielow, J. B., Thomma, B. P. H. J., & Crous, P. W. (2015). Alternaria section Alternaria: Species, formae speciales, or pathotypes? *Studies in Mycology*, 82, 1–21. https://doi.org/10.1016/j.simyco.2015.07.001

Yang, F., Jensen, J. D., Spliid, N. H., Svensson, B., Jacobsen, S., Jørgensen, L. N., Jørgensen, H. J. L., Collinge, D. B., & Finnie, C. (2010). Investigation of the effect of nitrogen on severity of Fusarium Head Blight in barley. *Journal of Proteomics*, 73(4), 743-752. https://doi.org/10.1016/j.jprot.2009.10.010

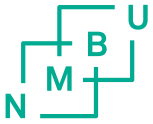

Norges miljø- og biovitenskapelige universitet
Noregs miljø- og biovitskapelege universitet
Norwegian University of Life Sciences

Postboks 5003
NO-1432 Ås
Norway